2018

Structural and Functional Consequences of HIV-1 Viral Protein Tat and Morphine Co-Exposure at the Blood-Brain Barrier

Crystal R. Leibrand

STRUCTURAL AND FUNCTIONAL CONSEQUENCES OF HIV-1 VIRAL PROTEIN TAT AND MORPHINE CO-EXPOSURE AT THE BLOOD-BRAIN BARRIER

A Dissertation submitted in partial fulfillment of the requirements for the degree of Doctor of Philosophy at Virginia Commonwealth University.

By

Crystal R. Leibrand

Bachelor of Science, Randolph-Macon College, Ashland, VA, USA

Director: Dr. MaryPeace McRae,

Assistant Professor, Department of Pharmacotherapy and Outcomes Science

Virginia Commonwealth University

Richmond, Virginia

April, 2018

Acknowledgements

First I would to thank my advisor **Dr. MaryPeace McRae** for giving me the opportunity to learn in her lab and for the constant support, encouragement, and advice with everything.

I also want to thank the members of my dissertation committee**, Drs. MaryPeace McRae, Patricia Fulco, Kurt Hauser, Joseph McClay, Patricia Slattum, and Douglas Sweet**. I appreciate your assistance and advice, as well as patience and time serving on my committee.

Dr. Patricia Fulco for allowing me to participate in her clinic throughout my graduate school years and serving as my mentor.

Dr. Vivian Bruzzese, Tom, and Millie for letting me volunteer at CrossOver and help the team in any way I could.

Dr. Krista Donohoe for guiding me through my teaching assistantship and completion of the Preparing Future Faculty program.

Dr. Patricia Slattum for always thinking of me and giving encouragement and insights during my combined degree path.

Iffie and Preetha for all of your lab help. I miss you both!

Dr. Kurt Hauser for co-mentoring me throughout my graduate research and providing optimism in the data even when I couldn't see it myself.

Dr. Jason Paris for training me to be the scientist I am today. I went from never touching a mouse before to becoming the mouse surgery queen. I am glad to have you as a mentor and colleague.

Drs. Woongi-Kim, Pamela Knapp, Yun Hahn, Angela Kashuba, Matthew Halquist, Quamrun Masuda, Said Ghandour for all of their help with my research.

The R25 MH080661 Pilot Award for Innovative NeuroAIDS Projects from **Johns Hopkins University/National Institute on Mental Health** which helped support my research.

The Deans Office and **Department of Pharmacotherapy and Outcomes Science Office** for their administrative help throughout my time here at VCU.

All of the members of **DPOS GSA**, including my cubicle buddy **Mohamad**. I'm going to miss our office and semester socials.

The **PharTech IT Department** for handling my shenanigans with grace.

My friends back from home including **Greg Eelman** (we must play Nintendo now in celebration), **Megan, Chris, and Zach**. Thank you for sticking by me, even when I was "missing in action" for several months at a time. Maybe another Mario Kart party is in order…

My closest friend throughout pharmacy school and post-P4 life, **Courtney Crocker**. You have always believed in me even when I didn't believe in myself.

My parents **Allen and Charlene Leibrand**, my sister **Rachel Leibrand**, and my future in-laws **Michael and Jolene Kaczmar** for your encouragement and support throughout this process.

My early morning study buddy **Oliver** the kitty and late night support dog **Ozzy**.

Last, but not least, my soon-to-be husband and best friend, **Kyle Kaczmar**. You are my rock in my otherwise hectic life. I would not have accomplished this without your constant love and support. I cannot wait to spend the rest of my life with you and experience all that life has to offer.

Table of Contents

Page

List of Tables

List of Figures

Abbreviations

ALCAM	activated leukocyte cell adhesion molecule
ANOVA	analysis of variance
APCI	atmospheric pressure chemical ionization
BCRP	breast cancer resistance protein
BBB	blood-brain barrier
cART	combination antiretroviral therapy
CNS	central nervous system
DOR	δ-opioid receptor
HAND	HIV-associated neurocognitive disorders
HIV-1	human immunodeficiency virus-1
HRP	horseradish peroxidase
Iba-1	ionized calcium-binding adaptor molecule 1
ICV	intracerebroventricular
IL-6	interleukin 6
INF-γ	interferon gamma
JAM-A	junctional adhesion molecule-A
KOR	κ-opioid receptor

LLQR	lower limit of quantification
M3G	morphine-3-glucuronide
M6G	morphine-6-glucuronide
MCP-1	monocyte chemoattractant protein 1
MDM	monocyte-derived macrophage
MOR	μ-opioid receptor
MRP	multidrug resistance protein
Na-F	sodium fluorescein
neuroAIDS	neuro-acquired immunodeficiency syndrome
NVU	neurovascular unit
OCT	organic cation transporter
Pgp	p-glycoprotein
PWID	people who inject drugs
RANTES	regulated on activation, normal T cell expressed and secreted
ROS	reactive oxygen species
SIV	simian immunodeficiency virus
Tat	trans-activator of transcription
TLR2	toll-like receptor 2

TLR4	toll-like receptor 4
TNF-α	tumor necrosis factor alpha
UDP	uridine diphosphate
UGT	UDP-glucuronosyltransferase
ZO	zonula occludens

Abstract

STRUCTURAL AND FUNCTIONAL CONSEQUENCES OF HIV-1 VIRAL PROTEIN TAT AND MORPHINE CO-EXPOSURE AT THE BLOOD-BRAIN BARRIER

By Crystal Reiko Leibrand

A dissertation submitted in partial fulfillment of the requirements for the degree of Doctor of Philosophy at Virginia Commonwealth University.

Virginia Commonwealth University, 2018

Major Advisor: MaryPeace McRae, Pharm.D., Ph.D.
Assistant Professor
Department of Pharmacotherapy and Outcomes Science

According to UNAIDS 2016, over 37 million people worldwide were infected with human immunodeficiency virus (HIV) in 2016, with over 1.2 million people living with HIV in the United States. Of those, approximately one half will suffer from HIV-associated neurocognitive disorders (HAND), which is a spectrum of neurocognitive disorders ranging from asymptomatic neurocognitive impairment, to mild neurocognitive disorder, to HIV-associated dementia. While combination antiretroviral therapy (cART) has decreased the incidence of the

most severe forms of HAND in patients with HIV, milder forms of HAND still persist. These defects can include decreased motor skills, cognitive abilities, memory, and attention. While patients with HIV are living longer thanks to cART, there are few to no long-term options for managing the neurocognitive defects caused by the chronic disease of HAND. Additionally, opiate abuse can increase both the incidence and severity of HAND. HAND may result due to poor antiretroviral drug (ARV) penetration across the blood-brain barrier (BBB). Thus, a better understanding of the effects of HIV and opiates on the BBB may result in improved therapies for HAND.

The Tat transgenic model was used to evaluate the effects of the HIV-1 viral protein Tat and morphine on blood-brain barrier leakiness using varied-sized paracellular compounds. Secondly, antiretroviral drug accumulation in the brain of Tat transgenic mice under Tat and/or morphine co-exposure was measured. Specifically, the single tablet regimen of Triumeq® (abacavir/lamivudine/dolutegravir) was studied in these mice and antiretroviral drug measured in both striatum and hippocampus brain regions and plasma via LC-MS/MS. Additionally, morphine and its metabolites were also measured via LC-MS/MS. Lastly, macrophage turnover within the caudate/putamen and phagocytic macrophage/microglia accumulation in the brain was measured in Tat transgenic mice under Tat and/or morphine conditions. Perivascular and parenchymal spaces were distinguished within the caudate/putamen, while overall phagocytic activity was measured in all other brain regions, including the nucleus accumbens, anterior cingulate cortex, primary motor cortex, somatosensory cortex, agranular insular cortex, and piriform cortex.

Chapter 1: Introduction

Over 37 million people were living with human immunodeficiency virus (HIV) infection worldwide in 2016, and of those up to 50% may develop symptoms of HIV-associated neurocognitive disorders (HAND) (McArthur 2004; Power et al. 2009; UNAIDS 2016). While combination antiretroviral therapy (cART) has decreased the incidence of most forms of neurocognitive impairment in patients with HIV, milder forms of HAND still persist. These milder defects include decreases in motor skills, cognitive abilities, attention, concentration, learning, and memory (Alfahad & Nath 2013; Antinori et al. 2007). This is a particularly alarming problem because despite advances in cART, which help prevent early death, there are few to no long-term options for managing the cognitive and neurobehavioral defects caused by what has become a chronic disease (Ellis et al. 2007). HAND may persist due to several factors. Inflammation in HIV infection leading to neurodegeneration may contribute to HAND, whether from immune reconstitution inflammatory syndrome (Fauci & Marston 2015; Saylor et al. 2016), translocation of gut bacteria disrupting the microbiome (Ancuta et al. 2008), or impediment of the proteasome to turnover folded proteins in brain cells (Saylor et al. 2016; Nguyen et al. 2010). Disruptions in bioenergetic homeostasis, including reductions in glucose uptake in the anterior cingulate cortex and in the mesial frontal gyrus in those patients even with undetectable HIV-1 RNA viral load (Andersen et al. 2010; Towgood et al. 2013). HAND may also persist due to poor antiretroviral drug (ARV) penetration across the blood-brain barrier (BBB) (Spudich & Ances 2012). Some studies have found that the use of antiretroviral drug regimens with high CNS penetration effectiveness were associated with better neurocognitive functioning (Smurzynski et al. 2011; Casado et al. 2014), though these findings have not been consistently found in other studies (Yilmaz et al. 2010). While cART is effective in restricting viral loads peripherally, HIV enters the brain early in disease and is challenging to eradicate. Thus, the brain

serves as an HIV reservoir, allowing for HIV to persist and cause chronic inflammation (Valcour et al. 2013). This theory is supported by the presence of detectable HIV in the cerebrospinal fluid (CSF) of some patients even with undetectable HIV-1 RNA viral load in the plasma, known as CSF escape (Fois & Brew 2015).

Opiate drug abuse can exacerbate HIV progression into AIDS (Kumar et al. 2006; Peterson et al. 1990) as well as increase the incidence and severity of HAND (Byrd et al. 2012; McArthur et al. 2010; Valcour 2011). People who inject drugs are at an increased risk of contracting HIV both through the sharing of HIV-contaminated needles and through risky sexual behavior (Reddy et al. 2012; Bell et al. 1998), with up to one-third of patients with HIV reporting opiate abuse (Bell et al. 1998; UNAIDS 2016). Studies have revealed an interactive link between opiates and HIV effects. Both HIV and opiates can suppress the immune system, and HIV can exacerbate HIV progression into AIDS and increase the rate and replication of HIV (Roy et al. 2011; K. F. Hauser et al. 2012; P K Peterson et al. 1990; Kumar et al. 2009; El-Hage et al. 2013). Patients with HIV who abuse opiates have poorer virologic suppression compared to those HIV patients who do not abuse opiates (Celentano & Lucas 2007; Weber et al. 2009). Even when receiving cART, patients with HIV who abuse opiates experience HAND, and at a higher rate and severity than those with HIV who do not abuse opiates (Byrd et al. 2011; Meyer et al. 2013; Nath et al. 2000; Robinson-Papp et al. 2012). In multiple *in vitro* and *in vivo* models, including simian immunodeficiency virus (SIV), morphine increases viral loads as well as neuropathological progression (Bokhari et al. 2011; Kumar et al. 2006).

1.A. Human Immunodeficiency Virus

Human immunodeficiency Virus (HIV) is a lentivirus that over time causes acquired immunodeficiency syndrome (AIDS) (Cohen et al. 2008; UNAIDS 2016). AIDS is a condition where the immune system is weakened and allows for the development of opportunistic infections, such as *Pneumocystis* pneumonia and *Mycobacterium avium* complex, and cancers, such as Kaposi sarcoma (Cohen et al. 2008; UNAIDS 2016). When left untreated, patients with HIV will succumb to the disease after 9-11 years after infection (UNAIDS 2016).

HIV was first recognized in the United States in the early 1980s, particularly affecting young men who have sex with men and intravenous (IV) drug users (Wing 2016). The number of deaths due to AIDS rose throughout the 1990s, until the introduction of combined antiretroviral therapy (cART) in 1996. The incorporation of cART into clinical care quickly declined the rates of AIDS-related death by 60-80% (Moore & Chaisson 1999). Today, the tolerability of therapies has increased, and fixed dose combinations are available to ease administration. Classes of antiretroviral medications include entry inhibitors, nucleoside/nucleotide reverse transcriptase inhibitors, non-nucleoside reverse transcriptase inhibitors, integrase inhibitors, and protease inhibitors (see Appendix 1 for HIV drugs in pipeline).

Survival following HIV infection has been shown to increase significantly with effective cART, with life expectancy nearly that of the non-HIV infected population in those patients with CD4 counts over 350 cells/μL a year after starting cART (Trickey et al. 2017). In 2016, there are over 37 million people worldwide are living with HIV, and over 1.2 million living in the United States (UNAIDS 2016). While life expectancy has improved in the post-cART era, there has been an increase in co-morbidities in patients with HIV, including non-AIDS cancers, cardiovascular disease, diabetes, kidney failure, osteoporosis, and neurocognitive disorders (UNAIDS 2016).

1.B. The Blood-Brain Barrier

The blood-brain barrier (BBB) functions to maintain a unique microenvironmental homeostasis within the brain, which allows selective substances to enter, while restricting others (Abbott 2013). The BBB is made up of endothelial cells and serves as both a physical and chemical barrier to compounds from the blood to reaching the brain (Abbott & Friedman 2012) (Figure 1.1). Tight junctions form a seal between endothelial cells, which contributes to the paracellular barrier. This barrier prevents large water-soluble molecules from crossing. but allows smaller molecules, such as essential nutrients and ions, to pass (Abbott & Friedman 2012). Tight junctions between the endothelial cells reduce permeation of compounds through the paracellular pathway (between the endothelial cells) from the blood into the brain. The major molecular components of the tight junctions include the structural proteins occludin, claudins, and junctional adhesion molecule (JAM), and the peripheral zona occludin (ZO) proteins (Arcangeli et al. 2013; Bazzoni et al. 2000; Furuse et al. 1999). Both claudins and occludin are linked to cytoplasmic scaffolding and ZO proteins (Abbott et al. 2010). Adherens junctions hold the endothelial cells together and provide structural support to the BBB. Cadherin proteins in adherens junctions span between the endothelial cells and are linked by scaffolding catenin proteins into the cell cytoplasm (Abbott et al. 2010). Disruption of adherens junctions is detrimental to tight junction protein formation, leading to BBB disruption (Abbott et al. 2010). Uptake and efflux drug transporters are also present which can help facilitate molecules to cross the BBB (uptake) or serve to exclude drugs by expelling them back into the blood (efflux) (Abbott 2013). Common efflux transporters at the BBB include P-glycoprotein (P-gp), Breast Cancer Resistance Protein (BCRP), and the multidrug resistance-associated protein family (MRPs) (Abbott & Friedman 2012). The brain endothelium of the BBB is supported by other cells within the neurovascular unit (NVU), which includes the perivascular astrocytes, pericytes,

and microglial cells (Abbott 2013; Abbott et al. 2006; Garcia-Segura & McCarthy 2004; Mäe et al. 2011). These surrounding cells may mediate the induction of many BBB properties, such as upregulating the expression of tight junction proteins as well as the expression of drug transporters such as P-glycoprotein (Abbott et al. 2006).

The paracellular route of the BBB refers to the pathway between the endothelial cells, while the transcellular route of the BBB refers to the pathway through the endothelial cells. Small, hydrophilic compounds tend to permeate the paracellular route, while large, lipophilic compounds tend to traverse the transcellular route (Abbott 2013). Many antiretroviral drugs are thought to traverse the transcellular route, as opposed to the paracellular route, due to their molecular weight and polarity (Ashraf et al. 2014).

There are few studies examining the combined effect of HIV and opiate abuse on transcellular antiretroviral drug transport. This is an important area of study as HAND likely persists due to poor penetration of antiretroviral drugs across the BBB (Mcarthur et al. 2010; Weksler et al. 2013).

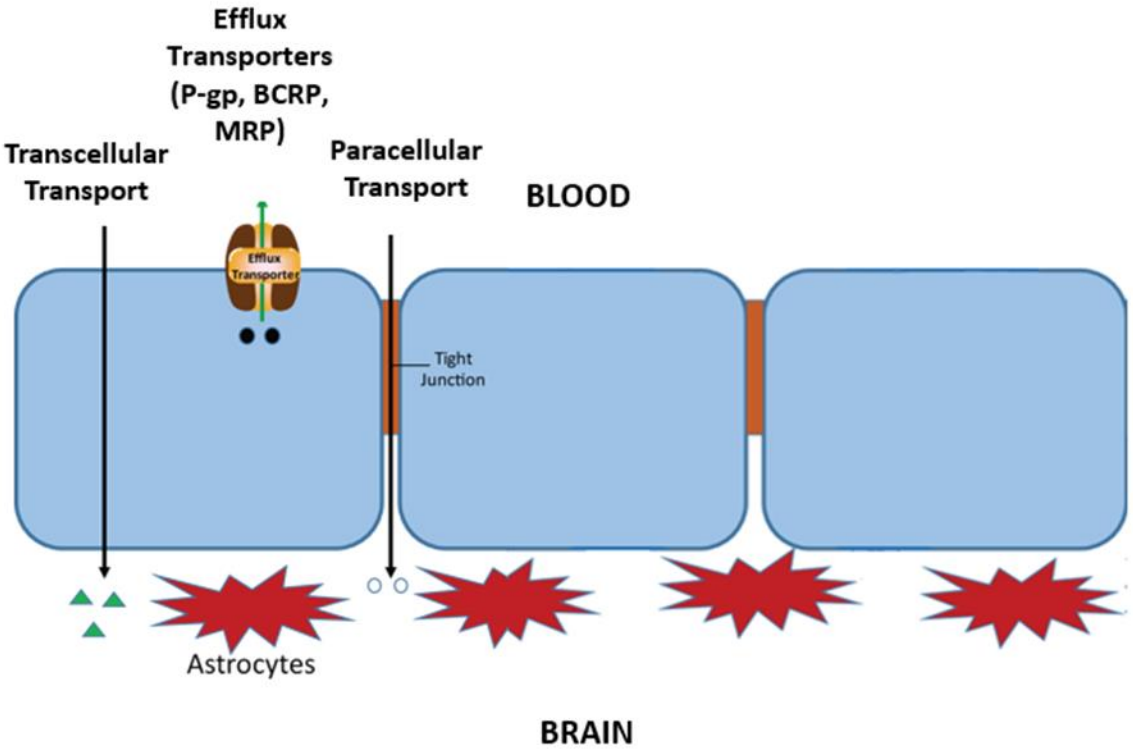

Figure 1.1 Mechanisms by which substances cross the blood-brain barrier. Lipid-soluble compounds favor diffusion across the endothelial lipid membrane via the transcellular route. The endothelium contains transport proteins including efflux transporter proteins such as P-glycoprotein (P-gp), breast cancer resistance protein (BCRP), and multidrug resistance protein (MRP). These proteins limit penetration of compounds across the blood-brain barrier by extruding these compounds back into blood. Tight junction proteins limit the penetration of water-soluble compounds via the paracellular route. Other mechanisms not explicitly shown include receptor-mediated endocytosis and transcytosis and adsorptive endocytosis.

1.C. HIV and HIV-Associated Neurocognitive Disorders (HAND)

Studies suggest that not only is the prevalence of HAND increasing, but that the life expectancy of those with HAND are shorter (Antinori et al. 2007; Heaton et al. 2011; McArthur et al. 2010; Tozzi et al. 2005). These individuals may have difficulty remembering to take their medications (Carey et al. 2006; McArthur 2004) and have difficulty maintaining employment (Alfahad & Nath 2013). Even in patients treated with combination antiretroviral therapy (cART), chronic opiate abuse aggravates CNS inflammation (Anthony et al. 2008). Opiates worsen HAND symptoms, including in the areas of recall and working memory (Byrd et al. 2011; Meyer et al. 2013). Despite advances in HIV treatment, no therapy has been found to completely treat or provide protection from HAND (McArthur 2004; McArthur et al. 2010), though there is evidence that the degree of antiretroviral penetration into the CNS influences the extent of neurocognitive improvement (Letendre et al. 2004). HIV infection can result in structural and function changes due to dendritic beading, which can be reversible with anatomy and function restored (Bellizzi et al. 2005). However, long-term exposure to neurotoxic factors due to HIV-1 infection can lead to irreversible neuronal damage (Kaul et al. 2001).

Disruption of the BBB is a primary characteristic of HAND (Dallasta et al. 1999; Eugenin et al. 2011; Eugenin et al. 2006). Low levels of HIV have been reported to infect astrocytes (Eugenin & Berman 2007; Wiley et al. 1986) and HIV-infected astrocytes have been shown to disrupt the BBB via a mechanism dependent on functional gap junction channels (Eugenin et al. 2011). HIV infection decreases the expression of tight junctions, including claudin-5, occludin, and ZO-1 (Eugenin et al. 2011; Persidsky et al. 1999; Persidsky et al. 2000). Studies have also shown that HIV increases monocyte transmigration across cultured endothelial cells (Coley et al. 2015; Eugenin et al. 2011; Persidsky et al. 1999; Persidsky et al. 2000). Perivascular macrophages and microglia are the predominately infected cell types by HIV in the

brain (Cosenza et al. 2002; Wiley et al. 1986). SIV-infected macrophages lower TEER in an endothelial monolayer (Sansing et al. 2012). *In vitro* studies have shown that HIV-1 viral protein Tat downregulates tight junction expression of claudin-1, claudin-5, and ZO-2 (András et al. 2003), as well as downregulates the expression of occludin (Mahajan et al. 2008; Wang & Ho 2011) Tat increases barrier permeability to paracellular compounds such as FITC-dextran and Evans Blue (András et al. 2005; Kanmogne et al. 2007), upregulates inflammation (Pu et al. 2003; Toborek et al. 2005), triggers monocyte trafficking into the brain (Pu et al. 2003), as well as triggers oxidative and inflammatory signaling in brain endothelium (András et al. 2005; Toborek et al. 2005).

1.D. HIV in Central Nervous System

Retroviruses, including members of the lentivirus family such as HIV, are capable of infecting the CNS (Clements & Zink 1996; González-Scarano & Martín-García 2005). HIV enters the CNS early following systemic infection (An et al. 1999). One theory proposed is that HIV enters the CNS by a "Trojan Horse" mechanism, where HIV infects monocytes which can then cross the blood-brain barrier and enter the brain (Meltzer et al. 1990; Verani et al. 2005). Other proposed mechanisms include HIV infection of CD4+ T cells which may cross the blood-brain barrier, adsorptive endocytosis across the blood-brain barrier, and by free cell entry via the paracellular route through openings in tight junction proteins of the blood-brain barrier. Secreted viral proteins, including Tat, can also across the blood-brain barrier into the brain parenchymal (González-Scarano & Martín-García 2005; Mattson et al. 2005; Eugenin et al. 2006) (Figure 1.2).

Once inside the brain, infected monocytes may differentiate into perivascular macrophages, which can then produce HIV. Perivascular macrophages are phenotypically distinct from resident brain macrophages, or microglia, which may also become infected and replicate HIV ("productive infection") (Hong & Banks 2015). Astrocytes have not been shown to produce the virus (Wiley et al. 1986; González-Scarano & Martín-García 2005). Neurons have not been shown to become infected by HIV nor are they capable of producing virus, likely since neurons lack the CD4 receptor (Hauser & Knapp 2014; González-Scarano & Martín-García 2005).

Although neurons are not directly infected by HIV, neurons are susceptible to injury from cellular and viral toxins from infected macrophages and microglia (Petito & Roberts 1995). Infected microglia can promote the production of soluble inflammatory mediators and cytokines (oxidative and inflammatory signaling), including the release of ROS, TNF-alpha, glutamate, CCL5/RANTES, IL-6, CCL2/MCP-1, and INF-γ, which can then lead to neuronal injury and death (Hong & Banks 2015; González-Scarano & Martín-García 2005; Williams & Hickey 2002). Chemokines mediate both the recruitment and activation of leukocytes by binding to cell surface receptors (Eugenin 2006). CCL2 is a chemoattractant for monocytes and CCL5 is chemotactic for T cells, eosinophils, and basophils (Eugenin 2006). INF-γ and Il-6 are pro-inflammatory cytokines which stimulate immune response. Additionally, this release of oxidative and inflammatory signaling triggers monocyte trafficking into the brain, which could allow for more HIV-infected monocytes and/or macrophages to enter the brain. This positive feedback loop can further promote irreversible neuronal injury and death (González-Scarano & Martín-García 2005; Kaul et al. 2001).

The perivascular space is a major site of bone-derived cell infiltration, including macrophages, which are continuously repopulated from the bone marrow (Fischer-Smith et al. 2001; Hickey et al. 1992). As much as 80-90% of HIV in the CNS is in perivascular macrophages (Filipowicz et al. 2016). The repopulation rate of macrophages can be accelerated during inflammation and infection (Burdo et al. 2010a; Hasegawa et al. 2009; Kim et al. 2003). Monocyte turnover has been linked to the progression into AIDS. While the depletion of CD4+ T cells is considered the primary cause for terminal progression into AIDS, it has been reported that increasing monocyte turnover was a significantly better predictor of disease progression in SIV-infected adult macaques (Hasegawa et al. 2009). Perivascular macrophage accumulation occurs during HIV infection, and is particularly seen in HIV encephalitis, which is also called HIV-associated dementia, the most severe form of HAND (Fischer-Smith et al. 2001; Kim et al. 2005; Nowlin et al. 2018). Pathological changes in the brains of patients with HIV-associated dementia correlate with an increase in activated bone-marrow-derived cells, including macrophages (Williams & Hickey 2002). Accumulation and increase in the recruitment and/or activity of phagocytic macrophages and microglia within the brain has been associated with worsening prognosis. Specifically Tat exposure has been shown in *in vitro* models to increase transmigration of peripheral monocytes across a blood-brain barrier model by increased production of CCL2 and upregulation of CCR5 on monocytes (J. Weiss et al. 1999). CCL2 is a chemokine which recruits monocytes, T cells, and dendritic cells to inflammatory sites, while CCL5 recruits leukocytes to inflammatory sites. Accumulation of inflammatory leukocytes within the brain may also occur by enhanced transmigration of human CD14+CD16+ monocytes (including infected and uninfected monocytes) into the brain. HIV infection can increase the expression of junctional adhesion molecule-A (JAM-A) and activated leukocyte cell adhesion

molecule (ALCAM) on monocytes, which can mediate this enhanced transmigration (Arcangeli et al. 2013; Williams et al. 2013).

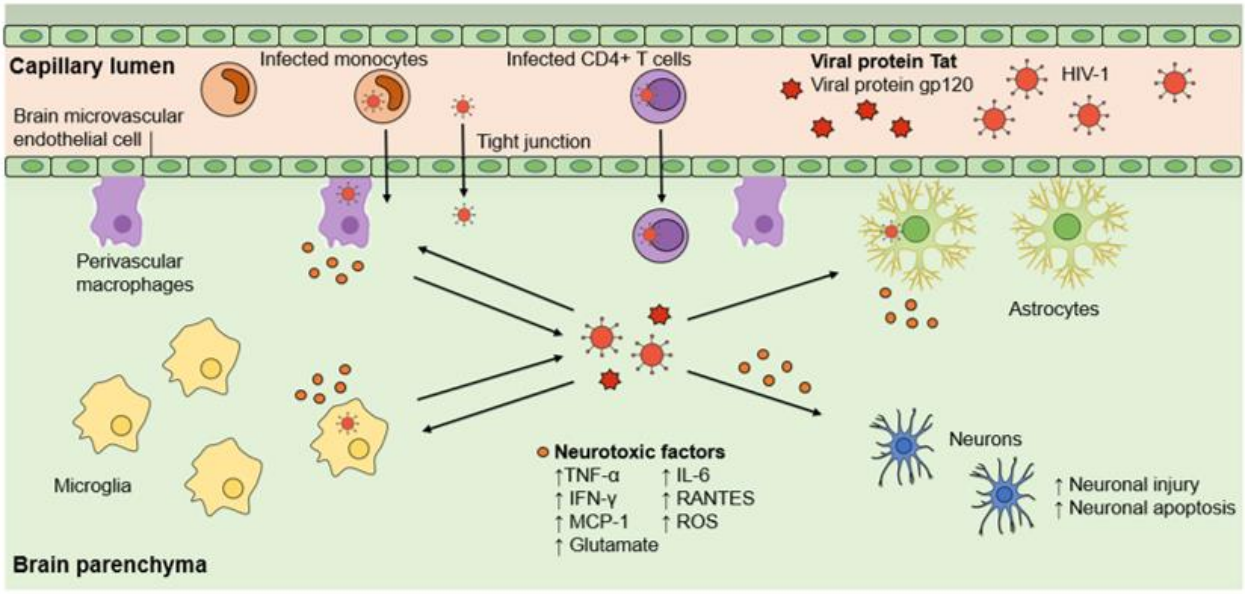

Figure 1.2. HIV Infection within the CNS. HIV infections enters the brain via a "Trojan Horse" mechanism by infecting monocytes which may cross the blood-brain barrier. Virus may also enter the brain via infected CD4+ T-cells and as free virus through the tight junctions between endothelial cell of the blood-brain barrier. Once in the brain virus can then infect microglia, which can then produce the virus. While virus can infect astrocytes, it has not been shown that astrocytes can produce virus under physiological conditions in the human CNS. While neurons are not infected by the virus, the release of neurotoxic factors, including oxidative and inflammatory signaling, by bystander cells can result in neuronal injury and neuronal death. Image adapted from Becker JT, et al. *Brain Imaging Behav* (2011) 5:77-85, González-Scarano F., et al. *Nature Reviews: Immunology* (2004) 5:69-81, Hauser KF, et al. *J Neurochem* (2007) 100:567-86.

1. E. HIV-1 Viral Protein Tat

HIV-1 viral protein Tat (transactivator of transcription) is expressed earlier in HIV-1 infection and is required for efficient HIV replication. While only certain CNS cell types can productively replicate HIV, HIV-1 Tat can be released from these infected cells to exhibit negative effects on neurons, brain microvascular endothelial cells, macrophages, macrophages, and astrocytes (González-Scarano & Martín-García 2005). HIV-1 Tat can contribute to neuronal injury and death via hyperpolarization of mitochondrial membranes and effects on synaptic signaling (Chauhan et al. 2003; Norman et al. 2007). Tat has also been shown to enhance the release of pro-inflammatory cytokines from CNS cells (Acheampong 2002, Woollard 2014) and alter molecular permeability across the BBB (András et al. 2003; Mahajan et al. 2008; Gandhi et al. 2010; Singh et al. 2004).

Our studies utilize doxycycline (DOX)-inducible HIV Tat_{1-86} transgenic mice as a model for HAND. Tat+ mice conditionally-express the HIV-1 Tat1-86 protein in a nervous system-targeted manner via a GFAP-driven Tet-on promoter (activated via consumption of chow containing doxycycline). Behavioral studies using tat transgenic mice have shown that the model recapitulates many cognitive deficits of HAND, including in spatial memory (Marks et al. 2016).

1.F. The Opioid Epidemic

Opiates refer alkaloids derived from the opium poppy plant *Papaver somniferum*, including morphine, codeine, and heroin (K. Hauser et al. 2012; Hauser & Knapp 2014). Opiates work by binding at specific opioid receptors, with those opiate drugs with abuse liability mainly acting on μ-opioid receptors (MOR) with lesser effects on δ-opioid receptors (DOR) and κ-opioid receptors (KOR) (Hutchinson et al. 2011; McCarthy et al. 2001; K. Hauser et al. 2012).

Heroin is deacetylated in the CNS into the main bioactive metabolite morphine (Wright 1940; K. Hauser et al. 2012)

The use of both prescription and non-prescription opioid medications has steadily increased in the United States since the late 1990's (Dart et al. 2015). One cause of the opioid epidemic or opioid crisis has been attributed to pharmaceutical companies in the late 1990s claiming to medical professionals that prescription opioid medications were not addictive (Morone & Weiner 2013; Van Zee 2009). Healthcare providers then began overprescribing prescription opioid medications, which led to diversion and misuse of opioid medications before their highly addictive potential was realized (Morone & Weiner 2013; Van Zee 2009). Other causes of the opioid epidemic have been the prevalence of pill mills (clinics prescribing medications for non-medical purposes) as well as the focus on treating pain with medications instead of non-pharmacologic measures like physical therapy. In 2015 the leading cause of accidental death in the United States was due to drug overdose, with 52,404 overdose deaths that year (Rudd 2016). Of the 52,404 overdose deaths in 2015, 20,101 deaths were due to prescription opioids and 12,990 deaths were due to heroin (Rudd 2016). An observed trend during the epidemic are those who begin by misusing prescription painkillers later misusing heroin. The National Surveys on Drug Use and Health revealed that over 80% of misusers of heroin report using prescription opioid pain medications prior to first initiating heroin (Jones 2013). Another survey published in *JAMA Psychiatry* in 2014 revealed that misusers of heroin prefer heroin over prescription opioids due to decreased cost, ease of access (likely due to increased illegal distribution of heroin in rural and suburban communities), and desire for greater "high" produced by heroin (Cicero et al. 2014).

HIV and opiate abuse are interlinked due to the common mode of HIV transmission via injection drug use. States such as New York have shown that needle exchange programs reduce the transmission of infections, including HIV, by people who inject drugs (PWID) (New York State Department of Health AIDS Institute. 2014). Unfortunately, needle exchange programs are not universally accepted and there are several legal and law enforcement challenges to their implementation nationwide (Beletsky et al. 2011). An example of the consequences due to the transmission interlink between PWID and HIV is the HIV outbreak that occurred in Austin, Indiana in 2015 (Conrad et al. 2015a; Peters et al. 2016a). While Austin, Indiana itself only has a population of about 5,000 people, over 150 diagnosed cases of HIV in 2015 have been attributed to syringe-sharing partners injecting oxymorphone (Opana®), an oral semi-synthetic opioid analgesic (Conrad et al. 2015b; Peters et al. 2016b). There are over 2 million PWID in both the United States and Canada, with a 15-20% prevalence of HIV in this population (Beyrer et al. 2010).

1.G. Antiretroviral Drugs and Efflux Drug Transporters

Understanding the pharmacokinetic properties of antiretroviral drugs is vital to the management of HIV infection. There are currently five classes of antiretroviral drugs: entry inhibitors, nucleoside/nucleoside reverse transcriptase inhibitors (NRTIs), non-nucleoside reverse transcriptase inhibitors (NNRTIs), integrase inhibitors (INSTIs), and protease inhibitors (PIs) (Pau & George 2014; Ashraf et al. 2014). Each of these classes act on part of the HIV life cycle. Entry inhibitors work early in the HIV life cycle, such as acting on the CCR5 receptor (maraviroc), gp41 protein (enfuvirtide), or the CD4 receptor (ibalizumab) (Pau & George 2014;

Ashraf et al. 2014). NRTIs block reverse transcriptase to prevent the conversion of HIV RNA to DNA (Pau & George 2014; Ashraf et al. 2014). Examples of NRTIs include abacavir, lamivudine, tenofovir, and emtricitabine. NNRTs work similarly but bind to a different site than NRTIs, specifically to a hydrophobic pocket near the catalytic site of reverse transcriptase (Pau & George 2014; Ashraf et al. 2014). Example of NNRTIs include efavirenz, etravirine, and rilpivirine. INSTIs block integrase, an enzyme which inserts viral DNA into host DNA (Pau & George 2014; Ashraf et al. 2014). Examples of INSTIs include dolutegravir, bictegravir, raltegravir, and elvitegravir. Protease inhibitors block protease, preventing cleavage of viral polypeptide precursors into mature enzymes and proteins (Pau & George 2014; Ashraf et al. 2014). Examples of protease inhibitors include darunavir, lopinavir, and atazanavir.

Many antiretroviral drugs are also substrates for efflux drug transporters, such as Pgp, BCPR, and MRP. Efflux drug transporters located at the blood-brain barrier can expel substrates back into the blood, which can limit the substrate from crossing into the brain. This is an importance consideration for HIV therapy since many antiretroviral drugs are substrates for efflux transporters at the blood-brain barrier, which may limit antiretroviral drug concentrations within the brain. Decreased antiretroviral drug concentrations in the brain may allow for HIV proliferation and additional inflammation to occur in the brain. The present study examines the effects of HIV-1 Tat and morphine on the accumulation three antiretroviral drugs in the brain, which are part of the single-tablet regimen Triumeq®: abacavir, lamivudine, and dolutegravir. The protein binding, metabolic, and excretion properties of these drugs, as well as that for morphine and doxycycline are included Table 1.1. All three drugs are known substrates for the efflux transporter BCRP (Table 1.2). Both dolutegravir and abacavir are known substrates for Pgp, while abacavir and lamivudine are known substrates for MRP-4 (Table 1.2).

Table 1.1. Pharmacokinetic properties of drugs used in the present studies, including antiretroviral drugs, morphine, and doxycycline. (Glare & Walsh 1991; Olsen 1974; Triumeq 2014; Epivir 1998; Tivicay 2013; Ziagen 1995; Bocedi et al. 2004; Yuen et al. 2008; Yeh et al. 1977; Chittick et al. 1999; Cottrell et al. 2013; Sun & He 2009; Dowell et al. 1999; Kucuk et al. 2009)

	Morphine	Abacavir	Lamivudine	Dolutegravir	Doxycycline
Protein Binding	• In adults is **20% to 35%** protein bound and largely to the albumin fraction.	• Binding to human plasma proteins is approximately **50%**.	• **< 36%** protein bound.	• **≥98.9%** to albumin and alpha-1 acid glycoprotein (AAG)	• **>90%**
Metabolism	• About 90% of morphine is converted into metabolites. • **Hepatic** via conjugation with glucuronic acid primarily to morphine-6-glucuronide (M6G) (10-15%) (active analgesic) and morphine-3-glucuronide (M3G) (45-55%) (inactive as analgesic; may contribute to CNS stimulation). • Morphine is a substrate of **CYP2D6** (minor), **P-glycoprotein, UGT1A1.**	• Hepatic via alcohol dehydrogenase and uridine diphosphate glucuronyltransferase (UGT) to inactive 5'carboxylic acid metabolite (~30% of dose recovered in urine) and inactive glucuronide metabolite (~36% of dose recovered in urine). • Remaining 15% of abacavir equivalents found in the urine are minor metabolites, each <2% of the total dose. • Intracellularly metabolized to carbovir triphosphate via phosphorylation by cellular kinases.	• Predominately cleared unchanged by renal excretion (70%). • Hepatic metabolism is low (5-10%). Only known metabolite is trans-sulfoxide metabolite.	• Primarily metabolized via UGT1A1 with some contribution from CYP3A. • Inhibited CYP3A4 but not 1A2, 2A6, 2B6, 2C8, 2C9, 2C19, or 2D6 in pooled human liver microsomes. • Substrate of CYP3A4 (minor), **UGT1A1**, UGT1A3, UGT1A9.	• Not metabolized hepatically, though is concentrated in bile by the liver. Partially inactivated in GI tract by chelate formation. • Excretion by the kidney is about 40% (29% to 55.4%). • No known inhibitory/transport effects.
Excretion	• Urine (primarily as M3G, adults: 2% to 12% excreted unchanged). Feces (7% to 10%) • Accumulation of M6G could lead to toxicity with renal insufficiency.	• ~83% is eliminated via urine, with 1.2% as unchanged drug, 30% as 5'-carboxylic acid metabolite, 36% as the glucuronide, and 15% as other metabolites. • Fecal elimination accounts for 16% of total dose.	• Primarily urine (majority as unchanged drug, 70%).	• Feces, 53% as unchanged drug. • Urine, 31% as metabolites, <1% as unchanged drug.	• Feces (30%); urine (23% to 40%)

Table 1.2. Relationship between efflux drug transporters and drugs present in this study.

Drug	Transporter Substrate	Transporter Upregulation
Dolutegravir	Pgp, BCRP	
Abacavir	Pgp, BCRP, MRP4	
Lamivudine	BCRP, MRP4	
Morphine	Pgp	Pgp
Doxycycline		

1.H. HIV and Opiate Interactions in the Brain and at the Blood-Brain Barrier

While the incidence of more severe cognitive symptoms including encephalitis has declined in the era of cART, HAND remains a significant problem as HIV has evolved into a chronic, long term care disease (Ellis et al. 2007; Sacktor et al. 2002). Opiate drug abuse not only increases the incidence of HIV encephalitis (Bell et al. 2006; UNAIDS 2016), it has been shown to increase the incidence of HAND (Byrd et al. 2012; Meyer et al. 2013; Robinson-Papp et al. 2012). Neurocognitive problems, such as worsening memory, have been reported in patients with HIV, and are reportedly worse in individuals who abuse drugs (Anthony et al. 2008; Bell et al. 2006; Byrd et al. 2011; Meyer et al. 2013; Nath 2015b; Robinson-Papp et al. 2012). Studies reveal that opiates have an interactive effect with HIV, such as by increasing rate of HIV replication (El-Hage et al. 2013; Peterson et al. 1990), SIV/SHIV (Simian Immunodeficiency Virus/Simian-Human Immunodeficiency Virus) replication (Bokhari et al. 2011; Chuang et al. 1993; Kumar et al. 2006; Kumar et al. 2004; Li et al. 2003; Li et al. 2002; Peterson et al. 1990) and suppressing immune function (K. Hauser et al. 2012; Roy et al. 2011).

The main metabolic pathway of morphine is by glucuronidation by UDP-glucuronosyltransferase (UGT) enzymes. UGT2B7 converts morphine into morphine-3-glucuronide (M3G), an inactive morphine metabolite, and morphine-6-glucoronide (M6G), an analgesically active metabolite with abuse liability (De Gregori et al. 2012). Human brain homogenates have been shown to metabolize morphine to M3G and M6G. Importantly, M6G can be formed directly in the CNS and penetrate across the BBB at a high rate (Yamada et al. 2003). Morphine has been shown to modulate tight junction protein expression, decrease TEER in a dose-dependent manner, increase P-gp expression, and increase the expression of pro-inflammatory cytokines (Mahajan et al. 2008). Chronic morphine exposure has been shown to alter the expression and function of cytoskeletal proteins and cytoskeleton-associated

components in rats (Marie-Claire et al. 2004). By contrast, acute co-exposure to the partial μ-MOR agonist, partial κ-opioid receptor (KOR) antagonist, buprenorphine was found to inhibit MCP1-induced monocyte chemotaxis (Carvallo, Lopez, Che, et al. 2015). Collectively, these results suggest that the effects of opiates on BBB function are complex.

Opiates depress the immune system, allowing HIV-1 to proliferate (Dronda et al. 2004; Li et al. 2005; McDonough et al. 1980; Nath et al. 2000; Peterson et al. 1990; Wybran et al. 1979). Opiates can act directly on microglia and astroglia resulting in neurodegenerative effects including neurotoxicity. Opiates have also been shown to synergistically potentiate Tat-induced increases in the release of IL-6, CCL5/RANTES, and CCL2/MCP-1 by astrocytes (El-Hage et al. 2005). Morphine also potentiates neurodegenerative effects of Tat through glia expressing the μ-opioid receptor with increased production of ROS (Zou et al. 2011). Together morphine and Tat have been shown to decrease ZO-1 and occludin gene expression, while increasing P-gp expression, JAM-2 expression, and increasing the production of pro-inflammatory cytokines TNF-α and IL-8 (Mahajan et al. 2008). Tat or morphine exposure decreases barrier tightness and increases immune cell transmigration *in vitro,* with co-exposure of Tat and morphine further exacerbating BBB permeability (Mahajan et al. 2008).

Chapter 2: Objective and Specific Aims

Objective.

Over 37 million people were living with human immunodeficiency virus (HIV) infection worldwide in 2016, and of those up to 70% may develop symptoms of HIV-associated neurocognitive disorders (HAND) (Peterson et al. 1990; Silva et al. 2014; Wybran et al. 1979). While combination antiretroviral therapy (cART) has decreased the incidence of most severe forms of neurocognitive impairment in patients with HIV, including HIV-associated dementia, milder forms of HAND still persist, including mild neurocognitive disorder and asymptomatic neurocognitive impairment. These milder defects can include decreases in memory, cognitive abilities, and motor skills (Alfahad & Nath 2013; Antinori et al. 2007). Despite advances in HIV medicine, there are currently no options to cure the neurocognitive defects caused by HAND (Ellis et al. 2007). While many factors are thought to contribute to the development of HAND, one theory is that HAND can result due to poor antiretroviral drug (ARV) penetration across the blood-brain barrier (BBB) (Spudich & Ances 2012). Complete eradication of HIV cannot be achieved when the brain serves as a reservoir for latent HIV, which can later reactivate and contribute to systemic infection (Saylor et al. 2016).

Opiate drug abuse can exacerbate HIV progression into AIDS (Kumar et al. 2006; Peterson et al. 1990) as well as increase the incidence and severity of HAND (Byrd et al. 2012; McArthur et al. 2010; Valcour 2011). Individuals abusing opiates are already at an increased risk of contracting HIV due to injection drug use, with up to one-third of patients with HIV reporting opiate abuse (Bell et al. 1998; UNAIDS 2016). Studies have revealed an interactive link between opiates and HIV effects. In multiple *in vitro* and *in vivo* models, including simian immunodeficiency virus (SIV), morphine increases viral loads as well as neuropathological progression (Bokhari et al. 2011; Kumar et al. 2006). Patients with HIV who abuse opiates have

poorer virologic suppression compared to those HIV patients who do not abuse opiates (Celentano & Lucas 2007; Weber et al. 2009). Even when receiving cART, patients with HIV who abuse opiates experience HAND, and at a higher rate and severity than those with HIV who do not abuse opiates (Byrd et al. 2011; Meyer et al. 2013; Nath et al. 2000; Robinson-Papp et al. 2012).

The objective of this dissertation is to determine if opiates in the presence of HIV-1 Tat exacerbates BBB disruption, alters ARV penetration into the brain, and increased monocyte turnover in the brain. To address these hypotheses, *in vivo* studies using the Tat transgenic mouse model will be used to study the effects of Tat and morphine exposure on BBB integrity (by measuring leakiness of the BBB), ARV penetration into the brain, and monocyte turnover. The goal of this proposal is to identify the extent to which opiates and HIV-1 exposure affects BBB structure and function.

Aim 1: Define the effects of HIV-1 viral protein Tat and morphine on BBB integrity and permeability.

Hypothesis: BBB integrity and permeability are compromised in the presence of both HIV-1 viral protein Tat and morphine. BBB integrity will be evaluated in Tat+ transgenic mice versus Tat− (control) mice ± morphine. Tracer dye mixtures (sodium fluorescein 0.376 kDa (NaFl), Cascade Blue 10 kDa, and Texas Red 70 kDa) will be injected intravenously and leakiness through the BBB into the brain will be observed.

Aim 2: Measure the effects of HIV-1 viral protein Tat and morphine on the flux of antiretroviral drug accumulation in the brain of mice.

Hypothesis: ARV accumulation in the brain is decreased in the presence of HIV-1 Tat and morphine. ARVs will be administered via subcutaneous minipump and steady-state levels of ARV accumulation in the brain will be assessed using HIV-1 Tat-1 transgenic mice exposed to morphine. P-glycoprotein protein expression will be measured via western blotting.

Aim 3: Determine the effects of the HIV-1 viral protein Tat and morphine on monocyte turnover and perivascular macrophage accumulation in the brain of mice.

Hypothesis: Monocyte turnover and perivascular macrophage accumulation in the brain is increased in the presence of HIV-1 Tat and morphine. Bilateral intracerebralventricular (i.c.v.) infusions of labeled-dextran will be administered to HIV-1 Tat-1 transgenic mice exposed to morphine. Cells will be counted via immunohistochemistry.

Chapter 3: HIV-1 Tat Disrupts Blood-Brain Barrier Integrity and Increases Phagocytic Perivascular Macrophages and Microglia in the Dorsal Striatum of Transgenic Mice

Leibrand CR, Paris JJ, Knapp PE, Kim W-K, Hauser KF, McRae MP. **HIV-1 Tat Disrupts Blood-Brain Barrier Integrity and Increases Phagocytic Perivascular Macrophages and Microglia in the Dorsal Striatum of Transgenic Mice.** *Neuroscience Letters*. February 2017; 640:136-143. PMID: 28057474

3.A. Introduction

About 37 million people globally were living with human immunodeficiency virus-1 (HIV-1) in 2016, with over 1.2 million HIV-infected individuals residing within the United States (UNAIDS 2016). Despite the use of combination antiretroviral therapy (cART), approximately half of infected individuals experience HIV-associated neurocognitive disorders (HAND) and display deficits in memory and learning, an increased prevalence of neuropsychiatric disorders, and motor impairments (Saylor et al. 2016; Antinori et al. 2007). Understanding the ability of HIV infection to disrupt the blood-brain barrier (BBB), and to alter the migration of inflammatory cells to the brain is critical to understanding the pathology of neuroAIDS.

The BBB is a major barrier against HIV-1 entry into the CNS. HIV is largely thought to enter the CNS through the trafficking of HIV-infected monocyte-derived macrophages (MDMs) (i.e., Trojan Horse model) (M. Meltzer et al. 1990; Verani et al. 2005). It is also hypothesized that some virions may enter the CNS via endothelial transcytosis or cross the BBB paracellularly, and that viral entry would be aided by breaches in BBB integrity (Mattson et al. 2005). Indeed, early post-mortem analyses of HIV-infected brains reveal an accumulation of serum proteins, consistent with barrier breakdown (Petito & Cash 1992; Power et al. 1993). Molecular alterations critical for leukocyte transmigration across the BBB are increased in the

HIV-infected CNS (Eugenin et al. 2006) and expression of the tight junction protein, claudin-5, is reduced (Chaudhuri et al. 2008). However, the mechanisms by which HIV disrupts BBB integrity are only partially understood.

One mechanism by which HIV may destabilize the BBB involves actions of the HIV-1 regulatory protein, trans-activator of transcription (Tat). Tat is an early-expressed gene product, secreted from infected cells (Ensoli et al. 1990), that induces the expression and release of cytokines, chemokines, and adhesion proteins *in vitro* and *in vivo* in mice receiving intracerebral Tat injections (Conant et al. 1998; Pu et al. 2003). *In vitro*, Tat decreases expression of the tight junction proteins, claudin-1, claudin-5, and zonula occludens-1 (ZO-1) and/or zonula occludens-2 (ZO-2) in brain microvascular endothelial cells (András et al. 2003; Mahajan et al. 2008; Pu et al. 2007). Tat-mediated effects on tight junction proteins may be dynamic given that Tat-promoted neuroinflammation may further contribute to BBB permeability, and inhibiting Tat-mediated translocation of NF-κB attenuates changes in claudin-5 (András et al. 2005). However, the extent to which these *in vitro* findings reflect changes in BBB function and integrity *in vivo* is uncertain (Bakri et al. 2001). Accordingly, the present investigation assessed BBB integrity in Tat transgenic mice.

We hypothesized that expression of HIV-1 Tat protein in a transgenic murine model would disrupt the BBB, resulting in increased barrier permeability and in the increased recruitment/activation of macrophages/microglia within the dorsal striatum. The dorsal striatum is reported to be selectively vulnerable in HIV-infected individuals (Nath 2015a) and the acute and chronic effects of Tat-induced neuropathogenesis in this region are well-characterized in our transgenic mouse model (Bruce-Keller et al. 2008; Fitting et al. 2010; Paris et al. 2016). To assess this, mice that conditionally expressed HIV-1 Tat (Tat+), or their control counterparts

(Tat−), received transcardial injections of sodium fluorescein (Na-F; 0.376 kDa), horseradish peroxidase (HRP; 44 kDa), or Texas Red®- labeled dextran (70 kDa) to determine the nature and extent of BBB leakiness. To assess phagocytic activity, mice were administered bilateral i.c.v. infusions of Alexa Fluor® 488- labeled dextran and numbers of phagocytic perivascular macrophages and microglia were examined 5 days later by quantitative fluorescence microscopy.

3.B. Experimental

3.B.1. Subjects and Housing

The use of mice in these studies was approved by the Institutional Animal Care and Use Committee at Virginia Commonwealth University and the experiments were conducted in accordance with ethical guidelines defined by the National Institutes of Health (NIH Publication No. 85-23).

Adult, female mice (approximately 70 days of age) that expressed the HIV-1 tat transgene (Tat +; N = 10), and their control counterparts that lacked the transgene (Tat−; N = 12), were generated in the vivarium at Virginia Commonwealth University. Briefly, Tat+ mice conditionally-expressed the HIV-1 Tat1-86 protein in a CNS-targeted manner via a GFAP-driven Tet-on promoter (activated via consumption of chow containing doxycycline). Tat− controls expressed only the doxycycline-responsive rtTA transcription factor as previously described (Bruce-Keller et al. 2008; Hauser et al. 2009). All mice were placed on doxycycline chow (Dox Diet #2018; 6 g/kg) obtained from Harlan Laboratories (Madison, WI) for the duration of the experiment (10 d). Mice were housed 4–5/cage and were maintained in a temperature- and humidity-controlled room on a 12:12 h light/dark cycle (lights off at 18:00 h) with ad libitum access to food and water.

3.B.2. Surgical Manipulation

All mice underwent bilateral stereotaxic infusions as modified from prior reports to target the same rostral-caudal region of the striatum as previously reported, except labeled dextran will be injected into the lateral ventricles rather than the striatum (El-Hage et al. 2006b; El-Hage et al. 2006). Briefly, mice received bilateral i.c.v. infusions (4 μL) under isoflurane (4%) anesthesia (Bregma: AP: −0.5 mm, Lat: ±1.6 mm, DV: −2 mm; (Naumenko et al. 2012a; Naumenko et al. 2013a). Following surgery, mice were monitored to ensure weight gain, muscle tone, and proper neurological response and general health (Crawley & Paylor 1997). While anesthesia, including isoflurane anesthesia, could have effects at the BBB, it is unethical to not administer anesthesia to mice during surgeries and infusions. Surgical records were maintained documenting how long each mouse was under anesthesia, including recovery time. All mice surgery and infusion times were approximately the same between each mouse.

3.B.3. Experiment 1: assessment of blood-brain barrier permeability

To assess the influence of HIV-1 Tat on BBB integrity, Tat− and Tat+ mice were transcardially infused with 50 μL of ~0.376 kDa Na-F (2%, w/v; 10 min prior to perfusion with 15 mL PBS), 10 μL ~44 kDa HRP (5 mg/mL; 5 min prior to perfusion with 15 mL PBS followed by 20 mL 4% paraformaldehyde), or 10 μL ~70 kDa dextran conjugated to Texas Red® (4 mg/mL; 10 min prior to perfusion with 15 mL PBS) per prior methods (Ben-Zvi et al. 2014; Hawkins & Egleton 2006; Ramirez et al. 2012). BBB permeability was assessed via multiple methods: HRP brain penetration was measured immunohistochemically in whole-brain sections, whereas Na-F and Texas Red®-labeled dextran were measured in brain homogenates. For HRP experiments, frozen coronal slices (40 μm; obtained 0.845–1.245 mm from Bregma) were

labeled with primary anti-HRP and visualized via appropriate secondary antibody conjugated to Alexa Fluor® 647 (Alexa 647, Thermo Fisher, Rockford, IL; far-red fluorescence). Slices were counterstained with Hoechst 33342 nuclear stain (Thermo Fisher; blue fluorescence) and imaged as described (Marks et al. 2016). HRP signal was normalized to background (signal intensity in the off-tissue area of the tiled image). HRP signal above background levels indicates BBB disruption and leakage of HRP into the brain (Ben-Zvi et al. 2014). Tiled images of HRP and Hoechst dual-labeled sections in the dorsal striatum were acquired from within a single z-plane (~0.50 μm-depth) within 5 μm from the surface of the section. HRP immunofluorescence was detected in the far-red range (Alexa 647) using diode laser excitation (637 nm) with a 640 nm long-pass filter. All images were acquired using a Zeiss LSM700 confocal microscope (Oberkochen, Germany) equipped with a 20× 1.0 NA objective. During image acquisition, the laser intensity, detector gain, and all other parameters were held constant within an identical volume of tissue across all treatment groups. Fluorescent densitometry was assessed in unaltered tagged image file (tif) format images using ImageJ software (National Institutes of Health).

For Na-F and 70 kDa dextran experiments, brains were homogenized and Na-F and fluorescein-labeled dextrans were measured via spectrophotometry (Na-F: 440/525 nm, ex/em; Texas Red®-dextrans: 575/620 nm, ex/em) using a PHERAstar FS Plus microplate reader (BMG Labtech). Na-F and 70 kDa dextran data are expressed as fold-change in fluorescent intensity/well (200 uL volume) compared to Tat− control mice (Ramirez et al. 2012).

3.B.4. Experiment 2: *in vivo* labeling of phagocytic macrophages/microglia in the CNS

To assess the effects of Tat on the number of phagocytic macrophages/microglia within the brain, Tat+ and Tat− mice received a bilateral i.c.v. infusion of ~10 kDa Alexa Fluor® 488-

dextran (Alexa 488-dextran; 4 mg/kg; Thermo Fisher; cat. # D22910) on day 5 of Tat exposure (approximately half-way through the Tat induction period). On day 10 of Tat exposure, mice were transcardially perfused with PBS followed by 4% paraformaldehyde and were prepared for immunohistochemistry as previously described (Marks et al. 2016). Coronal slices (40 μm; 0.845–1.245 mm from Bregma) were counterstained with Hoechst 33342 to detect cell nuclei. Alexa 488-dextran was infused at 5 days following induction when Tat causes significant pathology in the striatum; astrogliosis and microgliosis is evident at 48 h following Tat induction (Bruce-Keller et al. 2008), and synaptodendritic injury occurs 7–10 days following Tat induction (Fitting et al. 2010). To further demonstrate that the Alexa 488-dextran-labeled phagocytes were macrophages/microglia, anti-Iba-1 primary antibodies (Wako Pure Chemical Industries, Richmond, VA) were visualized using Alexa 647-conjugated secondary antibodies (Thermo Fisher) and co-localized with Alexa 488-dextran. Alexa 488-dextran and Iba-1 colocalization was confirmed in the same cell by 3-dimensional reconstruction of multiple zstack images using a Zeiss LSM 700 microscope (63× 1.4 NA objective) and presented as a single compressed image in the present paper. To determine the relative number of phagocytic macrophages/microglia in the caudate/putamen of Tat− and Tat+ mice, Hoechst+ cells were counted in sequential fields until a criterion of 200 cells/slice was met; the number of Alexa 488-dextran cells is reported as a proportion of the total number of Hoechst+ cells.

3.B.5. Statistical Analyses

Dependent measures for BBB permeability and phagocytic activity in perivascular macrophages/microglia were assessed by one-way analysis of variance (ANOVA) in the HRP experiment and by Student’s one-tailed t-tests for remaining experiments. Group differences in

main effects were determined using Fisher's Protected Least Significant Difference post-hoc tests determined group. No interactions were detected. Analyses were considered significant if $p < 0.05$.

3.C. Results

3.C.1. Experiment 1: HIV-1 Tat disrupts the blood-brain barrier of Tat-transgenic mice

Inducing HIV-1 Tat in transgenic mice significantly altered BBB permeability as assessed by HRP accumulation in brain [$F(3,9) = 8.20$, $p < 0.05$] (Fig, 1A–H′). Tat+ mice receiving transcardial infusions of HRP demonstrated significantly greater HRP signal in the brain compared to HRP-infused, Tat− control mice ($p = 0.008$), or the negative controls [Tat+ ($p = 0.001$) or Tat− ($p = 0.02$) mice that were not infused with HRP] (Fig. 1J). Moreover, Tat exposure compromised barrier integrity as assessed by Na-F accumulation in brain [$t(10) = 2.09$, $p < 0.05$] (Fig. 3.1I). However, the accumulation of Texas Red+ 70 kDa dextran in the brain did not significantly differ between Tat− or Tat+ mice (Fig. 3.1K), suggesting that there is an upper limit to barrier disruption induced by Tat under these experimental conditions.

3.C.2. Experiment 2: Phagocytic macrophage/microglial-activity is greater following HIV-1 Tat exposure

Alexa 488-dextran (i.c.v.) co-localized with perivascular Iba-1-labeled cells within the caudate/putamen of Tat− (Fig. 3.2A-A″) and Tat+ (Fig. 3.2B-B″) mice. Morphology and dextran accumulation were consistent with phagocytic perivascular macrophages (3.2A-2B″). Within the parenchyma of the caudate/putamen, Iba-1-labeled cells with microglial morphology co-localized with Alexa 488-dextran (Fig. 3.2C). Compared to Iba-1-labeled macrophages within the perivascular space, microglia within the parenchyma internalized notably less dextran;

however, greater amounts of dextran were observed within some microglia that were proximally closer to vascular boundaries (Fig. 3.2D). The co-localization of Alexa 488-dextran in phagocytic cells associated with the perivascular space (Fig. 3.3A–B″) and within the parenchyma was quantified. Compared to Tat− controls, HIV-1 Tat exposure significantly increased the proportion of dextran-labeled phagocytes both in the parenchyma [$F(1,20) = 9.08$, $p < 0.05$] (Fig. 3.3C) and in the perivascular space [$F(1,20) = 23.58$, $p < 0.05$] (Fig. 3.3D) of the caudate/putamen.

3.D. Discussion

Our findings support the hypothesis that Tat is a critical component mediating the known BBB disruptive effects of HIV-1. The results suggest that Tat-dependent disruptions to the BBB also contribute to the glial activation, inflammation, and neuronal injury seen in the dorsal striatum in the transgenic Tat mouse (Bruce-Keller et al. 2008; Fitting et al. 2010; Paris et al. 2016).

The leakage of Na-F and HRP tracers into the brains of mice was significantly increased in Tat+ compared with Tat− mice. These data are consistent with previous *in vitro* work demonstrating that Tat exposure increases brain vascular endothelial permeability to paracellular compounds such as Evans Blue or FITC-dextrans (Gandhi, Zainulabedin M Saiyed, et al. 2010; Pu et al. 2007). BBB disruption is not an “all-or-none” phenomenon and therefore varying the size of molecular tracers can infer the magnitude of BBB disruption (Hoffmann et al. 2011). In our studies, BBB breach occurred not only for a relatively small compound (Na-F; 0.376 kDa) but also for a compound ~100-fold larger (HRP; 44 kDa), while a 70 kDa dextran conjugate failed to cross, suggesting an intermediate level of disruption of the endothelium upon 10 d

exposure to Tat. Interestingly, HRP immunofluorescence was not uniformly distributed within the Tat+ mouse brain (Fig. 3.1G–1H′). Although differences in HRP leakage within the brain may be a specific feature of the Tat model, it may also reflect regional differences in the response of the BBB to Tat exposure. Future investigations may aim to examine these endpoints using additional models of central Tat expression, perhaps in a between-subjects design in which dextrans of varying size are assessed against the same fluorophore to eliminate any variance caused by differences in fluorescent labeling and/or the differences in the tracers themselves (e.g., NaF vs. HRP vs. dextran).

We also hypothesized that Tat exposure would increase the recruitment and/or activity of phagocytic macrophages and microglia within the brain, which was confirmed by the observed increases in Alexa 488-dextran labeled cells within the parenchyma and the perivascular space of the caudate/putamen. We observed strong co-localization of labeled dextran within perivascular macrophages (Fig. 3.2A-A″ and 3.2B-B″). Of interest, we also saw dextran-labeled Iba-1-immunoreactive microglia within the parenchyma (Fig. 3.2C). Dextran accumulation within microglia was notably reduced compared to that observed in perivascular macrophages; albeit, some microglia situated closer to the brain vasculature demonstrated increased amounts of dextran internalization (Fig. 3.2D) and dextran was not colocalized with some Iba-1+ microglia especially in the Tat− mice. Although astrogliosis and microgliosis have been observed in the Tat transgenic mouse (Bruce-Keller et al. 2008), alterations in macrophage/microglial function, as assessed by phagocytic activity, have not been previously characterized. Similar increases in microglia and perivascular macrophages are seen following intrahippocampal injections of Tat (Pu et al. 2003), though in these studies the BBB was partially disrupted by the stereotaxic injection of Tat. Additionally, others have demonstrated using *in vitro* models that Tat exposure

increases transmigration of peripheral monocytes across a BBB model via increased production of CCL2 (MCP-1) and upregulation of CCR5 on monocytes (J. M. Weiss et al. 1999). HIV infection increases expression of junctional adhesion molecule-A (JAM-A) and activated leukocyte cell adhesion molecule (ALCAM) on monocytes, both of which can mediate the enhanced transmigration of human CD14+, CD16+ monocytes (infected and uninfected) into the brain resulting in accumulation of these inflammatory leukocytes within the CNS. Despite the importance of JAM-A and ALCAM in monocyte trafficking, Tat's specific role in this process is not yet well described (Williams et al. 2015). It is also noteworthy that the rarefaction of brain capillaries and altered hemodynamics seen with chronic (6 months) Tat exposure in this Tat transgenic mouse model (Silva et al. 2014) are likely a direct result of sustained BBB disruption, macrophage activation, and inflammation that we observe after 10 d of Tat induction. Given Tat's dynamic capacity to decrease tight junction expression in brain microvascular endothelial cells (András et al. 2003; Mahajan et al. 2008; Pu et al. 2007), and to facilitate NF-κB signaling which may inhibit occludin expression (Wachtel et al. 2001), future studies are warranted that examine the importance of timing of Tat expression on BBB disruption and neuroinflammation.

Perivascular macrophages are phenotypically distinct from resident brain macrophages, the microglia, and play a central role in HIV neuropathogenesis (Kim et al. 2006; Fischer-Smith et al. 2001; Buckner et al. 2011). Perivascular macrophages can be productively infected with HIV and produce soluble inflammatory mediators and cytokines which contribute to breakdown of the BBB (Hong & Banks 2015). Additionally, the perivascular space is a major site of infiltration of blood-derived cells under normal and inflammatory conditions (Ransohoff et al. 2003; Hickey et al. 1992). They are continuously repopulated from bone marrow (Fischer-Smith et al. 2001; Hickey et al. 1992) and the rate of this repopulation can be accelerated in

inflammation and infection (Williams et al. 2001; Burdo et al. 2010b; Hasegawa et al. 2009; Kim et al. 2003). Accumulation of perivascular macrophages is a feature of HIV infection, including HIV encephalitis and HIV-associated dementia (Fischer-Smith et al. 2001; Kim et al. 2005; Nowlin et al. 2018). Our findings support the hypothesis that Tat has a critical role in mediating the increased numbers of phagocytic macrophages and microglia within the brain that are observed in HIV infection.

HIV-1-infected cells within the CNS may secrete viral proteins besides Tat (such as gp120), which activate surrounding macrophages, microglia and astrocytes to increase the release of inflammatory factors and escalate recruitment of monocytes into the CNS (Buckner et al. 2011; Williams et al. 2012; Gendelman et al. 2009; Carvallo et al. 2015; Eugenin & Berman 2003). Gp120 can affect the BBB and may act in concert with Tat to further exacerbate BBB disruption and monocyte expansion and transmigration (Zembala et al. 1997; Nakamuta et al. 2008). Exposure to gp120 *in vitro* results in the expansion of high CD16 expressing monocytes, which is similar to the expansion observed *in vivo* following HIV infection (Thieblemont et al. 1995; Pulliam et al. 1997). Unlike most other HIV proteins, Tat appears to continue to be expressed by infected cells despite the suppression of viral replication by cART (Johnson et al. 2013), and our studies demonstrate that this sustained expression of Tat could be of clinical importance to BBB alterations in virally suppressed patients. Current antiretroviral therapy does not target the early phase of HIV-1 mRNA transcription when Tat is expressed (Karn & Stoltzfus 2012).

3.E. Conclusions

The present findings demonstrate HIV-1 Tat to be a critical mediator of HIV-associated disruption of the intact BBB. Furthermore, *in vivo* Tat exposure resulted in increases in the proportion of dextran-labeled macrophages within the perivascular space and striatal tissue, which is a region of clinical significance in HAND. This Tat transgenic mouse model may be a useful tool in further examining BBB dynamics in monocyte trafficking within the context of HIV-1 Tat exposure.

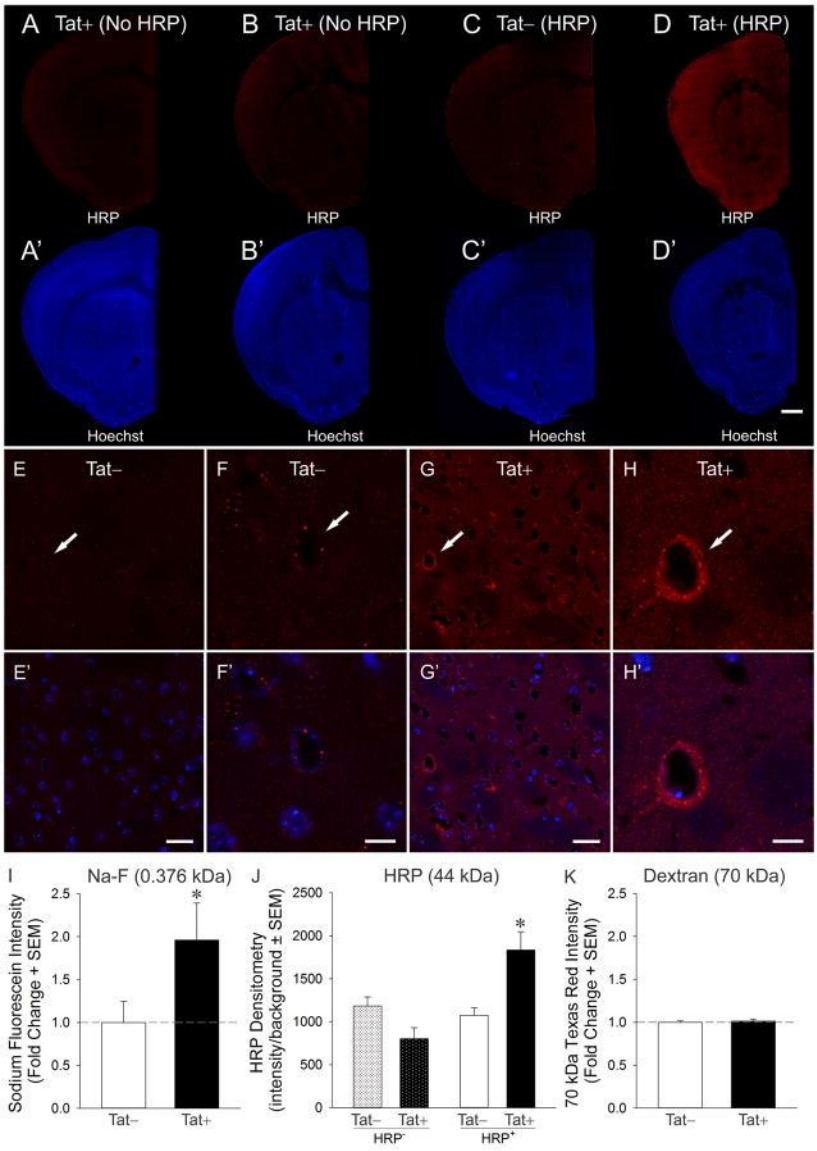

Figure 3.1. Effects of HIV-1 Tat expression on the penetration of horseradish peroxidase (HRP; red) from the vasculature into the forebrain of Tat transgenic mice (A–D; Scale bar = 1 mm). Tat expressing (Tat+) mice that were transcardially injected with HRP showed increased BBB permeability (D), while mice lacking the Tat transgene (Tat−) (C) or mice that were injected with saline instead of HRP (A–B) served as controls. The same sections as in A–D were counterstained with Hoechst 33342 (blue) to reveal the underlying cytoarchitecture (A′–D′). Higher magnification image showing a gradient of HRP penetration from some small blood vessels (capillaries and some venules, indicated by arrows) into the striatal parenchyma in Tat+ mice (G–H′) that was minimally evident in Tat− control mice (E–F′). Scale bar = 50 μm (E, E′,

G, G′) or 10 μm (F, F′, H, H′). Effects of Tat expression on mice transcardially injected with 0.376 kDa sodium fluorescein (Na-F) (I), 44 kDa HRP (J), and 70 kDa Texas Red®-labeled dextran (K). Tat expression increased the permeability of the BBB to Na-F and HRP, but not to the higher molecular weight Texas Red®-labeled dextran. * indicates $p < 0.05$ compared to all other groups.

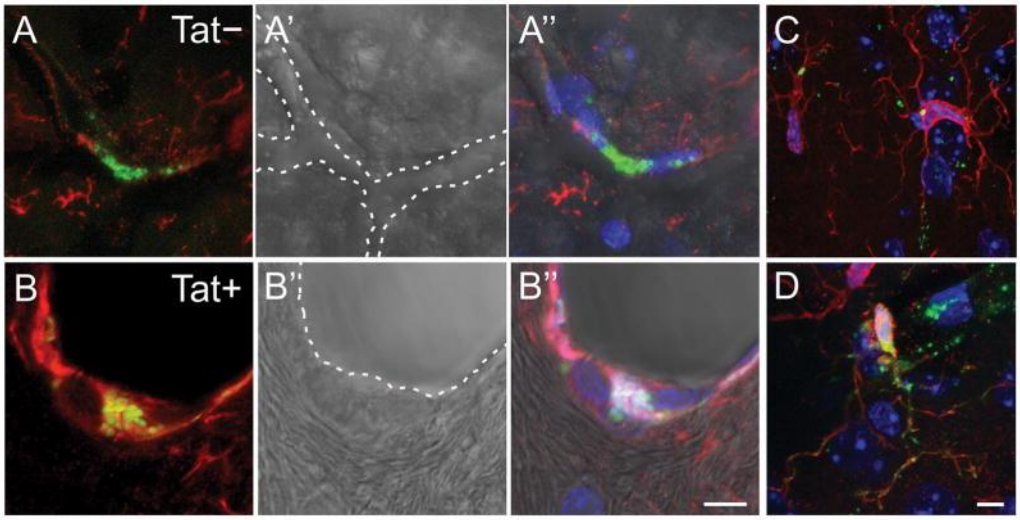

Figure 3.2. Photomicrographs of phagocytic perivascular macrophages within the caudate/putamen of Tat− (A-A″) and Tat+ (B-B″) transgenic mice (A–B). Perivascular macrophages labeled with Iba-1 (red) typically phagocytosed Alexa 488-conjugated dextran (infused i.c.v. at 5 d following continuous Tat induction; green). Dotted lines indicate the boundaries of small blood vessels. Alexa 488-dextran was also observed within Iba-1-labeled microglia residing in the caudate/putamen parenchyma of Tat− (C) and Tat+ (D) transgenic mice. Scale bar = 10 μm.

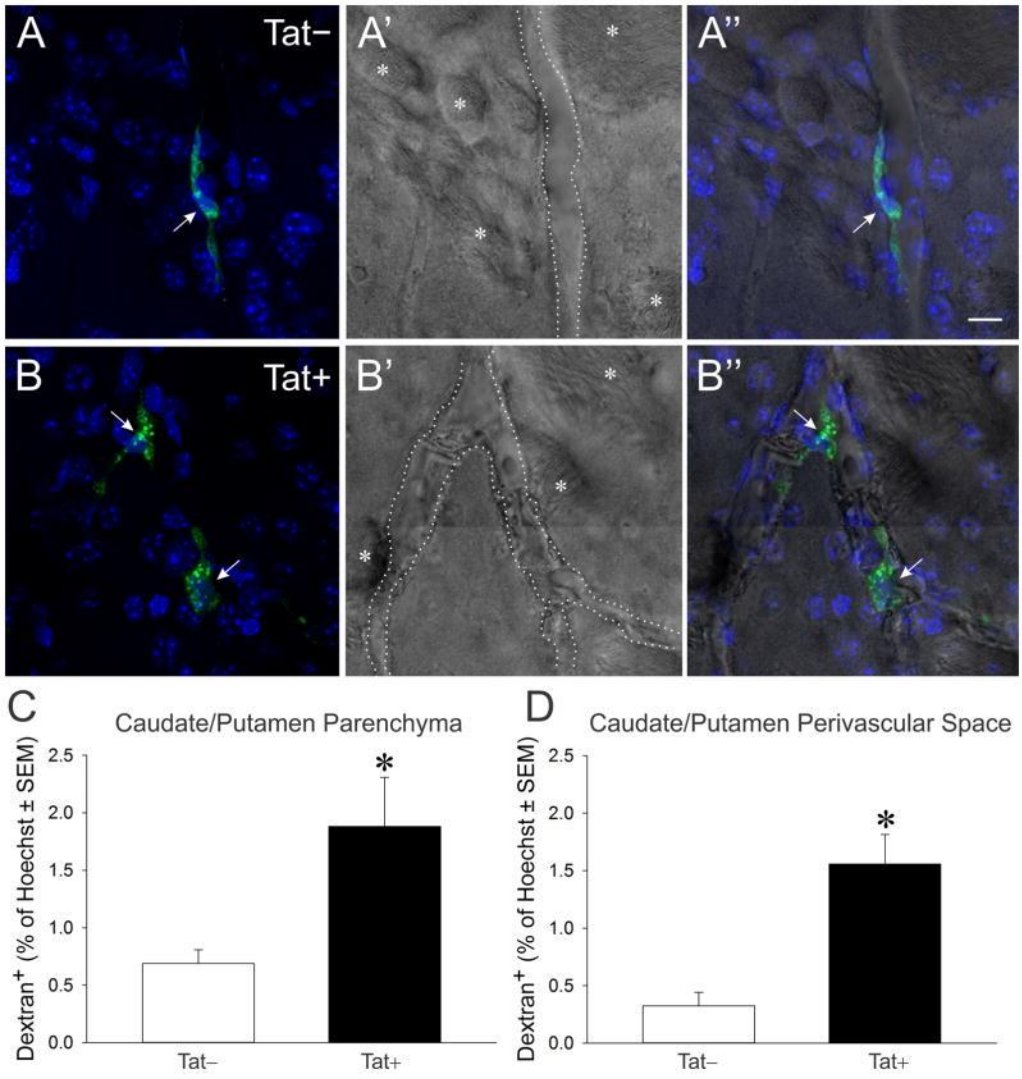

Figure 3.3. Photomicrographs of phagocytic perivascular macrophages within the caudate/putamen of Tat− (A-A) and Tat+ (B-B″) transgenic mice (A–B). Macrophages (arrows) were labeled with Alexa 488-dextran (infused i.c.v. at 5 d following continuous Tat induction; green). The dotted line indicates the boundaries of small blood vessel, while the asterisk (*) indicates white matter tracts indicative of the striatum. Scale bar = 10 μm. HIV-1 Tat exposure significantly increased the proportion of dextran-labeled phagocytes compared to Tat− control mice (C–D). Quantification of the proportion of phagocytic cells labeled with green within the parenchyma (C) or perivascular space (D). * indicates $p < 0.05$ compared to Tat− mice.

Chapter 4: Effects of Tat and/or Morphine on Monocyte Turnover in the Brain and Regional Distribution of Macrophages Using the Tat Transgenic Mouse Model

4.A. Introduction

Monocytic phagocytes are the primary cell type to host and proliferate human HIV within the CNS (Williams & Hickey 2002). Given that HIV does not infect neurons, activation of bystander cells, such as microglia, underlies many of the neuroinflammatory and subsequent toxic effects associated with central infection (Hauser et al. 2007; Becker et al. 2011). One such target of infection includes the blood-brain barrier (BBB), which typically serves to maintain homeostasis within the brain, but may be compromised following infection, prompting influx of activated monocytes into the CNS (González-Scarano & Martín-García 2005). Understanding which brain regions are most affected by the accumulation of activated monocytes, and detecting any trends in phagocytic cellular infiltration, are critical to further elucidate the neuropathogenesis of AIDS.

It has been reported that HIV-1 Tat and morphine can trigger CNS inflammation, thus recruiting monocyte-derived macrophages from the periphery into the CNS. While the progression into AIDS is typically described by the decrease in CD4+ T cells, it has been shown that increases in monocyte turnover are a better predictor of disease progression in SIV-infected adult macaques (Hasegawa et al. 2009). However, the effects of HIV-1 Tat and morphine on monocyte turnover and macrophage accumulation in the Tat transgenic mouse model are not yet known.

The purpose of this study is to examine the effects of HIV-1 Tat on regional distribution of phagocytic macrophages/microglia. We hypothesized that expression of HIV-1 Tat protein in a transgenic murine model would promote changes in regional activation of monocyte-derived

cells within the brain. In particular, we hypothesized an increase in recruitment/activation of monocyte-derived macrophages (MDMs) within the caudate/putamen, a region reported to be selectively vulnerable in patients with HIV (Nath 2015a). Several studies have examined both the acute and chronic effects of Tat-induced neuropathogenesis in the caudate/putamen regimen in the transgenic mouse model and have demonstrated that Tat exposure is associated with glial activation, neuronal injury, dendritic spine loss, and increased protein oxidation (Bruce-Keller et al. 2008; Fitting 2010; Paris et al. 2016). To assess phagocytic activity, Tat expression was induced for 10 days in transgenic mice. On day 10 of tat induction, mice were administered bilateral i.c.v. infusions of Alexa Fluor® 594- labeled dextran with sacrifice 4 hours later. The number of Alexa Fluor® 594-dextran-labeled macrophages were counted by fluorescence microscopy.

The purpose of this study is to examine the effects of HIV-1 Tat and/or morphine on monocyte turnover. We also hypothesized that HIV-1 Tat and/or morphine co-exposure would increase monocyte turnover and macrophage accumulation in the caudate/putamen of Tat transgenic mice. Worsening neurological prognosis has been associated with the accumulation and increase in recruitment/activity of phagocytic macrophages and microglia within the brain (Fischer-Smith et al. 2001). Monocyte turnover has been associated with SIV progression (Hasegawa et al. 2009) and SIV encephalitis (Burdo et al. 2010a). To examine changes in monocyte trafficking into the CNS, mice that conditionally expressed HIV-1 Tat (Tat+), or their control counterparts (Tat−), received i.c.v. infusions of multi-color labeled-dextran at different time intervals of Tat induction and/or morphine exposure.

4.B. Materials and Methods

4.B.1. Subjects and Housing

The use of mice in these studies was approved by the Institutional Animal Care and Use Committee at Virginia Commonwealth University and the experiments were conducted in accordance with ethical guidelines defined by the National Institutes of Health (NIH Publication No. 85-23). Adult, female mice (approximately 70 days of age) were utilized for these initial studies given their capacity for a more dynamic neuroimmune response to a range of insults compared to adult males (Hanamsagar et al. 2017; Schwarz et al. 2012) Mice were generated in the vivarium at Virginia Commonwealth University and either expressed an HIV-1 *tat* transgene (Tat+), or were control counterparts that lacked the *tat* transgene (Tat−). Tat+ mice conditionally-expressed the HIV-1 Tat_{1-86} protein in a nervous system-targeted manner via a GFAP-driven, Tet-on promoter, which is activated by consumption of chow containing doxycycline. Tat− controls expressed only the doxycycline-responsive rtTA transcription factor as previously described (Bruce-Keller et al. 2008; Hauser et al. 2009). All mice were placed on doxycycline-containing chow (Dox Diet #2018; 6 g/kg) obtained from Harlan Laboratories (Madison, WI) for the duration of Tat induction and then placed on regular feed. Mice were housed 4–5/cage and were maintained in a temperature- and humidity-controlled room on a 12:12 h light/dark cycle (lights off at 18:00 h) with *ad libitum* access to food and water.

4.B.2. Surgical Manipulation

Experiment 1: In vivo labeling assessment of regional phagocytic macrophage/microglia distribution in the CNS

All mice underwent bilateral stereotaxic dextran infusions as modified from prior reports (El-Hage et al. 2006b; El-Hage et al. 2006). Briefly, mice received bilateral i.c.v. infusions (4 μL) under isoflurane (4%) anesthesia (Bregma: AP: −0.5 mm, Lat: ±1.6 mm, DV: −2 mm;

(Naumenko et al. 2012b; Naumenko et al. 2013b). Following surgery, mice were monitored to ensure weight gain, muscle tone, and proper neurological response and general health (Crawley & Paylor 1997).

Experiment 2: Assessment of monocyte turnover via in vivo labeling of phagocytic macrophages/microglia in the caudate/putamen

Infusion guide cannulas (including internal and "dummy cap" cannulas to close the guide cannula when not in use) (PlasticsOne Inc., Roanoke, VA) were stereotaxically positioned under inhaled isoflurane anesthesia (4%) into the lateral ventricles of all mice (Bregma: AP: −0.5 mm, Lat: ±1.6 mm, DV: −2 mm) (Naumenko et al. 2012b; Naumenko et al. 2013b). The guide cannula avoids the need for repeated stereotaxic infusion of labeled dextran. Following surgery, mice were monitored to ensure weight gain, muscle tone, and proper neurological response and general health (Crawley & Paylor 1997). Guide cannula surgeries were performed two days prior to the initial dextran infusion (and three days prior to Tat induction) to allow for adequate recovery prior to labelling of phagocytes.

4.B.3. Morphine Administration

Only those mice in the monocyte turnover study received morphine treatment. On the same day as Tat induction, mice underwent osmotic minipump surgery. Briefly, mice were anesthetized with isoflurane (4% induction, 2% maintenance). A small mid-scapular entry was made through the skin and an ALZET® osmotic pump (2002 model, flow rate 0.5 µL/hr) delivering 0.77 mg morphine/day or placebo was implanted. Bupivacaine was applied to all surgical sites immediately after implantation.

4.B.4. Experiment 1: *In vivo* labeling assessment of regional phagocytic macrophage/microglia distribution in the CNS

Tat+ and Tat− mice received a bilateral i.c.v. infusion of ~10 kDa Alexa Fluor® 594-dextran (Alexa 594-dextran; 4 mg/kg; Thermo Fisher; cat. # D22910) on day 5 of Tat exposure (approximately half-way through the Tat induction period) (Fig. 4.1). On day 10 of Tat exposure, mice were transcardially perfused with PBS followed by 4% paraformaldehyde and were prepared for immunohistochemistry as previously described (Marks et al. 2016). Coronal slices (40 μm; 0.845–1.245 mm from Bregma) were counterstained with Hoechst 33342 to detect cell nuclei.

To determine the relative number of phagocytic macrophages/microglia in the caudate/putamen, nucleus accumbens, anterior cingulate cortex, primary motor cortex, somatosensory cortex, agranular insular cortex, and piriform cortex of Tat− and Tat+ mice, the number of Alexa 594-dextran cells that were Hoechst+ in the whole brain section per region were counted using a Zeiss LSM 700 microscope (20× objective). Brain regions were distinguished using Allen Mouse Brain Atlas (http://www.brain-map.org).

4.B.5. Experiment 2: Assessment of monocyte turnover via *in vivo* labeling of phagocytic macrophages/microglia in the caudate/putamen

An initial i.c.v. infusion of 10 kDa, Cascade Blue® (blue fluorescence) dextran (Thermo-Fisher, catalog number D1976) were administered one day prior to Tat induction (Fig. 4.1). One day after Tat induction, a second infusion of dextran, 10 kDa, Alexa Fluor® 488 (green fluorescence) dextran (Thermo-Fisher, catalog number D22910), were infused to visualize potential changes in macrophage populations immediately after Tat induction. After 13 d of Tat induction, a third infusion of dextran, 10 kDa, Alexa Fluor® 594 (red fluorescence) dextran

(Thermo-Fisher, catalog number D22913), were administered to visualize potential changes in macrophage populations after a longer duration of Tat induction. After 14 d of Tat induction, mice were perfused with buffered paraformaldehyde and the tissue processed for fluorescence microscopy. Frozen coronal slices (40 μm; obtained 0.845–1.245 mm from Bregma) were counterstained with Hoechst 33342 nuclear stain (Thermo Fisher; blue fluorescence). The number of labeled macrophages in each treatment group were determined morphologically at 63× objective counting Hoechst+ cells in sequential fields until a criterion of 600 cells/slice was met.

In a previous macrophage turnover study (Appendix II), Alexa Fluor® 488 –dextran (day 5 of Tat induction, "early") and Alexa Fluor® 594 –dextran (day 10 of Tat induction, "late", 4 hours prior to sacrifice) was infused into the mice bilaterally. However, we did not see a difference in the proportion of phagocytes labeled early vs. late in the duration of Tat exposure. This provides the rationale for our current macrophage turnover experiment timeline, which includes the addition of the Cascade Blue®-dextran (1 day prior to Tat induction) to label phagocytes prior to Tat induction, as well as infusing Alexa Fluor® 488 earlier during Tat induction (1 day after Tat induction vs 5 days) and Alexa Fluor® 594 later during Tat induction (13 days after tat induction vs 10 days). These adjustments may better parse monocyte trafficking in the present *in vivo* model.

4.B.6. Statistical Analyses

Dependent measures for monocyte turnover and phagocytic activity in various brain regions were assessed by one-way analysis of variance (ANOVA) using Tukey's *post-hoc* tests in the monocyte turnover experiment and by Student's one-tailed t-tests for remaining experiments. Group differences in main effects were determined using Fisher's Protected Least Significant

Difference post-hoc tests determined group. No interactions were detected. Analyses were considered significant if $p < 0.05$.

4.C. Results

4.C.1. Experiment 1: HIV-1 Tat Causes CNS Regional Differences in Phagocytosis

The number of Alexa Fluor® 594-dextran-labeled macrophages significantly decreased in Tat+ mice in cortical regions, including the somatosensory cortex [$F(1,11) = 45.009$, $p < 0.05$], agranular insular cortex [$F(1,11) = 15.471$, $p < 0.05$], and piriform cortex [$F(1,11) = 55.596$, $p < 0.05$], compared to Tat− controls (Fig. 4.2). No significant differences were observed within the nucleus accumbens, anterior cingulate cortex, or primary motor cortex. Within the caudate/putamen, an area shown vulnerable in HIV patients (Annadora J Bruce-Keller et al. 2008; Fitting, Xu, et al. 2010) and susceptible to *in vivo* Tat neurotoxicity (Bansal et al. 2000), there was a significant increase in the number of Alexa Fluor® 594-dextran-labeled macrophages [$F(1,11) = 73.205$, $p < 0.05$] in Tat+ mice compared to Tat− controls (Figure 4.2).

4.C.2. Experiment 2: Tat and Morphine Increase Monocyte Turnover in the Perivascular Space

No significant differences in the percent of Cascade Blue®-labeled cells, the baseline population prior to Tat induction and/or morphine exposure, was observed among the treatment groups in the parenchyma or perivascular space (Figure 4.3). These Cascade Blue®-labeled cells are triple-labeled (Cascade Blue®, Alexa Fluor® 488-dextran, and Alexa Fluor® 594-dextran) indicating that these cells were located in the caudate/putamen prior to Tat and/or morphine induction and remained there throughout the course of the experiment. No significant differences in the percent of triple-labeled cells (labeled Cascade Blue®, Alexa Fluor® 488-dextran, and

Alexa Fluor® 594-dextran; "stable population") was observed among the treatment groups in the parenchyma or perivascular space (Fig. 4.4).

Dual-colored cells (Alexa Fluor® 488-dextran and Alexa Fluor® 594-dextran) are the population of cells which trafficked into the caudate/putamen with 1 day after Tat induction and/or morphine exposure. There was a significant increase in the percent of dual-colored cells (Alexa Fluor® 488-dextran and Alexa Fluor® 594-dextran co-localization; "newly recruited cells") within the parenchyma in Tat+ morphine mice compared to Tat− placebo mice ($p < 0.008$). Similarly within the perivascular space, there was a significant increase in the percent of dual-colored cells Tat+ morphine, Tat− morphine, and Tat+ placebo compared to Tat− placebo ($p < 0.008$). In addition, there was a significant difference between Tat+ morphine and Tat− morphine compared to Tat+ placebo ($p < 0.008$) (Fig. 4.5). There were no single-color Alexa Fluor® 594-dextran labeled cells, or the population of cells which trafficked into the caudate/putamen beyond 1 day of Tat induction and/or morphine exposure. There were no single-color Alexa Fluor® 488-dextran detected in the present study, nor any instance where a Cascade Blue®-labeled cell was not also co-localized with Alexa Fluor® 488-dextran and Alexa Fluor® 594-dextran.

4.D. Discussion

These findings suggest that the expression of HIV-1 Tat facilitates regional activation of monocyte-derived cells in an *in vivo* murine model. These findings also support the notion of phagocytic cellular infiltration from cortical to subcortical regions, but additional studies need to be conducted to verify this infiltration. In the present chapter, we detected a significant increase in the number of 594-labeled macrophages in the caudate/putamen in Tat+ mice

compared to Tat− controls. Chapter 3 determined labeling at a 63× objective, counting Hoechst+ cells in sequential fields until a criterion of 200 cells/slice was met. The present chapter examined the entire coronal slice at 20× objective, thereby counting all labeled cells within each region. Since cells were counted at the 20× objective, perivascular and parenchymal cells count not be discerned from one another.

Additionally, monocyte turnover increased upon exposure to Tat and morphine exposure in the perivascular space of the caudate/putamen. Additional cells were counted in these studies (600 Hoechst+ cells versus 200 Hoechst+ cells) due to high variability in Cascade Blue®-labeled cells when counting only to 200 cells. Additional studies may also explore a varied timeline for measuring monocyte turnover, since Alexa Fluor® 594-dextran ("late" infiltrating cells) was always co-localized with Alexa Fluor® 488-dextran. One explanation could be that increased monocyte turnover occurs quickly following Tat and/or morphine insult, before returning to baseline turnover rate. A longer study, injecting Alexa Fluor® 594-dextran after 28 days of morphine exposure and/or Tat induction may help further elucidate Tat and morphine influence on monocyte turnover in the caudate/putamen.

4.E. Conclusions

The present findings demonstrate that Tat influences the accumulation of phagocytic macrophages/microglia in the CNS. In particular, Tat exposure increased regional distribution of phagocytic macrophages/microglia within the caudate/putamen, while decreasing distribution within the somatosensory cortex, agranular insular cortex, and piriform cortex. Furthermore, HIV-1 Tat and morphine play an important role in promoting monocyte turnover in the caudate/putamen of transgenic mice. Future studies may include the use of flow cytometry to detect changes in cell populations within the brain under Tat and/or morphine conditions.

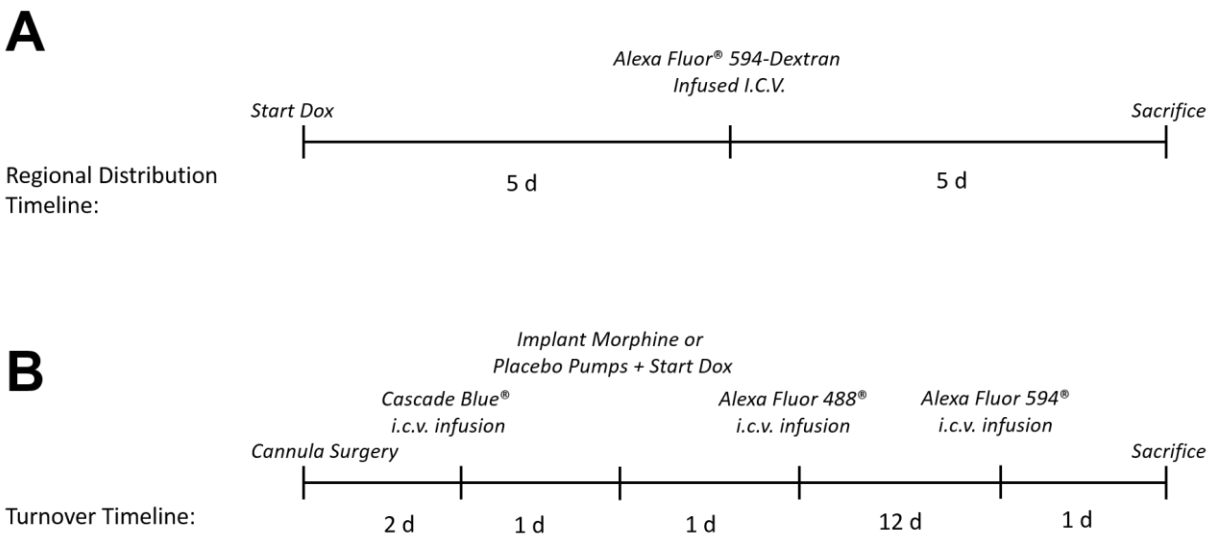

Figure 4.1. Timeline for regional distribution of phagocytic monocytes timeline (A) and monocyte turnover timeline (B).

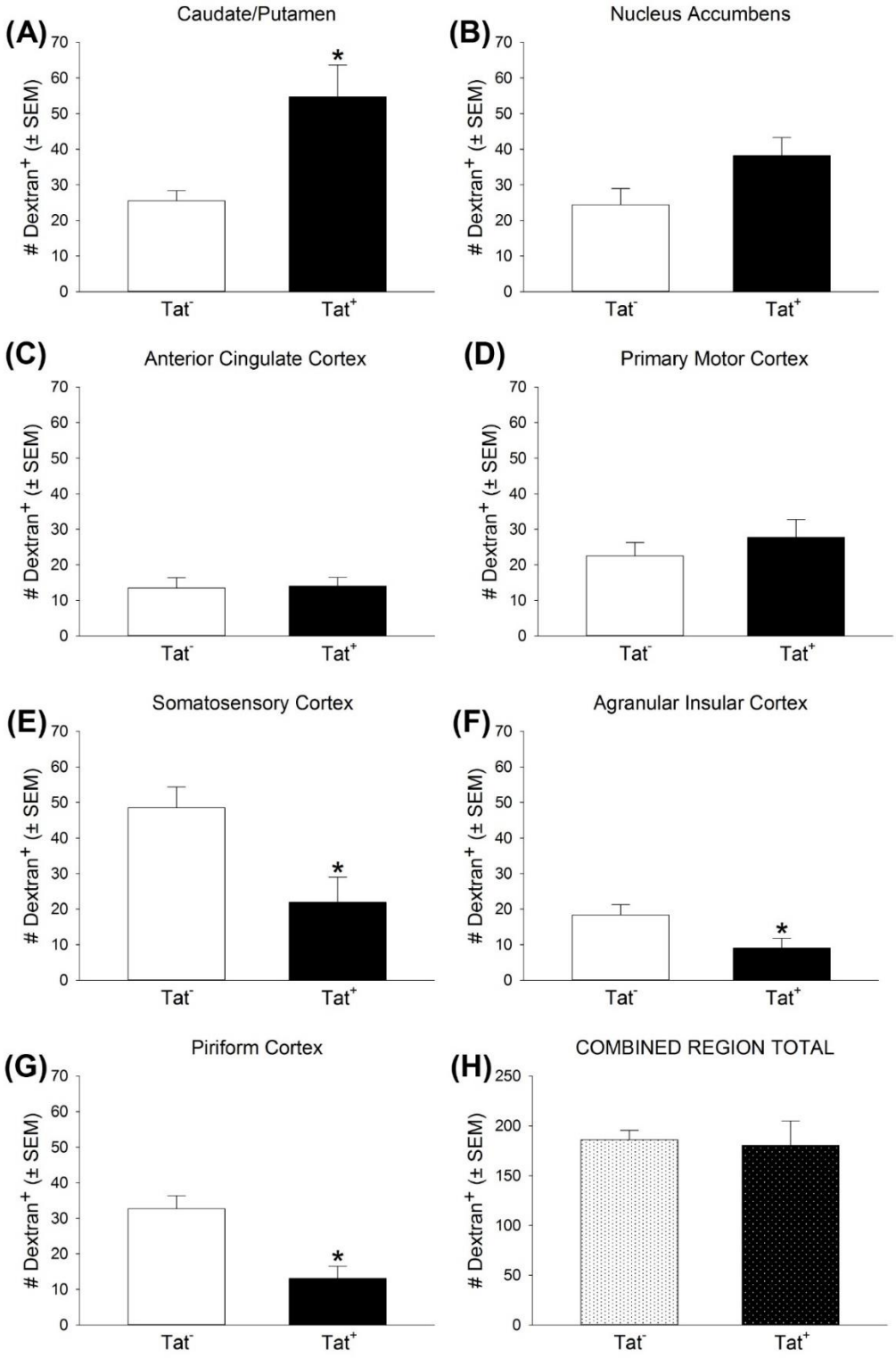

Figure 4.2. Regional differences in phagocytosis. The number of Alexa Fluor® 594-dextran-labeled macrophages significantly increased in Tat+ mice in the caudate/putamen (A), compared to Tat− controls (*$p < 0.05$). No significant differences observed within nucleus accumbens (B),

anterior cingulate cortex (C), or primary motor cortex (D). The number of Alexa Fluor® 594-dextran-labeled macrophages significantly decreased in Tat+ mice in cortical regions, including the somatosensory cortex (E), agranular insular cortex (F), and piriform cortex (G), compared to Tat− controls (*$p < 0.05$).

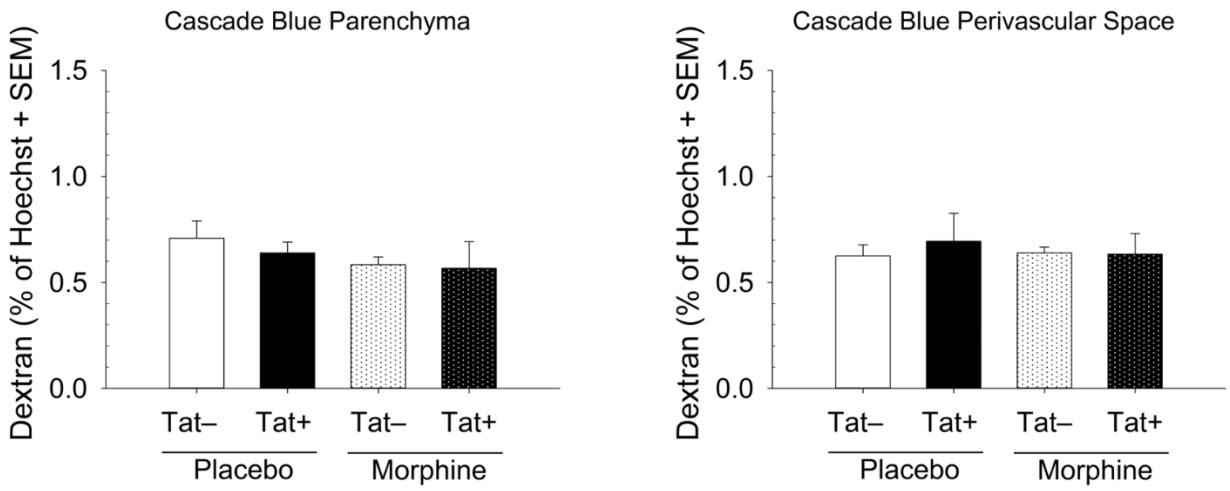

Figure 4.3 Differences in percent of Cascade Blue®-labeled cells within the parenchymal and perivascular space were not statistically significant ($p > 0.05$).

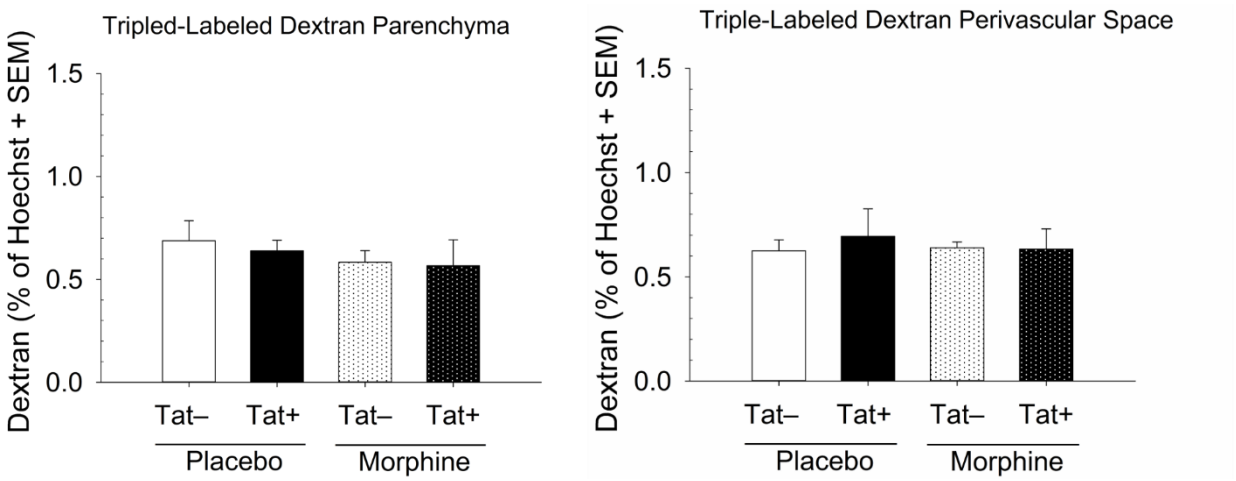

Figure 4.4. Differences in percent of triple-labeled cells within the parenchymal and perivascular space, representing the stable population present prior to Tat induction and/or morphine exposure, were not statistically significant after treatment ($p > 0.05$).

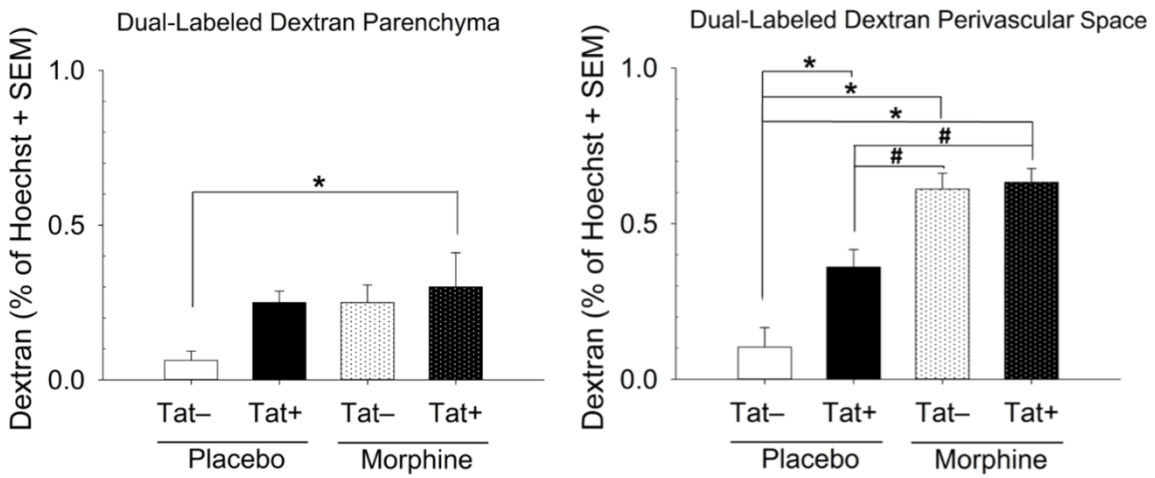

17

Figure 4.5. Dual-labeled cells within the parenchyma and the perivascular space of the caudate/putamen. There was a significant increase in the percent of dual-labeled cells within the parenchymal in Tat+ morphine mice compared to Tat− mice (*$p < 0.008$). There was a significant increase in the percent of dual-labeled cells within the perivascular space in Tat+ morphine mice, Tat− morphine mice, and Tat+ placebo mice compared to Tat− placebo mice (*$p < 0.008$), as well as a significant increase in Tat+ morphine and Tat− morphine compared to Tat+ placebo ($^{\#}p < 0.008$)

Chapter 5: HIV-1 Tat and Opioids Act Independently to Limit Antiretroviral Brain Concentrations and Reduce Blood-Brain Barrier Integrity

5.A. Introduction

Despite the aggressive use of combination antiretroviral therapy (cART), HIV infection results in neurocognitive and neurobehavioral impairment, collectively termed neuro-acquired immunodeficiency syndrome (neuroAIDS) in about half of infected individuals (Cysique & Brew 2009; Tozzi et al. 2007; Sacktor et al. 2002; Ellis et al. 2007). Although the severity has diminished in the post-cART era, HIV-associated neurocognitive disorders (HAND) persist as HIV/AIDS evolves into a chronic disease (Vivithanaporn et al. 2011; Ellis et al. 2007). Poor central nervous system (CNS) penetration of antiretroviral drugs likely contributes to HIV persistence and chronic inflammation within the brain, despite the fact that viral loads are often reduced to non-detectable levels in the peripheral circulation.

Opiate drug abuse can exacerbate the cognitive impairment and pathologic CNS changes in HIV-infected persons. HIV neuropathogenesis and cognitive deficits are exacerbated with opiate co-exposure (Hauser et al. 2007; Donahoe & Vlahov 1998), potentiating HIV replication (Peterson et al. 1990; Li et al. 2002; Peterson et al. 1993; Peterson et al. 1994; Kumar et al. 2006; Nath et al. 2002), glial activation (El-Hage et al. 2005; El-Hage et al. 2006a; El-Hage et al. 2008; Turchan-Cholewo et al. 2009; Zou et al. 2011), neurotoxicity (Gurwell et al. 2001; Fitting et al. 2010; Fitting et al. 2014) and blood-brain barrier (BBB) breakdown (Dutta & Roy 2012; Mahajan et al. 2008). Despite HIV and drug abuse being inextricably linked, morphine- and HIV-interactive effects on the actual penetration of therapeutic drugs into the brain are not well studied.

HIV-derived cellular and viral toxins are known to alter the integrity of the BBB. Exposure to HIV alters tight junction expression (Dallasta et al. 1999; Boven et al. 2000; Eugenin et al. 2011; Chaudhuri et al. 2008; Persidsky et al. 2006; Chaudhuri et al. 2008) and also increases transmigration of cells across the barrier (Saukkonen et al. 1997; Eugenin 2006; Persidsky et al. 2000; Persidsky et al. 1999; Buckner et al. 2011; Coley et al. 2015; Williams et al. 2012; Eugenin et al. 2011). The HIV proteins Tat (transactivator of transcription) and/or gp120 (glycoprotein 120) decrease tight junction protein expression (Louboutin & Strayer 2012; Kanmogne et al. 2002; Shiu et al. 2007; Nakamuta et al. 2008; Louboutin et al. 2010; Price et al. 2005; Kanmogne et al. 2007), increase transmigration of monocytes (Weiss et al. 1999; Williams et al. 2015; Wu et al. 2000; Buckner et al. 2006; Williams et al. 2013; Buckner et al. 2011), and increase barrier permeability to paracellular compounds (Xu et al. 2012; Pu et al. 2007; Zhong et al. 2008; Pu et al. 2005; Gandhi et al. 2010; Banerjee et al. 2010; Andras et al. 2003; András et al. 2005; Leibrand et al. 2017)

Morphine exposure has been reported to regulate the expression of tight junction proteins (Wen et al. 2011; Mahajan et al. 2008) and can alter transendothelial electrical resistance (TEER; a measure of barrier integrity) (Mahajan et al. 2008), although the findings of the effects of opiates on barrier permeability are inconsistent. These differences may be attributed to the use of different study models, morphine concentrations, duration of exposure, and route of morphine administration. The range of findings include claims that morphine exposure increases BBB permeability (a ‘leaky’ barrier) (Wen et al. 2011), to those asserting there is no change in permeability (Yousif et al. 2008; Strazza et al. 2016) or even decreased permeability to paracellular markers, suggesting enhanced barrier function (Sharma & Ali 2006). While the mechanisms by which opiates effect the paracellular permeability of the BBB are uncertain,

morphine has been shown to disrupt tight junctional complexes in columnar epithelium lining the small intestine (Meng et al. 2013). In the small intestine, morphine acts via a signaling pathway involving the upregulation of TLR2 and TLR4 and a myosin light chain kinase-dependent redistribution of the tight junctional proteins, ZO-1 and occludin (Meng et al. 2013). Besides having effects on paracellular transport, morphine exposure can also affect the expression of drug efflux transporters associated with transcellular transport through the endothelial cell component of the BBB (Miller et al. 2008; Yousif et al. 2008; Mahajan et al. 2008). Thus, the nature of opiate-dependent reductions or improvements in barrier function likely result from independent actions on paracellular and transcellular processes, and are likely subject to the timing and duration of exposure (Aquilante et al. 2000; Yousif et al. 2008; Miller et al. 2008; Mahajan et al. 2008).

The rate and extent to which a drug will cross the BBB and penetrate into the brain is influenced by the physicochemical properties of drugs, including lipophilicity, molecular weight, charge at physiologic pH and protein binding (Abbott et al. 2010). Additionally, depending on the transporter(s) involved, active transport systems can facilitate or hinder brain penetration of drugs. Furthermore, BBB "breakdown", which classically refers to tight junction disruption and/or flux of paracellular compounds, does not necessarily predict changes in the flux of drugs that typically traverse the BBB by transcellular (through the cells) mechanisms (Gan et al. 1993; Troutman & Thakker 2003).

The purpose of this study was to examine the effects of the HIV-1 protein Tat and morphine on antiretroviral penetration into the brain in concert with measurements of any alterations in the integrity of the BBB. We hypothesized that chronic opiate abuse would exacerbate HIV-1 Tat-mediated BBB breakdown, but also that antiretroviral penetration into the

brain would be limited by Tat and/or morphine exposure. To assess this, mice that conditionally expressed HIV-1 Tat (Tat+), or their control counterparts (Tat−) were exposed to morphine or a placebo treatment. All mice received the antiretroviral drug combination dolutegravir/abacavir/lamivudine by continuous administration via an osmotic pump. After 5 days of antiretroviral drug exposure, brain and plasma were collected for quantitation of antiretroviral drug concentrations. To determine the extent of BBB leakiness, mice were exposed to Tat, with or without morphine, and given transcardial injections of labeled dextrans with Cascade Blue® (10 kDa), fluorescein (40 kDa), and Texas Red® (70 kDa).

Understanding how opioid abuse alters the penetration of antiretroviral drugs into the brain may lead to an improved understanding of why opioid abusers have more severe neurocognitive impairment and may lead to the development of better therapeutic drug regimens for neuroAIDS.

5.B. Materials and Methods

5.B.1. Subjects and Housing

The use of mice in these studies was approved by the Institutional Animal Care and Use Committee at Virginia Commonwealth University and the experiments were conducted in accordance with ethical guidelines defined by the National Institutes of Health (NIH Publication No. 85-23). Adult, female mice (approximately 70 days of age) were utilized for these initial studies given their capacity for a more dynamic neuroimmune response to a range of insults compared to adult males (Hanamsagar et al. 2017; Schwarz et al. 2012) Mice were generated in the vivarium at Virginia Commonwealth University and either expressed an HIV-1 tat transgene (Tat+), or were control counterparts that lacked the tat transgene (Tat−). Tat+ mice conditionally-expressed the HIV-1 Tat_{1-86} protein in a nervous system-targeted manner via a

GFAP-driven, Tet-on promoter, which is activated by consumption of chow containing doxycycline. Tat− controls expressed only the doxycycline-responsive rtTA transcription factor as previously described (Bruce-Keller et al. 2008; Hauser et al. 2009). All mice were placed on doxycycline-containing chow (Dox Diet #2018; 6 g/kg) obtained from Harlan Laboratories (Madison, WI) for the duration of Tat induction and then placed on regular feed. Mice were housed 4–5/cage and were maintained in a temperature- and humidity-controlled room on a 12:12 h light/dark cycle (lights off at 18:00 h) with *ad libitum* access to food and water.

5.B.2. Antiretroviral Drug Administration

Triumeq® (ViiV Healthcare) is a combination tablet containing abacavir (600 mg), dolutegravir (50 mg) and lamivudine (300 mg), and was purchased from the VCU Health Systems Pharmacy. The dosing for mice was calculated via allometric scaling (Nair & Jacob 2016), based on an average 20 g mouse and was as follows: abacavir 2.5 mg/day (123.5 mg/kg/day), dolutegravir 0.2 mg/day (10.3 mg/kg/day) and lamivudine 1.2 mg/day (61.7 mg/kg/day). In brief, tablets were crushed to a fine power and resuspended in normal saline. After centrifugation at 1000 rpm for 5 min to pellet tablet excipients, the supernatant was sterile filtered twice (0.45 µm followed by 0.22 µm filter). Following filtration, 220 µL was loaded into the ALZET® osmotic pump (Model 2001, 1 µl/h delivery). For morphine groups, morphine salt pentahydrate powder was diluted directly into the antiretroviral solution prior to loading into the pump at a concentration sufficient to deliver 2.5 mg/day. Drug preparations were made in batches to minimize dosing variability. Each pump was weighed before and after loading, with consistent weights among all pumps.

5.B.3. Morphine Administration

For dextran exclusion studies, morphine or placebo administration was achieved by subcutaneous implantation of 25 mg morphine or placebo time-release pelleted implants (National Institute on Drug Abuse, Rockville, MD) under aseptic conditions and 4% isoflurane anesthesia. The use of time-release morphine pelleted implants or tablets is a standard method to continuously administer morphine during a period of 5 to 7 d. The 25 mg pelleted implants produce morphine drug levels in the brain sufficient to cause tolerance (Chefer & Shippenberg 2009) and physical dependence (Bogulavsky et al. 2009) within 3 d in C57BL/6 mice and that are comparable to plasma/tissue levels achieved in humans who are opiate-dependent (Ghazi-Khansari et al. 2006).

Briefly, mice were anesthetized with isoflurane (4% induction, 2% maintenance). A small mid-scapular entry was made through the skin and either a time-release 25-mg morphine or placebo pellet (dextran exclusion studies) or an ALZET® osmotic pump delivering 2.5 mg morphine/day or placebo (antiretroviral and morphine accumulation studies) was implanted. Bupivacaine was applied to all surgical sites immediately post-op. Sample sizes range from 6-9 mice/group for dextran exclusion studies and antiretroviral accumulation studies.

5.B.4. Assessment of Blood-Brain Barrier Permeability

To assess the influence of HIV-1 Tat and morphine on BBB integrity, Tat+ and Tat− mice received Tat induction for 14 days followed by a 5-day washout period. At the conclusion of the 5-day washout period, Tat+ and Tat− mice were subcutaneously implanted with either morphine or placebo pellets. Five days after pellet implantation, mice were transcardially infused with 10 mL of dextran solution in PBS containing 10 kDa dextrans conjugated to Cascade Blue® (0.1 mg/mL), 40 kDa dextrans conjugated to fluorescein (0.1 mg/mL), and 70 kDa dextrans

conjugated to Texas Red® (0.1 mg/mL) over 5 minutes. Brains were homogenized in a 10× volume of 50% trichloroacetic acid, centrifuged at 5,000 x *g* at 4°C for 10 min, and then the supernatant was neutralized with 5 M NaOH (1:8 ratio) per prior methods (Ramirez et al. 2012; Leibrand et al. 2017). Cascade Blue, fluorescein, and Texas Red-labeled dextrans were measured via spectrophotometry (Cascade Blue®-dextrans: 380/460 nm, ex/em; fluorescein-dextrans: 485/520 nm, ex/em; and Texas Red®-dextrans: 575/620 nm, ex/em) using a PHERAStar FS Plus microplate reader (BMG Labtech) on a glass-bottom multi-well cell culture plate. Dextran data are expressed as fold-change in fluorescent intensity/well (500 µL volume) compared to Tat− placebo pellet control mice (Hawkins & Egleton 2006; Leibrand et al. 2017).

5.B.5. Antiretroviral Accumulation in Dorsal Striatum and Hippocampus

To assess the effects of HIV-1 Tat and morphine on antiretroviral accumulation in the dorsal striatum and hippocampus, Tat+ and Tat− mice received Tat induction for 14 d followed by a 5 d period in which doxycycline is not administered to clear the antibiotic from the system. Prior (Ngwainmbi et al. 2014) and unpublished studies indicate that Tat mRNA expression remains elevated (including that detected in striatum and hippocampus) for at least 3 weeks after withholding doxycycline. On day 5 of the doxycycline washout period, Tat+ and Tat− mice were subcutaneously implanted with an ALZET® osmotic pump containing antiretroviral drug combination dolutegravir/abacavir/lamivudine (Triumeq®) with or without morphine. Mice were continuously exposed to dolutegravir, abacavir, and lamivudine ± morphine for 5 d to allow drugs to reach steady state (corresponding to day 10 of experiment). After 5 d drug exposure, the mice were anesthetized under isoflurane and transcardially perfused with PBS (Fig. 5.1). The dorsal striatum and hippocampus were isolated, weighed, and snap-frozen for analysis.

LC-MS/MS methods were used to quantify dolutegravir, abacavir and lamivudine in mouse plasma and tissues. Frozen tissues were weighed, then homogenized in Precellys® hard tissue grinding kit tubes (Cayman Chemical, MI, USA) with cold 70:30 acetonitrile:1 mM ammonium phosphate buffer (pH 7.4). Analytes were extracted from plasma and tissue homogenates following protein precipitation with the following stable isotopically labeled internal standards: abacavir-d_4, lamivudine-^{15}N-d_2 and dolutegravir-^{13}C-d_5. Chromatographic separation of analytes and internal standards from matrix components was achieved using reverse-phase chromatography on a Waters Atlantis T3 (50 x 2.1 mm, 3 μm) column for abacavir and lamivudine or a Waters XTERRA MS C18 (50 x 2.1 mm, 3.5 μm) column for dolutegravir. Analytes were detected on an AB Sciex API-5000 triple quadrupole mass spectrometer using electrospray ionization in the positive ion mode for abacavir and lamivudine or atmospheric pressure chemical ionization (APCI) in the positive ion mode for dolutegravir. The calibrated ranges for abacavir, lamivudine and dolutegravir were 1-200 ng/mL, 0.125-50 ng/mL and 0.025-50 ng/mL of tissue homogenate, respectively. The calibrated range for abacavir, lamivudine and dolutegravir in plasma was 1-10000 ng/mL, 1-4000 ng/mL, and 50-10000 ng/mL, respectively. Precision and accuracy was ± 20% (25% at the lower limit of quantification; LLOQ). All antiretroviral data are expressed as a brain tissue-to-plasma ratio to normalize for systemic exposure.

5.B.6. Morphine and Morphine Metabolite Accumulation in Dorsal Striatum and Hippocampus

In the same mice in which antiretroviral concentrations were quantified, the contralateral brain regions were used for quantification of morphine concentrations. LC-MS/MS methods were used to quantify morphine and its glucuronidated metabolites, morphine-3-β-glucuronide

(M3G) and 6-β-glucuronide (M6G). Frozen samples are weighed and thawed at ambient temperature. A 0.50 mL aliquot of water was added to each tissue or plasma sample. Each sample underwent homogenization with a micro-tissue tearor for 30 sec. Following centrifugation, the sample supernatant was loaded onto pre-conditioned solid phase extraction cartridges (Waters HLB, Waters Corporation, Milford, MS). Samples were washed with 5% methanol, and then eluted into a 96-well plate with 95% methanol (twice). Eluent was then dried under a nitrogen stream at 55°C. Samples were then reconstituted with 0.1 mL of mobile phase prior to a 20 µL injection undergoing liquid chromatography tandem mass spectrometry (LC-MS/MS). Morphine and its glucuronide metabolites were separated using hydrophilic interaction chromatography (HILIC) with a Polaris Silica 2.0 x 30 mm, 5 µm (Agilent, Santa Clara, CA, USA) HPLC column under gradient conditions. Each analyte and stable isotopic internal standard employed the following selected reaction monitoring transitions: 286.0 > 165.0 (morphine), 462.0 > 286.0 (M3G), 462.0 > 286.0 (M6G), 289.0 > 165.00 (morphine-d3), 465.0 > 289.0 (M3G-d3), and 465.0 > 289.0 (M6G-d3). M3G and M6G are chromatographically separated (resolution >2.0), which is used for quantitative analysis. The linear range of all three analytes was 0.50–50 ng/mL, 1-100 ng/mL, and 10-1000 ng/mL for morphine, morphine-3-β-glucuronide, and morphine-6-β-glucuronide, respectively. Precision and accuracy acceptance criteria were ± 15% (20% at the lower limit of quantification; LLOQ).

5.B.7. Western Blotting

Protein expression within striatum, hippocampus, and liver (as positive control) were analyzed by immunoblotting using standard techniques. Brain tissue samples were homogenized in lysis buffer containing protease inhibitor (Roche, Indianapolis, IN). Homogenized lysates were incubated at 4 °C for 30 minutes with end-over-end mixing. Liver samples were also

subjected to lysis buffer containing protease inhibitor (Roche, Indianapolis, IN) but using a Precellys 24 homogenizer (Bertin Technologies, Aix en Provence, France) at 3 rounds of 10 s of bead-beating at 6,000 rpm at 4 °C with ceramic beads (1.4 mm diameter, Mobio Laboratories, Carlsbad, CA). Cell debris from both brain and liver tissue samples was removed by centrifugation at 12,000 rpm for 15 min at 4 °C. Supernatants were transferred to new tubes stored at −80 °C until ready for use. Protein concentrations were quantified using the BCA protein assay (Pierce, Rockford, IL). Thirty micrograms of cell lysate was loaded on a 12% Mini-Protean TGX gel (Bio-Rad, Hercules, CA) for all proteins except for Tat− transgenic mouse liver positive control, for which 10 micrograms was used. Following electrophoresis and transfer to polyvinylidene difluoride (PVDF), the membrane was blocked in 5% non-fat milk solution and incubated overnight with appropriate primary antibody. Antibodies used include mouse anti-actin (1:4,000; Sigma-Aldrich; catalog number A1978) and mouse anti-P-glycoprotein (C219; 1 µg/ml dilution; Calbiochem, Billerica, MA; catalog number 517310). Blots were then incubated at RT for 1 h with horseradish peroxidase-conjugated anti-mouse [1:20,000] secondary antibody. Signals were enhanced using chemiluminescence using the SuperSignal West Femto system (Thermo Fisher Scientific) and detected by exposure to the ChemiDoc system (Bio-Rad). The chemiluminescence signal intensity was quantified using ImageLab software (Bio-Rad). All protein expression data is expressed as relative density, which was calculated by the ratio of the absolute density of P-glycoprotein to that of β-actin absolute density.

5.B.8. Statistical Analyses

Dependent measures for BBB permeability and antiretroviral drug accumulation were assessed by two-way analyses of variance (ANOVA). Fisher's Protected Least Significant

Difference *post-hoc* tests determined group differences following main effects. Interactions were determined via simple main effects and main effect contrasts with error controlled for multiple comparisons. Morphine content was assessed via Student's two-tailed *t*-tests. All analyses were considered significant when $p < 0.05$.

5.C. Results

5.C.1. HIV-1 Tat and Morphine Independently Disrupt the Blood-Brain Barrier of Mice

Following 14 d of Tat induction, accumulation of the smallest tracer, 10 kDa labeled dextran, was significantly increased among Tat+ mice compared to their Tat− counterparts ($p = 0.02$). Moreover, morphine exposure significantly increased 10 kDa dextran accumulation among Tat− mice, compared to those that received placebo pellets ($p = 0.047$) (Fig. 5.1). There was no additive effect of Tat and morphine co-exposure on dextran leakage into the brain.

With the larger tracers, significant main effects for morphine were observed. Morphine exposure significantly increased brain accumulation of the 40 kDa-labeled fluorescein-conjugated dextran [$F(1,26) = 6.187$, $p = 0.02$), as well as the 70 kDa-labeled Texas Red®-conjugated dextran [$F(1,26) = 5.696$, $p = 0.02$], irrespective of Tat exposure (Fig. 5.1).

5.C.2. Morphine Alters Antiretroviral Drug Penetration into the Brain

Morphine exposure significantly influenced antiretroviral accumulation in the brain. The greatest influence was observed for morphine to significantly decrease the tissue-to-plasma ratio of dolutegravir within the striatum [$F(1,28) = 17.43$, $p = 0.0004$] and the hippocampus [$F(1,28) = 13.80$, $p = 0.0009$], irrespective of Tat exposure. Morphine exposure also significantly decreased the tissue-to-plasma ratio of abacavir in the striatum (but not hippocampus),

irrespective of Tat exposure [$F(1,28) = 8.87$, $p = 0.007$]. No effects were observed on the tissue-to-plasma ratio of lamivudine (Fig. 5.2).

When comparing raw concentrations (not normalized for systemic exposure) of antiretroviral accumulation in the brain, morphine exposure was observed to significantly decrease abacavir content in striatum [$F(1,28) = 6.37$, $p = 0.02$], irrespective of Tat exposure (Table 5.1). No other significant differences in raw antiretroviral content were observed in striatum, hippocampus, or plasma (Table 5.1).

5.C.3. Morphine LC/MS Results

The effects of Tat exposure on the both tissue-to-plasma ratios and raw concentrations of morphine and its M3G metabolite in plasma, striatum, and hippocampus were investigated. Tat+ mice was a strong trend towards significantly increased morphine concentrations in plasma ($p = 0.059$) as compared to their Tat− counterparts (Fig. 5.3). In contrast, there was a significant decrease in the tissue-to-plasma morphine ratio within the hippocampus in Tat+ ($p = 0.0499$) compared to Tat− mice. No significant changes in morphine concentrations were noted in the striatum. Raw concentrations of M3G content within the plasma, hippocampus and striatum between Tat+ and Tat− mice were also compared. In the hippocampus, Tat exposure resulted in significantly increased M3G concentrations in the hippocampus [$F(1,13) = 10.43$, $p = 0.0066$), but no significant changes in M3G concentrations were observed in the plasma or striatum (Table 4.1).

Additionally, M3G metabolite levels in the hippocampus positively correlated with dolutegravir levels in hippocampus ($r^2 = 0.31$, $p = 0.0310$) and morphine levels in the plasma negatively correlated with dolutegravir levels in striatum (r^2 0.31) = 0.32, $p = 0.0344$).

5.C.4. P-glycoprotein Displays Similar Baseline levels of Expression in the Striatum and Hippocampus, but Increases in Response to Morphine Exposure

There were no significant differences in baseline P-gp expression levels between striatum and hippocampus in either Tat− placebo mice ($p = 0.9727$) or in Tat+ placebo mice ($p = 0.3460$) at baseline (Fig. 5.4). However, exposure to morphine, irrespective of Tat status, resulted in significant increases in P-gp expression in both striatum [$F(1,12) = 4.752$, $p = 0.0499$) and hippocampus [$F(1,12) = 4.810$, $p = 0.0487$) compared with the non-morphine exposed groups. (Fig. 5.4).

5.D. Discussion

The data from these studies support three main findings. The experimental results demonstrate that 1) morphine, and to a lesser extent Tat, exposure in mice can result in damage to the blood brain barrier, 2) morphine exposure results in decreased penetration of select antiretroviral drugs within the brain, and 3) Tat exposure results in altered distribution of morphine; with lower concentrations of morphine within the hippocampus of Tat+ mice.

5.D.1. Tat Increased BBB Leakiness for 10 kDa Compound

Our findings suggest that while Tat and morphine can independently disrupt the integrity of the BBB, morphine exposure results in greater damage to the BBB than Tat. We have previously demonstrated that following Tat induction, there is a size limited leakage of tracers into the brain; with 0.4 kDa and 44 kDa tracers freely leaking into the brain, while the entry of a larger 70 kDa tracer was unaffected by Tat (Leibrand et al., 2017). These findings are recapitulated within the current study, with the exception that the intermediate sized tracer did not display significant extravasation into the brain parenchyma in Tat exposed mice. There are a

few potential reasons for the discrepancy. The time course was slightly different between the two studies. In the previous study, BBB leakiness was measured at the end of day 10 of doxycycline; with no doxycycline-free period prior to sacrifice. In the present experiments, mice were fed doxycycline (to cause Tat induction) for 14 d, followed by a doxycycline-free period of a total of 10 d; in which there was a 5 d washout period prior to starting ARV ± morphine. The washout period was designed to minimize any potential pharmacokinetic drug-drug interactions between doxycycline and the antiretroviral drugs ± morphine cocktail. The specific pharmacokinetic, metabolic and excretion profiles of each drug suggested limited potential for drug-doxycycline interactions; however, any unexpected interactions would potentially have confounded our results. Tat mRNA expression remains elevated in the striatum even after doxycycline has been removed for 4 weeks (Knapp and Xu, unpublished); therefore, it was expected that Tat levels would remain elevated over the entire study. However, it is possible that Tat protein levels waned in the time frame of our studies, allowing for some repair or recovery of barrier properties/integrity. Another potential explanation is related to the difference in the physical properties between dextran solutions and HRP. Dextrans are polydisperse and therefore any one dextran solution, even when characterized as a particular kDa size, will actually have a broad distribution of sizes. This variability in size range could affect our ability to make a direct size comparison between dextrans and other tracers, such as HRP, used in previous studies (Venturoli & Rippe 2005). Regardless, the findings within this study demonstrate that morphine exposure resulted in greater breakdown of the BBB than that of Tat. Morphine-exposed mice, regardless of Tat status, had significant leakage of even the largest tracer (70 kDa).

5.D.2. Morphine Exposure Increased BBB Leakiness but Decreased ARV Brain Concentrations

Furthermore, morphine exposure resulted in decreased ARV brain concentrations, despite increased BBB leakiness. Initially, it might seem paradoxical that morphine exposure *increases* the penetration of the dextran tracers, while *decreasing* the penetration of dolutegravir and abacavir without affecting the accumulation of lamivudine within the brain. It must be recognized that tracer leakage is a measure paracellular flux of molecules or compounds. An increase in the flux of compounds that traverse the BBB paracellularly, or between the endothelial cells of the BBB, does not necessarily predict changes in flux of drugs that cross via transcellular mechanisms. For example, alterations in barrier integrity by manipulating tight junctions increases the influx of ranitidine, a polar paracellular compound (Gan et al. 1993). However, these same tight junction changes have no impact on the overall flux of two different substances known to traverse the BBB by transcellular mechanisms, ondansetron and testosterone (Gan et al. 1993; Troutman & Thakker 2003). The antiretroviral drugs used in this study traverse the membrane via transcellular mechanisms. The ability of drugs to cross lipid bilayers, such as the endothelial cells of the BBB, is influenced by the physicochemical properties (such as lipophilicity, size, and protein binding), as well as by active uptake transport processes. Abacavir, which is moderately lipophilic and not highly protein bound, would be expected to have some passive permeability. Lamivudine is a lower molecular weight than abacavir. Although lamivudine also binds proteins minimally, it is less lipophilic than abacavir, which may hamper its passive penetration across the BBB (Reis et al. 2013). Alternatively, the entry of abacavir and lamivudine into cells is also known to be partially mediated by the uptake transporters organic cation transporters (OCT), OCT1, OCT2, and OCT3 (Minuesa et al. 2009; Casado et al. 2014; Yuen et al. 2008; Reis et al. 2013). Dolutegravir, a lipophilic drug, can

permeate cells through passive permeability (Reese et al. 2013), but the net penetration of dolutegravir into the brain may be limited by its extensive protein binding (99%) (Reese et al. 2013). Additionally, net flux across the BBB is also influenced by active efflux transporters, such as P-glycoprotein (P-gp), where the efflux transporter itself can be a major determinant of CNS penetration (Edwards et al. 2002; Polli et al. 1999). Dolutegravir and abacavir, but not lamivudine, are substrates for P-gp (Shaik et al. 2007; Reese et al. 2013). Herein, we demonstrate increased protein expression of P-gp within the brain (striatum and hippocampus) in the morphine exposed mice (Fig. 5.5), which could account for the net decrease tissue-to-plasma ratio of each of these drugs within the brain. The finding that P-gp expression is increased in response to morphine is consistent with several other studies. Acute morphine increases P-gp mRNA (Yousif et al. 2008; Mahajan et al. 2008). Chronic morphine exposure increases protein expression of P-gp within the brain and decreases antinociceptive responses in rats (Bauer et al. 2004; Aquilante et al. 2000). In contrast, others have demonstrated no change in P-gp activity with chronic morphine treated rats (Yousif et al. 2008). Other drug transporters, such as BCRP, are also involved in the efflux of the antiretrovirals we studied, although because P-gp is the only efflux transporter in common between dolutegravir and abacavir, a role of BCRPs in mediating the observed changes in dolutegravir and abacavir concentrations in the present study is less likely (Kis et al. 2010; Giri et al. 2008; Reese et al. 2013). The implications for these findings could be potentially widespread. If morphine exposure results in the net decrease of brain concentrations of P-gp substrates, this could potentially have a negative impact on the treatment of HIV by other antiretroviral drugs within the brain, or may even impact the efficacy of other CNS active drugs that are P-gp substrates.

5.D.3. No Regional Differences in ARV Penetration

HIV is known to preferentially affect certain regions within the brain. Maximal viral loads can be found in the basal ganglia, as well as the medial temporal lobes, hippocampus and frontal lobes (Nath 2015a). The striatum and hippocampus were examined within this study because they preferentially show high viral loads in HIV-infected individuals (Nath 2015a), express high levels of μ-opioid receptors (Mansour et al. 1995; Arvidsson et al. 1995), and display substantial pathology in the HIV-1 Tat transgenic mouse (Marks et al. 2016; Schier et al. 2017; Fitting et al. 2010). Brain regional differences in response to HIV or HIV viral proteins have been demonstrated previously, including regional differences in cytokine release and regional and cell specific dysregulation of opioid receptors (Fitting et al. 2010; Fitting et al. 2010; Stiene-Martin et al. 1998). Within this study, the observed differences in abacavir concentrations between striatum (decreased) and hippocampus (no change) suggested regional differences in penetration of each drug. However, upon analysis, there were no significant regional differences in dolutegravir, abacavir or lamivudine raw concentrations between striatum and hippocampus within this study. Therefore, caution must be used not to over-interpret the abacavir results.

5.D.4. Tat Altered Morphine Distribution with Brain and Plasma

Another important finding was that Tat exposure resulted in altered morphine distribution within the plasma and brain as compared to Tat− mice. Decreased penetration of morphine within the hippocampus of Tat+ mice was not reflected, nor could have been predicted by plasma concentrations within these animals, which strongly trended towards an increase in morphine concentration. Furthermore, although the parent concentrations decreased, M3G concentrations within the hippocampus significantly increased. P-gp expression was increased within the

hippocampus and could have mediated the efflux of morphine, resulting in the observed decrease in morphine concentration within the hippocampus. While the mechanism(s) underlying increased M3G in hippocampus are not known, M3G is not thought to be a substrate for P-gp (Xie et al. 2000) and therefore alterations in P-gp would not have been expected to result in changes in the concentration of M3G systemically or in different brain regions

Within this study, total, not unbound, antiretroviral concentrations were measured; therefore, we do not have a precise estimate of free drug within the brain. However, the focus of the present study was to assess the directionality of effects of Tat and morphine exposure on drug concentrations. Because ARV concentrations were measured at steady state, and because we have no evidence to suggest that either Tat or morphine would cause ARV displacement from its protein binding sites, the impact on ARV tissue concentrations would be expected to be proportional between total and unbound concentrations.

5.E. Conclusions

The present findings demonstrate that HIV-1 Tat and morphine are critical mediators of BBB disruption and that Tat exposure can alter the distribution of morphine within the mouse brain, resulting in decreased morphine concentrations within the hippocampus. Furthermore, decreases in concentrations of dolutegravir and abacavir, along with increased expression of the efflux transporter P-gp, were observed within the striatum and hippocampus. Additional studies need to be conducted to verify the role of P-gp in mediating the observed changes in concentrations of cART and/or morphine and its metabolites. Furthermore, to more fully understand the functional impact of altered brain concentrations, future studies may include an infectious HIV model in order to assess the impact of morphine administration on antiviral efficacy.

Table 5.1. Raw concentrations within plasma, striatum and hippocampus. These data are expressed as concentration (not the tissue-to-plasma ratios); *$p < 0.05$; significant difference between morphine or M3G groups. †$p < 0.05$; significant main effect of morphine. Values are the mean ± SEM.

	Plasma Drug concentration (ng/mL)			
	Placebo		Morphine	
Drug	Tat–	Tat+	Tat−	Tat+
Dolutegravir	433.2 ± 80.9	485.7 ± 60.9	634.5 ± 63.0	537.7 ± 26.2
Abacavir	1790.6 ± 607.0	1519.6 ± 184.4	1326.7 ± 84.8	1311.1 ± 62
Lamivudine	829.7 ± 320.9	500.6 ± 66.8	471.3 ± 60.2	507.8 ± 33.2
Morphine			232.1 ± 44.5	555.5 ± 122.7
M3G			2297.6 ± 369.3	2714.6 ± 279.0

	Striatum Drug concentration (ng/mg)				**Hippocampus** Drug concentration (ng/mg)			
	Placebo		Morphine		Placebo		Morphine	
Drug	Tat−	Tat+	Tat−	Tat+	Tat−	Tat+	Tat−	Tat+
Dolutegravir	4.6 ± 1.1	5.3 ± 1.4	3.4 ± 1.0	2.4 ± 0.6	4.8 ± 1.1	5.8 ± 1.1	3.7 ± 0.4	3.7 ± 0.4
Abacavir	134.4 ± 26.1	165.8 ± 24.6	**99.9 ± 10.6†**	**93.2 ± 5.9†**	129.2 ± 26.4	163.1 ± 25.7	110.1 ± 11.5	100.2 ± 6.0
Lamivudine	25.9 ± 3.5	26.7 ± 4.9	21.5 ± 4.0	19.4 ± 1.6	27.3 ± 3.4	26.3 ± 4.5	20.8 ± 1.8	26.0 ± 3.0
Morphine			259.0 ± 107.6	322.7 ± 94.2			143.9 ± 31.1	113.2 ± 20.1
M3G			3.0 ± 1.6	11.6 ± 7.5			**6.6 ± 3.4***	**33.7 ± 6.4***

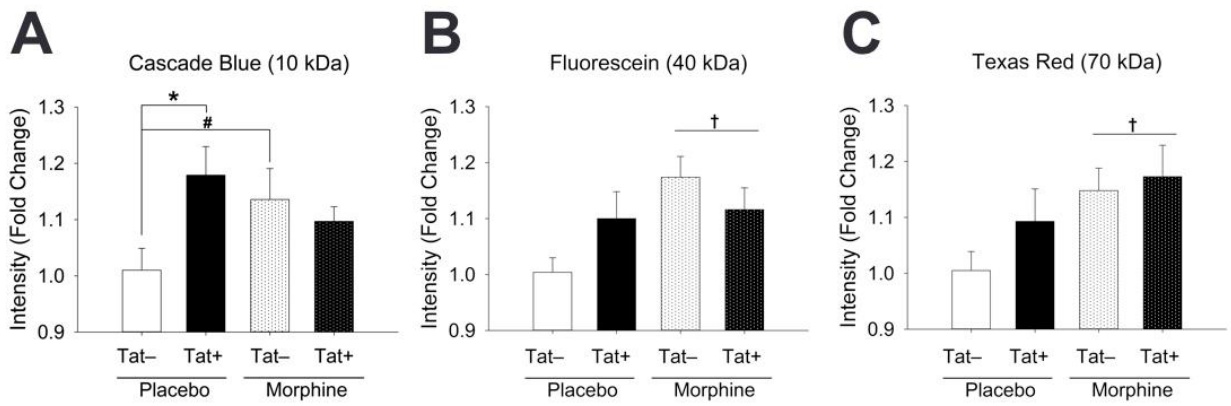

Figure 5.1. Effects of HIV-1 Tat and morphine on BBB leakiness after 14-day Tat induction. A) Tat exposure significantly increased 10 kDa (Cascade Blue®) tracer leakage in placebo-treated mice (*$p < 0.05$) and morphine increased 10 kDa (Cascade Blue®) tracer leakage in Tat− mice ($^{\#}p < 0.05$). B, C) Additionally, there was a significant main effect of morphine to reduce the integrity of the BBB to higher molecular weight (40 kDa and 70 kDa) tracers ($^{\dagger}p < 0.05$; significant main effect of morphine). Data represent the fold-change in mean fluorescence intensity ± the SEM sampled from $n = 8$ Tat−/placebo, $n = 6$ Tat+/placebo, $n = 9$ Tat−/morphine, and $n = 7$ Tat+/morphine mice.

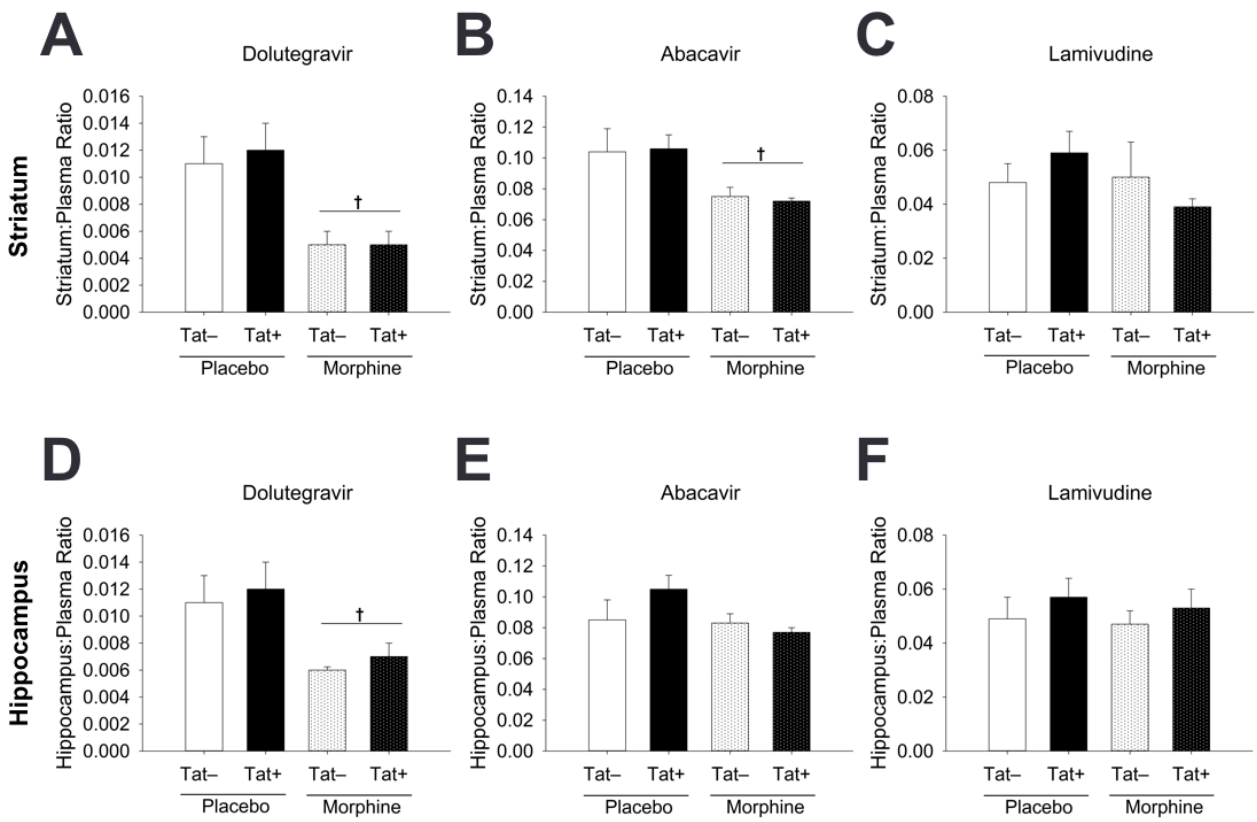

Figure 5.2. Antiretroviral tissue-to-plasma ratios in striatum and hippocampus. Morphine significantly reduced the levels of dolutegravir (A, D) and abacavir (B, E), but not lamivudine (C, F), depending on the brain region ($^{\dagger}p < 0.05$; main effect). Data represent the tissue-to-plasma ratios ± the SEM sampled from $n = 9$ Tat−/placebo, $n = 9$ Tat+/placebo, $n = 6$ Tat−/morphine, and $n = 8$ Tat+/morphine mice.

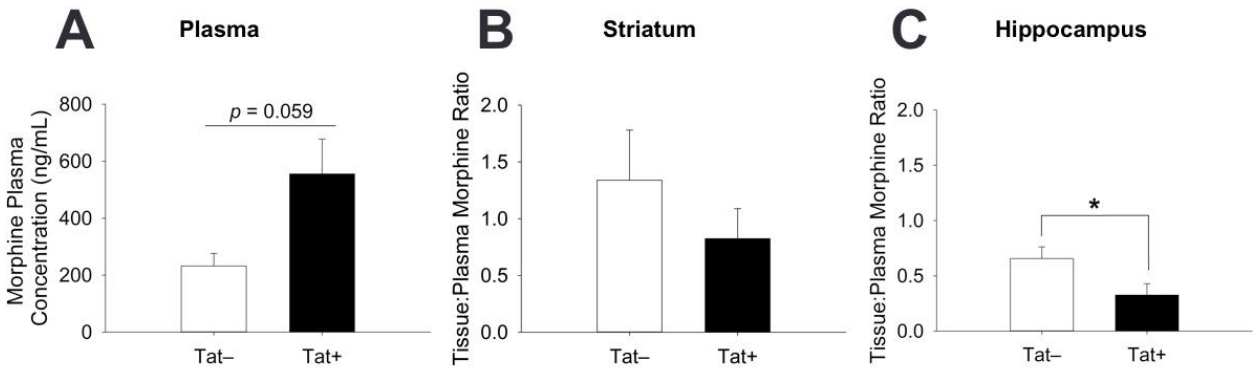

Figure 5.3. Morphine plasma concentrations and tissue-to-plasma ratios in striatum and hippocampus. Morphine levels were assessed by LC-MS/MS in both plasma and brain tissue. Morphine plasma levels showed a strong trend towards an increase in concentration with Tat exposure (A). Tat exposure decreased the morphine tissue-to-plasma ratio in the hippocampus (C) but not in the striatum (B) (*$p < 0.05$). Data represent the tissue-to-plasma ratios ± the SEM sampled from $n = 6$ Tat−, $n = 9$ Tat+ mice.

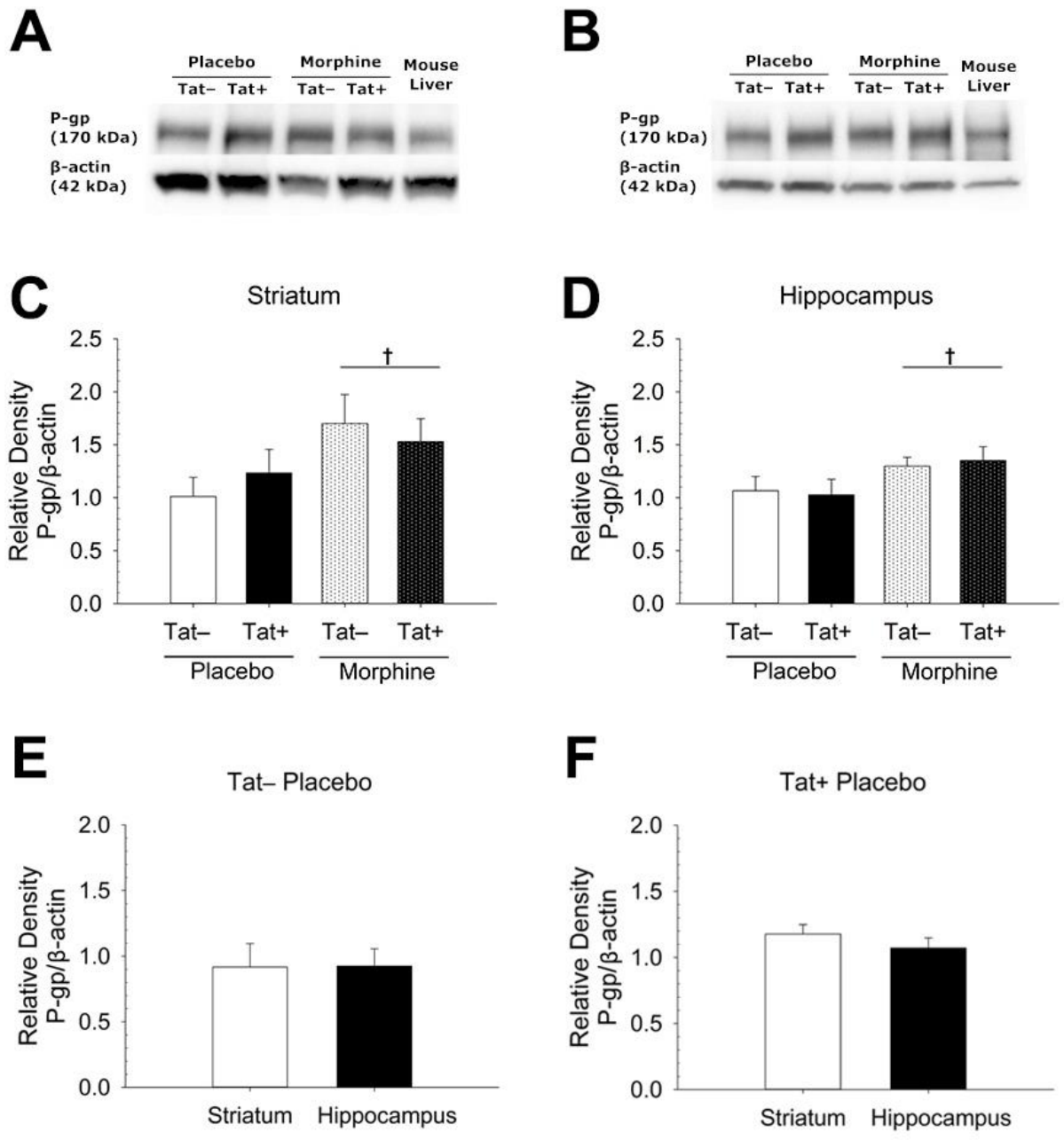

Figure 5.4. Western blots of P-gp levels in the striatum (A, C) and hippocampus (B, D) of Tat− or Tat+ mice ± morphine co-exposure. Western blots of P-glycoprotein (P-gp) levels in the striatum and hippocampus of Tat− placebo mice (E) and Tat+ placebo mice (F) at baseline. Data represent the relative density of P-gp (absolute density of P-gp over the absolute density of β-actin) ± the SEM. Exposure to morphine treatment, irrespective of Tat status, significantly increased P-gp expression in both striatum (A, C) (†$p < 0.05$) and hippocampus (B, D) (†$p < 0.05$) compared with those groups unexposed to morphine. Differences in regional P-gp

expression between striatum and hippocampus were not statistically significant in Tat− placebo mice or in Tat+ placebo mice at baseline (E, F); $n = 4$ for all groups.

Chapter 6: Overall Conclusions and Future Directions

In Chapter 3, we concluded that HIV-1 Tat plays an important role in the HIV-associated disruption of the BBB. Tat exposure results in increased proportion of dextran-labeled macrophages within the perivascular space and parenchymal tissue of the caudate/putamen, which is a region of clinical significance in HAND. In Chapter 4, acute morphine experiment and (to a lesser extent) Tat induction alter MDM turnover suggest that leukocyte trafficking also altered. In Chapter 5, we explored the role of morphine and HIV-1 Tat on BBB disruption, concluding that both morphine and HIV-1 Tat are critical mediators of BBB disruption. Tat exposure can influence morphine distribution within the brain, resulting decreased morphine concentrations within the hippocampus. We found that morphine decreased the concentrations of dolutegravir and abacavir, along with increased the expression of the efflux transporter P-gp, within the striatum and hippocampus.

Future directions include studies examining the effects of P-gp function as well as changes in cell populations in the brain under Tat and/or morphine exposure. Since Chapter 5 revealed morphine effects on P-gp expression and ARV penetration into the striatum and hippocampus, P-gp function studies will focus on morphine effects without regard to Tat exposure. To further complement studies in Chapter 3 assessing phagocytic macrophage/microglia accumulation in the CNS, as well as in Chapter 4 assessing monocyte turnover under Tat and/or morphine exposure, flow cytometry studies will be performed to determine how cell populations (microglia, monocytes/macrophages, neutrophils) change in response to Tat and/or morphine.

Pgp Function Study

The purpose of this study is to determine how morphine affects P-gp function, using quinidine as a P-gp substrate and PSC833 as a P-gp inhibitor. Morphine (1.5 mg/day) or placebo will be delivered for 5 days in Tat transgenic mice without Tat induction. After 5 days mice will be administered PSC833 (10 mg/kg orally via gavage) or saline 60 minutes prior to quinidine or saline (40 mg/kg, I.P.). Sixty minutes after quinidine or saline administration, mice are sacrificed, plasma and brains harvested (striatum and hippocampus), weighted and frozen until analysis. Quinidine concentrations will be measured via LC-MS/MS.

Flow Cytometry Study

The purpose of this study is to determine how HIV-1 Tat and morphine may influence changes in cell populations within the brain. Populations to study include neutrophils, classical (previously inflammatory) monocytes, and non-classical (previously resident or patrolling) monocytes. Antibodies to identify these populations used include CD11b, CD45, Ly6C, and Ly6G. The experiment timeline would match that from the monocyte turnover study (Chapter 4), which includes 14 days of Tat induction and morphine exposure.

Appendix I.

Mononuclear Phagocytic Activity.

Tat effects on the number of phagocytic macrophages/microglia within the brain were assessed with the following procedure. Tat^+ (n = 6) and Tat^- (n = 6) mice received two sets of bilateral i.c.v. infusions of ~10 kDa fluorophore-conjugated dextrans separated by five days. On separate days after Tat-induction, Alexa Fluor® 488 –dextran (day 5) and Alexa Fluor® 594 – dextran (day 10) (4 mg/kg; Thermo Fisher; cat.# D22910 and D22913, respectively) was infused into the mice bilaterally. On day 10, 4 h after dextran infusion, mice were transcardially-perfused with 4% paraformaldehyde and were prepared for immunohistochemistry as previously described (Marks et al., 2016). Coronal slices (40 µm; 0.845 – 1.245mm from Bregma) were counterstained with Hoechst 33342 to detect nuclei. Dextran infusates are taken up by phagocytic cells within the CNS, labeling activated mononuclear cells. As such, greater proportions of 488- or 594-labeled cells indicate longer (488- and 594- dual labeled cells), or shorter residing (594- single labeled cells) cells which phagocytosed the label. Cells with only the 594-single label were actively phagocytosing only at the later stages (10d); which could indicate late activation or that these cells recently migrated into the CNS (after 5d) and can be suggestive of turnover of these MDMs.

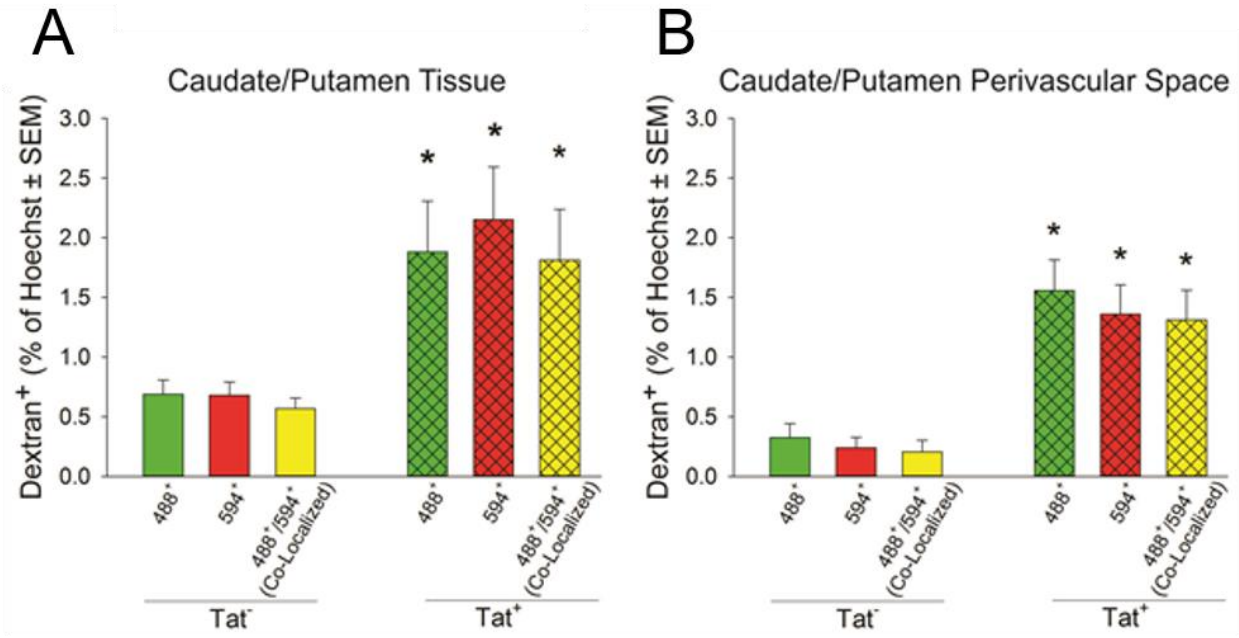

Figure A.1. No significant differences were observed between early-labeled phagocytes after 5 days of Tat exposure (488+), vs. late-labeled phagocytes after 10 days of Tat exposure (594+). However, there existed a notable trend for late-labeled (594+) cells to present in greater proportion than dual- (488+/594+) labeled cells [$F(2,20) = 3.24$, $p = 0.06$, n.s.] within the caudate/putamen tissue (Figure. 2C).

References

Abbott, N.J., 2013. Blood–brain barrier structure and function and the challenges for CNS drug delivery. *Journal of Inherited Metabolic Disease*, 36(3), pp.437–449. Available at: http://link.springer.com/10.1007/s10545-013-9608-0.

Abbott, N.J. et al., 2010. Structure and function of the blood-brain barrier. *Neurobiology of Disease*, 37(1), pp.13–25. Available at: http://dx.doi.org/10.1016/j.nbd.2009.07.030.

Abbott, N.J. & Friedman, A., 2012. Overview and introduction: the blood-brain barrier in health and disease. *Epilepsia*, 53 Suppl 6, pp.1–6. Available at: http://www.pubmedcentral.nih.gov/articlerender.fcgi?artid=3625728&tool=pmcentrez&rendertype=abstract.

Abbott, N.J., Rönnbäck, L. & Hansson, E., 2006. Astrocyte-endothelial interactions at the blood-brain barrier. *Nature reviews. Neuroscience*, 7, pp.41–53.

Alfahad, T.B. & Nath, A., 2013. Update on HIV-associated neurocognitive disorders. *Current neurology and neuroscience reports*, 13(10), p.387. Available at: http://www.ncbi.nlm.nih.gov/pubmed/23954972 [Accessed December 17, 2013].

An, S.F. et al., 1999. Early entry and widespread cellular involvement of HIV-1 DNA in brains of HIV-1 positive asymptomatic individuals. *Journal of neuropathology and experimental neurology*, 58(11), pp.1156–1162.

Ancuta, P. et al., 2008. Microbial translocation is associated with increased monocyte activation and dementia in AIDS patients. *PLoS ONE*, 3(6), pp.10–20.

Andersen, Å.B. et al., 2010. Cerebral FDG-PET scanning abnormalities in optimally treated HIV patients. *Journal of Neuroinflammation*, 7, pp.2–7.

Andras, I.E. et al., 2003. HIV-1 Tat Protein Alters Tight Junction Protein Expression and Distribution in Cultured Brain Endothelial Cells. *Journal of Neuroscience Research*, 74, pp.255–265.

András, I.E. et al., 2003. HIV-1 Tat Protein Alters Tight Junction Protein Expression and Distribution in Cultured Brain Endothelial Cells. *J Neurosci Res.*, 74(2), pp.255–65.

András, I.E., Pu, H., Tian, J., Deli, M.A., Nath, A., Hennig, B. & Toborek, M., 2005. Signaling mechanisms of HIV-1 Tat-induced alterations of claudin-5 expression in brain endothelial cells. *Journal of Cerebral Blood Flow & Metabolism*, 25(9), pp.1159–1170.

András, I.E., Pu, H., Tian, J., Deli, M.A., Nath, A., Hennig, B., Toborek, M., et al., 2005. Signaling mechanisms of HIV-1 Tat-induced alterations of claudin-5 expression in brain endothelial cells. *Journal of Cerebral Blood Flow & Metabolism*, 25(9), pp.1159–1170.

Anon, 1995. Epivir (lamivudine) package insert. Research Triangle Park, NC: ViiV Healthcare. , pp.1–26.

Anon, 2013. Tivicay (Dolutegravir) package insert. Research Triangle Park, NC: ViiV Healthcare. , pp.1–37.

Anon, 2014. Triumeq (abacavir, dolutegravir, and lamivudine) package insert. Research Trinagle park, NC: ViiV Healthcare.

Anon, 1998. Ziagen (abacavir) package insert. Research Triangle Park, NC: ViiV Healthcare. , pp.1–29.

Anthony, I.C. et al., 2008. The effects of illicit drugs on the HIV infected brain. *Frontiers in Bioscience*, 13, pp.1294–1307.

Antinori, A., Heaton, R.K. & Marder, K., 2007. Updated research nosology for HIV- associated neurocognitive disorders. *Neurology*, pp.1789–1799.

Aquilante, C.L. et al., 2000. Increased Brain P-glycoprotein in Morphine Tolerant Rats. *Pharmacology Letters*, 66(4), pp.47–51.

Arcangeli, M.L., Frontera, V. & Aurrand-Lions, M., 2013. Function of junctional adhesion molecules (JAMs) in leukocyte migration and homeostasis. *Archivum Immunologiae et Therapiae Experimentalis*, 61, pp.15–23.

Arvidsson, U. et al., 1995. Distribution and targeting of a mu-opioid receptor (MOR1) in brain and spinal cord. *Journal of Neuroscience*, 15(5), pp.3328–3341.

Ashraf, T. et al., 2014. Role of CNS transporters in the pharmacotherapy of HIV-1 associated neurological disorders. *Current Pharmaceutical Design*, 20, pp.1543–1563.

Bakri, Y. et al., 2001. The susceptibility of macrophages to human immunodeficiency virus type 1 X4 isolates depends on their activation state. *Biomedicine and Pharmacotherapy*, 55(1), pp.32–38.

Banerjee, A. et al., 2010. HIV proteins (gp120 and Tat) and methamphetamine in oxidative stress-induced damage in the brain: potential role of the thiol antioxidant N-acetylcysteine amide. *Free radical biology & medicine*, 48(10), pp.1388–98. Available at: http://www.pubmedcentral.nih.gov/articlerender.fcgi?artid=2873898&tool=pmcentrez&rendertype=abstract [Accessed January 12, 2014].

Bansal, A.K. et al., 2000. Neurotoxicity of HIV-1 proteins gp120 and Tat in the rat striatum. *Brain Research*, 879(1–2), pp.42–49.

Bauer, B. et al., 2004. Pregnane X receptor up-regulation of P-glycoprotein expression and transport function at the blood-brain barrier. *Molecular pharmacology*, 66(3), pp.413–419.

Bazzoni, G. et al., 2000. Interaction of Junctional Adhesion Molecule with the Tight Junction Components ZO-1, Cingulin, and Occludin. *J Biol Chem*, 275(27), pp.20520–6.

Becker, J.T. et al., 2011. Subcortical brain atrophy persists even in HAART-regulated HIV disease. *Brain Imaging and Behavior*, 5(2), pp.77–85.

Beletsky, L. et al., 2011. The roles of law, client race and program visibility in shaping police interference with the operation of US syringe exchange programs. *Addiction*, 106(2), pp.357–365.

Bell, J.E. et al., 1998. HIV encephalitis, proviral load and dementia in drug users and homosexuals with AIDS Effect of neocortical involvement. *Brain*, 121, pp.2043–2052.

Bell, J.E., Arango, J.C. & Anthony, I.C., 2006. Neurobiology of multiple insults: HIV-1-associated brain disorders in those who use illicit drugs. *Journal of Neuroimmune Pharmacology*, 1, pp.182–191.

Bellizzi, M.J. et al., 2005. Synaptic activity becomes excitotoxic in neurons exposed to elevated levels of platelet-activating factor. *Journal of Clinical Investigation*, 115(11), pp.3185–3192.

Ben-Zvi, A. et al., 2014. MSFD2A is critical for the formation and function of the blood brain barrier. *Nature*, 509(7501), pp.507–11.

Beyrer, C. et al., 2010. Time to act: A call for comprehensive responses to HIV in people who use drugs. *The Lancet*, 376(9740), pp.551–563.

Bocedi, A. et al., 2004. Binding of anti-HIV drugs to human serum albumin. *IUBMB Life*, 56(10), pp.609–614.

Bogulavsky, J.J. et al., 2009. Deletion of the Glutamate Receptor 5 Subunit of Kainate Receptors Affects the Development of Morphine Tolerance. *Journal of Pharmacology and Experimental Therapeutics*, 328(2), pp.579–587.

Bokhari, S.M. et al., 2011. Morphine Potentiates Neuropathogenesis of SIV Infection in Rhesus Macaques. *J Neuroimmune Pharmacol*, 6(4), pp.626–39.

Boven, L.A. et al., 2000. Monocyte infiltration is highly associated with loss of the tight junction protein zonula occludens in HIV-1-associated dementia. *Neuropathology and Applied Neurobiology*, 26(4), pp.356–360.

Bruce-Keller, A.J. et al., 2008. Morphine causes rapid increases in glial activation and neuronal injury in the striatum of inducible HIV-1 tat transgenic mice. *Glia*, 56(13), pp.1414–1427.

Bruce-Keller, A.J. et al., 2008. Morphine Causes Rapid Increases in Glial Activation and Neuronal Injury in the Striatum of Inducible HIV-1 Tat Transgenic Mice. *Glia*, 56, pp.1414–1427.

Buckner, C.M. et al., 2011. Characterization of monocyte maturation/differentiation that facilitates their transmigration across the blood-brain barrier and infection by HIV: Implications for NeuroAIDS. *Cellular Immunology*, 267(2), pp.109–123.

Buckner, C.M. et al., 2006. Neuroimmunity and the blood-brain barrier: Molecular regulation of leukocyte transmigration and viral entry into the nervous system with a focus on neuroAIDS. *Journal of Neuroimmune Pharmacology*, 1(2), pp.160–181.

Burdo, T.H. et al., 2010a. Increased Monocyte Turnover from Bone Marrow Correlates with Severity of SIV Encephalitis and CD163 Levels in Plasma. *PLoS Pathogens*, 6(4), p.e1000842. Available at: http://dx.plos.org/10.1371/journal.ppat.1000842.

Burdo, T.H. et al., 2010b. Increased Monocyte Turnover from Bone Marrow Correlates with Severity of SIV Encephalitis and CD163 Levels in Plasma. *PLoS Pathogens*, 6(4), p.e1000842.

Byrd, D. et al., 2012. Impact of opiate addiction on neuroinflammation in HIV. *Journal of neurovirology*, 18(5), pp.364–73.

Byrd, D.A. et al., 2011. Neurocognitive Impact of Substance Use in HIV Infection. *Journal of Acquired Immune Deficiency Syndromes*, 58(2), pp.154–162.

Carey, C.L. et al., 2006. Prospective Memory in HIV-1 Infection. *Journal of Clinical and Experimental Neuropsychology Journal of Clinical and Experimental Neuropsychology Journal of Clinical and Experimental Neuropsychology Neuropathology Component Clinical Trials Data Management UnitData Systems Manager*, 28(4), pp.536–548.

Carvallo, L., Lopez, L., Che, F., et al., 2015. Buprenorphine Decreases the CCL2-Mediated Chemotactic Response of Monocytes. *J Immunol*, 194, pp.3246–3258.

Carvallo, L., Lopez, L., Che, F.-Y., et al., 2015. Monocytes CCL2-Mediated Chemotactic Response of Buprenorphine Decreases the Buprenorphine Decreases the CCL2-Mediated Chemotactic Response of Monocytes. *The Journal of Immunology*, 194, pp.3246–3258. Available at: http://www.jimmunol.org/content/194/7/3246.

Casado, J.L. et al., 2014. Central nervous system antiretroviral penetration and cognitive functioning in largely pretreated HIV-infected patients. *Journal of NeuroVirology*, 20(1).

Celentano, D.D. & Lucas, G., 2007. Optimizing treatment outcomes in HIV-infected patients with substance abuse issues. *Clinical Infectious Diseases*, 45(SUPPL. 4), pp.S318–S323. Available at: http://www.embase.com/search/results?subaction=viewrecord&from=export&id=L351417236%5Cnhttp://dx.doi.org/10.1086/522557%5Cnhttp://vb3lk7eb4t.search.serialssolutions.com?sid=EMBASE&issn=10584838&id=doi:10.1086%2F522557&atitle=Optimizing+treatment+outcomes+in+H.

Chaudhuri, A., Duan, F., et al., 2008. HIV-1 activates proinflammatory and interferon-inducible genes in human brain microvascular endothelial cells: putative mechanisms of blood–brain barrier dysfunction. *Journal of Cerebral Blood Flow & Metabolism*, 28(4), pp.697–711.

Chaudhuri, A., Yang, B., et al., 2008. STAT1 signaling modulates HIV-1 – induced inflammatory responses and leukocyte transmigration across the blood-brain barrier. *Blood*, 111(4), pp.2062–2072.

Chauhan, A. et al., 2003. Intracellular human immunodeficiency virus Tat expression in

astrocytes promotes astrocyte survival but induces potent neurotoxicity at distant sites via axonal transport. *Journal of Biological Chemistry*, 278(15), pp.13512–13519.

Chefer, V.I. & Shippenberg, T.S., 2009. Augmentation of morphine-induced sensitization but reduction in morphine tolerance and reward in delta-opioid receptor knockout mice. *Neuropsychopharmacology : official publication of the American College of Neuropsychopharmacology*, 34(4), pp.887–98.

Chittick, G.E. et al., 1999. Abacavir: absolute bioavailability, bioequivalence of three oral formulations, and effect of food. *Pharmacotherapy*, 19(8), pp.932–942. Available at: http://onlinelibrary.wiley.com/o/cochrane/clcentral/articles/584/CN-00166584/frame.html.

Chuang, L.F., Killiam, K.F.J. & Chuang, R.Y., 1993. Increased replication of simian immunodeficiency virus in CEm x174 cells by morphine sulfate. *Biochemical and biophysical research communications*, 195(3), pp.1165–1173.

Cicero, T.J. et al., 2014. The changing face of heroin use in the United States a retrospective analysis of the past 50 years. *JAMA Psychiatry*, 71(7), pp.821–826.

Clements J.E. & M.C., Z., 1996. *Molecular biology and pathogenesis of animal lentivirus infections*, Available at: http://books.google.com/books?id=Ku2wPAAACAAJ.

Cohen, M.S. et al., 2008. Review series The spread , treatment , and prevention of HIV-1 : evolution of a global pandemic. *The Journal of Clinical Investigation*, 118(4), pp.1244–1254.

Coley, J.S. et al., 2015. Dopamine Increases CD14 + CD16 + Monocyte Migration and Adhesion in the Context of Substance Abuse and HIV Neuropathogenesis. *PLoS ONE*, 10(2), pp.1–22.

Conant, K. et al., 1998. Induction of monocyte chemoattractant protein-1 in HIV-1 Tat-stimulated astrocytes and elevation in AIDS dementia. *Proceedings of the National Academy of Sciences of the United States of America*, 95(March), pp.3117–3121. Available at: http://www.pubmedcentral.nih.gov/articlerender.fcgi?artid=19704&tool=pmcentrez&rendertype=abstract.

Conrad, C. et al., 2015a. Community Outbreak of HIV Infection Linked to Injection Drug Use of Oxymorphone—Indiana, 2015. *Annals of Emergency Medicine*, 66(3), pp.315–316. Available at: http://linkinghub.elsevier.com/retrieve/pii/S0196064415004783.

Conrad, C. et al., 2015b. Community Outbreak of HIV Infection Linked to Injection Drug Use of Oxymorphone—Indiana, 2015. *Annals of Emergency Medicine*, 66(3), pp.315–316.

Cosenza, M.A. et al., 2002. Up-regulation of MAP2e-expressing oligodendrocytes in the white matter of patients with HIV-1 encephalitis. *Neuropathology and Applied Neurobiology*, 28, pp.480–488.

Cottrell, M.L., Hadzic, T. & Kashuba, A.D.M., 2013. Clinical pharmacokinetic, pharmacodynamic and drug-interaction profile of the integrase inhibitor dolutegravir. *Clinical Pharmacokinetics*, 52(11), pp.981–994.

Crawley, J.N. & Paylor, R., 1997. A proposed test battery and constellations of specific behavioral paradigms to investigate the behavioral phenotypes of transgenic and knockout mice. *Hormones and Behavior*, 31(3), pp.197–211.

Cysique, L. a. & Brew, B.J., 2009. Neuropsychological functioning and antiretroviral treatment in HIV/AIDS: A review. *Neuropsychology Review*, 19(2), pp.169–185.

Dallasta, L.M. et al., 1999. Blood-Brain Barrier Tight Junction Disruption in Human Immunodeficiency Virus-1 Encephalitis. *The American Journal of Pathology*, 155, pp.1915–1927.

Dart, R.C. et al., 2015. Trends in Opioid Analgesic Abuse and Mortality in the United States. *New England Journal of Medicine*, 372(3), pp.241–248. Available at: http://www.nejm.org/doi/10.1056/NEJMsa1406143.

Donahoe, R.M. & Vlahov, D., 1998. Opiates as potential cofactors in progression of HIV-1 infections to AIDS. *Journal of Neuroimmunology*, 83(1–2), pp.77–87.

Dowell, J.A.M.C. et al., 1999. Pharmacokinetics of [14 C] Abacavir , a Human Immunodeficiency Virus Type 1 (HIV-1) Reverse Transcriptase Inhibitor , Administered in a Single Oral Dose to HIV-1-Infected Adults : a Mass Balance Study. , 43(12), pp.2855–2861.

Dronda, F. et al., 2004. CD4 cell recovery during successful antiretroviral therapy in naive HIV-infected patients: the role of intravenous drug use. *AIDS*, 18(16), pp.2210–2.

Dutta, R. & Roy, S., 2012. Mechanism(s) Involved in Opioid Drug Abuse Modulation of HAND. *Current HIV Research*, 10(5), pp.469–477.

Edwards, J.E., Brouwer, K.R. & McNamara, P.J., 2002. GF120918, a P-glycoprotein modulator, increases the concentration of unbound amprenavir in the central nervous system in rats. *Antimicrobial agents and chemotherapy*, 46(7), pp.2284–2286.

El-Hage, N. et al., 2013. A novel bivalent HIV-1 entry inhibitor reveals fundamental differences in CCR5-μ-opioid receptor interactions between human astroglia and microglia. *AIDS (London, England)*, 27(14), pp.2181–90. Available at: http://www.pubmedcentral.nih.gov/articlerender.fcgi?artid=3918492&tool=pmcentrez&rendertype=abstract%5Cnhttp://www.ncbi.nlm.nih.gov/pubmed/23751259.

El-Hage, N. et al., 2006. CCR2 medites increases in glial activation caused by exposure to HIV-1 Tat and opiates. *J Neuroimmunol*, 178, pp.9–16.

El-Hage, N. et al., 2006a. HIV-1 Tat and opiate-induced changes in astrocytes promote chemotaxis of microglia through the expression of MCP-1 and alternative chemokines. *Glia*, 53(2), pp.132–146.

El-Hage, N. et al., 2006b. HIV Tat 1-72 and Opiate-induced changes in astrocytes promote chemotaxis of microglia through the expression of MCP-1 and alternative chemokines NIH Public Access. *Glia. January*, 15(532), pp.132–146.

El-Hage, N. et al., 2008. Morphine exacerbates HIV-1 Tat-induced cytokine production in astrocytes through convergent effects on [Ca(2+)](i), NF-kappaB trafficking and transcription. *PloS one*, 3(12), p.e4093. Available at: http://www.pubmedcentral.nih.gov/articlerender.fcgi?artid=2605563&tool=pmcentrez&rendertype=abstract [Accessed January 12, 2014].

El-Hage, N. et al., 2005. Synergistic increases in intracellular Ca2+, and the release of MCP-1, RANTES, and IL-6 by astrocytes treated with opiates and HIV-1 Tat. *Glia*, 50(2), pp.91–106. Available at: http://www.ncbi.nlm.nih.gov/pubmed/15630704 [Accessed January 12, 2014].

Ellis, R., Langford, D. & Masliah, E., 2007. HIV and antiretroviral therapy in the brain: neuronal injury and repair. *Nature Reviews Neuroscience*, 8(1), pp.33–44. Available at: http://www.ncbi.nlm.nih.gov/pubmed/17180161 [Accessed December 17, 2013].

Ensoli, B. et al., 1990. Tat protein of HIV-1 stimulates growth of cells derived from Kaposi's sarcoma lesions of AIDS patients. *Nature*, 345(6270), pp.84–6. Available at: http://www.ncbi.nlm.nih.gov/pubmed/16290341%5Cnhttp://link.springer.com/10.1007/BF01177222%5Cnhttp://linkinghub.elsevier.com/retrieve/pii/0021979780905019%5Cnhttp://scitation.aip.org/content/aip/journal/pof2/10/9/10.1063/1.869740%5Cnhttp://www.sciencedire.

Eugenin, E.A. et al., 2006. CCL2/monocyte chemoattractant protein-1 mediates enhanced transmigration of human immunodeficiency virus (HIV)-infected leukocytes across the blood-brain barrier: a potential mechanism of HIV-CNS invasion and NeuroAIDS. *The Journal of neuroscience : the official journal of the Society for Neuroscience*, 26(4), pp.1098–106.

Eugenin, E.A., 2006. CCL2/Monocyte Chemoattractant Protein-1 Mediates Enhanced Transmigration of Human Immunodeficiency Virus (HIV)-Infected Leukocytes across the Blood-Brain Barrier: A Potential Mechanism of HIV-CNS Invasion and NeuroAIDS. *The Journal of neuroscience : the official journal of the Society for Neuroscience*, 26(4), pp.1098–1106.

Eugenin, E.A. & Berman, J.W., 2003. Chemokine-dependent mechanisms of leukocyte trafficking across a model of the blood – brain barrier. *Methods*, 29, pp.351–361.

Eugenin, E.A. & Berman, J.W., 2007. Gap Junctions Mediate Human Immunodeficiency Virus-Bystander Killing in Astrocytes. *J Neurosci.*, 27(47), pp.12844–12850.

Eugenin, E. a et al., 2011. Human immunodeficiency virus infection of human astrocytes disrupts blood-brain barrier integrity by a gap junction-dependent mechanism. *The Journal of neuroscience : the official journal of the Society for Neuroscience*, 31(26), pp.9456–9465.

Fauci, A.S. & Marston, H.D., 2015. Ending the HIV–AIDS Pandemic — Follow the Science Anthony. *New England Journal of Medicine*, 373(23), pp.2193–2197. Available at: http://www.nejm.org/doi/10.1056/NEJMp1508256.

Filipowicz, A.R. et al., 2016. Proliferation of Perivascular Macrophages Contributes to the Development of Encephalitic Lesions in HIV-Infected Humans and in SIV-Infected Macaques. *Scientific Reports*, 6(August), pp.1–13. Available at: http://dx.doi.org/10.1038/srep32900.

Fischer-Smith, T. et al., 2001. CNS invasion by CD14 + / CD16 + peripheral blood-derived monocytes in HIV dementia : perivascular accumulation and reservoir of HIV infection. *Journal of NeuroVirology*, 7, pp.528–541.

Fitting, S., Xu, R., et al., 2010. Interactive Comorbidity between Opioid Drug Abuse and HIV-1 Tat Chronic Exposure Augments Spine Loss and Sublethal Dendritic Pathology in Striatal Neurons. *Am J Pathol*.

Fitting, S. et al., 2014. Interactive HIV-1 Tat and Morphine-Induced Synaptodendritic Injury Is

Triggered through Focal Disruptions in Na+ Influx, Mitochondrial Instability, and Ca2+ Overload. *The Journal of neuroscience : the official journal of the Society for Neuroscience*, 34(38), pp.12850–12864.

Fitting, S., Zou, S., et al., 2010. Regional Heterogeneity and Diversity in Cytokine and Chemokine Production by Astroglia: Differential Responses to HIV-1 Tat, gp120, and Morphine Revealed by Multiplex Analysis. *Journal of Proteome Research*, 9(4), pp.1795–1804.

Fois, A.F. & Brew, B.J., 2015. The Potential of the CNS as a Reservoir for HIV-1 Infection: Implications for HIV Eradication. *Current HIV/AIDS Reports*, 12(2), pp.299–303.

Furuse, M., Sasaki, H. & Tsukita, S., 1999. Manner of Interaction of Heterogeneous Claudin Species Within and Between Tight Junction Strands. *The Journal of Cell Biology*, 147(4), pp.891–903. Available at: http://www.jcb.org.

Gan, L.-S. et al., 1993. Mechanism of Intestinal Absorption of Ranitidine and Ondeansetron: Transport Across Caco-2 Cell Monolayers. *Pharmaceutical research*, 10(12), pp.1722–1725.

Gandhi, N., Saiyed, Z.M., et al., 2010. Interactive role of human immunodeficiency virus type 1 (HIV-1) clade-specific Tat protein and cocaine in blood-brain barrier dysfunction: implications for HIV-1-associated neurocognitive disorder. *Journal of neurovirology*, 16(4), pp.294–305.

Gandhi, N., Saiyed, Z.M., et al., 2010. Interactive role of human immunodeficiency virus type 1 (HIV-1) clade-specific Tat protein and cocaine in blood-brain barrier dysfunction: implications for HIV-1-associated neurocognitive disorder. *Journal of neurovirology*, 16(4), pp.294–305.

Garcia-Segura, L.M. & McCarthy, M.M., 2004. Minireview: Role of Glia in Neuroendocrine Function. *Endocrinology*, 145(3), pp.1082–1086.

Gendelman, H.E. et al., 2009. Monocyte chemotactic protein-1 regulates voltage-gated K+ channels and macrophage transmigration. *J Neuroimmune Pharmacol.*, 4(1), pp.47–59.

Ghazi-Khansari, M. et al., 2006. Determination of morphine in the plasma of addicts in using Zeolite Y extraction following high-performance liquid chromatography. *Clinica Chimica Acta*, 364(1–2), pp.235–238.

Giri, N. et al., 2008. Investigation of the Role of Breast Cancer Resistance Protein (Bcrp/ Abcg2) on Pharmacokinetics and Central Nervous System Penetration of Abacavir and Zidovudine in the Mouse. *Drug Metabol. Dispos.*, 36(8), pp.1476–1484.

Glare, P.A. & Walsh, T.D., 1991. Clinical pharmacokinetics of morphine. *Therapeutic Drug Monitoring*, 13(1), pp.1–23.

González-Scarano, F. & Martín-García, J., 2005. The neuropathogenesis of AIDS. *Nature reviews. Immunology*, 5(1), pp.69–81.

De Gregori, S. et al., 2012. Morphine metabolism, transport and brain disposition. *Metab Brain Dis*, 27, pp.1–5.

Gurwell, J.A. et al., 2001. Synergistic neurotoxicity of opioids and human immunodeficiency virus-1 Tat protein in striatal neurons in vitro. *NEUROSCIENCE*, 102(3), pp.555–563.

Hanamsagar, R. et al., 2017. Generation of a microglial developmental index in mice and in humans reveals a sex difference in maturation and immune reactivity: HANAMSAGAR et al. (Glia, (2017), 65, 9, (1504-1520), 10.1002/glia.23176). *Glia*, 65, pp.1504–1520.

Hasegawa, A. et al., 2009. The level of monocyte turnover predicts disease progression in the macaque model of AIDS. *Blood*, 114(14), pp.2917–2925.

Hauser, K. et al., 2009. HIV-1 Tat and morphine have interactive effects on oligodendrocyte survival and morphology. *Glia*, 57, pp.194–206.

Hauser, K. et al., 2012. Opiate drug use and the pathophysiology of neuroAIDS. *Current HIV Research*, 10, pp.435–452.

Hauser, K.F. et al., 2007. HIV-1 neuropathogenesis: glial mechanisms revealed through substance abuse. *Journal of neurochemistry*, 100(3), pp.567–86. Available at: http://www.ncbi.nlm.nih.gov/pubmed/17173547 [Accessed January 12, 2014].

Hauser, K.F. et al., 2009. HIV-1 Tat and morphine have interactive effects on oligodendrocyte survival and morphology. *Glia*, 57(2), pp.194–206.

Hauser, K.F. et al., 2012. Opiate drug use and the pathophysiology of neuroAIDS. *Current HIV research*, 10(5), pp.435–52. Available at:

http://www.pubmedcentral.nih.gov/articlerender.fcgi?artid=3431547&tool=pmcentrez&rendertype=abstract.

Hauser, K.F. & Knapp, P.E., 2014. Interactions of HIV and drugs of abuse: the importance of glia, neural progenitors, and host genetic factors. In *Neuroimmune Signaling in Drug Actions and Addictions*. pp. 231–313.

Hawkins, B.T. & Egleton, R.D., 2006. Fluorescence imaging of blood-brain barrier disruption. *Journal of Neuroscience Methods*, 151(2), pp.262–267.

Hawkins, B.T. & Egleton, R.D., 2006. Fluorescence imaging of blood–brain barrier disruption. *Journal of Neuroscience Methods*, 151, pp.262–267.

Heaton, R.K. et al., 2011. HIV-associated neurocognitive disorders before and during the era of combination antiretroviral therapy: Differences in rates, nature, and predictors. *Journal of NeuroVirology*, 17(1), pp.3–16.

Hickey, W.F., Vass, K. & Lassman, H., 1992. Bone marrow-derived elements in the central nervous system: an immunohistochemical and ultrastructural survey of rat chimeras. *Journal of neuropathology and experimental neurology*, 51(3), pp.246–256.

Hoffmann, A. et al., 2011. High and Low Molecular Weight Fluorescein Isothiocyanate (FITC)-Dextrans to Assess Blood-Brain Barrier Disruption: Technical Considerations. *Translational stroke research*, 2(1), pp.106–11. Available at: http://www.pubmedcentral.nih.gov/articlerender.fcgi?artid=3037479&tool=pmcentrez&rendertype=abstract [Accessed January 12, 2014].

Hong, S. & Banks, W.A., 2015. Role of the immune system in HIV-associated neuroinflammation and neurocognitive implications. *Brain Behav Immun*, 45, pp.1–12.

Hutchinson, M.R. et al., 2011. Exploring the Neuroimmunopharmacology of Opioids: An Integrative Review of Mechanisms of Central Immune Signaling and Their Implications for Opioid Analgesia. *Pharmacological Reviews*, 63(3), pp.772–810. Available at: http://pharmrev.aspetjournals.org/cgi/doi/10.1124/pr.110.004135.

Johnson, T.P. et al., 2013. Induction of IL-17 and nonclassical T-cell activation by HIV-Tat protein. *PNAS*, 110(33), pp.13588–13593.

Jones, C.M., 2013. Heroin use and heroin use risk behaviors among nonmedical users of

prescription opioid pain relievers - United States, 2002-2004 and 2008-2010. *Drug and Alcohol Dependence*, 132(1–2), pp.95–100. Available at: http://dx.doi.org/10.1016/j.drugalcdep.2013.01.007.

Kanmogne, G.D. et al., 2007. HIV-1 gp120 compromises blood-brain barrier integrity and enhances monocyte migration across blood-brain barrier: implication for viral neuropathogenesis. *Journal of cerebral blood flow and metabolism : official journal of the International Society of Cerebral Blood Flow and Metabolism*, 27(1), pp.123–34. Available at: http://www.pubmedcentral.nih.gov/articlerender.fcgi?artid=2232899&tool=pmcentrez&rendertype=abstract [Accessed January 12, 2014].

Kanmogne, G.D., Kennedy, R.C. & Grammas, P., 2002. HIV-1 gp120 proteins and gp160 peptides are toxic to brain endothelial cells and neurons: possible pathway for HIV entry into the brain and HIV-associated dementia. *Journal of neuropathology and experimental neurology*, 61(11), pp.992–1000.

Karn, J. & Stoltzfus, C.M., 2012. Transcriptional and posttranscriptional regulation of HIV-1 gene expression. *Cold Spring Harbor Perspectives in Medicine*, 2(2), pp.1–17.

Kaul, M., Garden, G. a & Lipton, S. a, 2001. Pathways to neuronal injury and apoptosis in HIV-associated dementia. *Nature*, 410(6831), pp.988–994.

Kim, W. et al., 2006. CD163 Identifies Perivascular Macrophages in Normal and Viral Encephalitic Brains and Potential Precursors to Perivascular Macrophages in Blood. *American Society for Investigative Pathology*, 168(3), pp.822–834.

Kim, W.-K. et al., 2003. Monocyte / Macrophage Traffic in HIV and SIV Encephalitis. *Journal of Leukocyte Biology*, 74, pp.650–656.

Kim, W., Alvarez, X. & Williams, K., 2005. The Role of Monocytes and Perivascular Macrophages in HIV and SIV Neuropathogenesis : Information from non- Human Primate Models. *Neurotoxicity Research*, 8, pp.107–116.

Kis, O. et al., 2010. The complexities of antiretroviral drug-drug interactions: role of ABC and SLC transporters. *Trends in Pharmacological Sciences*, 31(1), pp.22–35.

Kucuk, A. et al., 2009. Protective effects of doxycycline in ischemia/reperfusion injury on kidney. *Journal of Physiology and Biochemistry*, 65(2), pp.183–191.

Kumar, A.M. et al., 2009. Human immunodeficiency virus type 1 in the central nervous system leads to decreased dopamine in different regions of postmortem human brains. *Journal of neurovirology*, 15(3), pp.257–74. Available at: http://www.ncbi.nlm.nih.gov/pubmed/19499455 [Accessed January 12, 2014].

Kumar, R. et al., 2006. Chronic morphine exposure causes pronounced virus replication in cerebral compartment and accelerated onset of AIDS in SIV/SHIV-infected Indian rhesus macaques. *Virology*, 354, pp.192–206.

Kumar, R. et al., 2004. Modulation by morphine of viral set point in rhesus macaques infected with simian immunodeficiency virus and simian-human immunodeficiency virus. *Journal of virology*, 78(20), pp.11425–11428.

Leibrand, C.R. et al., 2017. HIV-1 Tat disrupts blood-brain barrier integrity and increases phagocytic perivascular macrophages and microglia in the dorsal striatum of transgenic mice. *Neuroscience Letters*, 640, pp.136–143. Available at: http://linkinghub.elsevier.com/retrieve/pii/S0304394016310217.

Letendre, S.L. et al., 2004. Enhancing antiretroviral therapy for human immunodeficiency virus cognitive disorders. *Annals of Neurology*, 56(3), pp.416–423.

Li, W. et al., 2005. Molecular and cellular mechanisms of neuronal cell death in HIV dementia. *Neurotoxicity Research*, 8(1–2), pp.119–134.

Li, Y., Wang, X., Tian, S., Guo, C.-J., et al., 2002. Methadone Enhances Human Immunodeficiency Virus Infection of Human Immune Cells. *Journal of Infectious Diseases*, 185(1), pp.118–122.

Li, Y., Wang, X., Tian, S., Guo, C., et al., 2002. Methadone Enhances Human Immunodeficiency Virus Infectionof Human Immune Cells. *The Journal of Infectious Diseases*, 185(1), pp.118–122. Available at: http://jid.oxfordjournals.org/lookup/doi/10.1086/338011.

Li, Y. et al., 2003. Morphine enhances HIV infection of neonatal macrophages. *Pediatric Research*, 54(2), pp.282–288.

Louboutin, J.-P. et al., 2010. HIV-1 gp120-induced injury to the blood-brain barrier: role of metalloproteinases 2 and 9 and relationship to oxidative stress. *Journal of neuropathology and experimental neurology*, 69(8), pp.801–816.

Louboutin, J.-P. & Strayer, D.S., 2012. Blood-Brain Barrier Abnormalities Caused by HIV-1 gp120: Mechanistic and Therapeutic Implications. *The Scientific World Journal*, 2012, pp.1–15.

Mäe, M., Armulik, A. & Betsholtz, C., 2011. Getting to Know the Cast -Cellular Interactions and Signaling at the Neurovascular Unit. *Current Pharmaceutical Design*, 17, pp.2750–2754.

Mahajan, S.D. et al., 2008. Tight Junction Regulation by Morphine and HIV-1 Tat Modulates Blood–Brain Barrier Permeability. *J Clin Immunol*, 28, pp.528–541.

Mansour, A. et al., 1995. Opioid-receptor mRNA expression in the rat CNS: anatomical and functional implications. *Trends in Neurosciences*, 18(1), pp.22–29.

Marie-Claire, C. et al., 2004. Cytoskeletal Genes Regulation by Chronic Morphine Treatment in Rat Striatum. *Neuropsychopharmacology*, 29, pp.2208–2215.

Marks, W.D. et al., 2016. HIV-1 Tat causes cognitive deficits and selective loss of parvalbumin, somatostatin, and neuronal nitric oxide synthase expressing hippocampal CA1 interneuron subpopulations. *Journal of neurovirology*, pp.1–16.

Mattson, M.P., Haughey, N.J. & Nath, A., 2005. Cell death in hiv dementia. *Cell Death and Differentiation*, 12, pp.893–904.

McArthur, J.C., 2004. HIV dementia: An evolving disease. In *Journal of Neuroimmunology*. pp. 3–10.

McArthur, J.C. et al., 2010. Human Immunodeficiency Virus- Associated Neurocognitive Disorders Mind the Gap. *Ann Neurol*, 67, pp.699–714.

McCarthy, L. et al., 2001. Opioids, opioid receptors, and the immune response. *Drug and Alcohol Dependence*, 62(2), pp.111–123.

McDonough, R. et al., 1980. Alteration of T and null lymphocyte frequencies in the peripheral blood of human opiate addicts: in vivo evidence for opiate receptor sites on T lymphocytes. *J Immunol*, 125, pp.2539–2543.

Meltzer, M. et al., 1990. The role of mononuclear phagocytes in the pathogenesis of human immunodeficiency virus. *Ann Rev Immunol*, 8, pp.169–94.

Meltzer, M.S. et al., 1990. Macrophages as susceptible targets for HIV infection, persistent viral reservoirs in tissue, and key immunoregulatory cells that control levels of virus replication and extent of disease. *AIDS research and human retroviruses*, 6(8), pp.967–71. Available at: http://www.ncbi.nlm.nih.gov/pubmed/2223243.

Meng, J. et al., 2013. Morphine Induces Bacterial Translocation in Mice by Compromising Intestinal Barrier Function in a TLR-Dependent Manner S. J. Buch, ed. *PloS one*, 8(1), p.e54040.

Meyer, V.J. et al., 2013. HIV and Recent Illicit Drug Use Interact to Affect Verbal Memory in Women. *J Acquir Immune Defic Syndr*, 63, pp.67–76.

Miller, D.S., Bauer, B. & Hartz, A.M.S., 2008. Modulation of P-Glycoprotein at the Blood-Brain Barrier: Opportunities to Improve Central Nervous System Pharmacotherapy. *Pharmacological Reviews*, 60(2), pp.196–209.

Minuesa, G. et al., 2009. Transport of Lamivudine [( ) - - L -2 J , 3 J -Dideoxy-3 J - thiacytidine] and High-Affinity Interaction of Nucleoside Reverse Transcriptase Inhibitors with Human Organic Cation Transporters 1 , 2 , and 3 □. , pp.252–261.

Moore, R.D. & Chaisson, R.E., 1999. Natural history of HIV infection in the era of combination antiretroviral therapy. *AIDS*, 13, pp.1933–1942.

Morone, N.E. & Weiner, D.K., 2013. Pain as the fifth vital sign: Exposing the vital need for pain education. *Clinical Therapeutics*, 35(11), pp.1728–1732.

Nair, A.B. & Jacob, S., 2016. A simple practice guide for dose conversion between animals and human. *Journal of basic and clinical pharmacy*, 7(2), pp.27–31.

Nakamuta, S. et al., 2008. Human immunodeficiency virus type 1 gp120-mediated disruption of tight junction proteins by induction of proteasome-mediated degradation of zonula occludens-1 and -2 in human brain microvascular endothelial cells. *Journal of neurovirology*, 14(3), pp.186–195.

Nath, A., 2015a. Eradication of human immunodeficiency virus from brain reservoirs. *Journal of neurovirology*, 21(3), pp.227–34.

Nath, A. et al., 2002. Molecular basis for interactions of HIV and drugs of abuse. *Journal of acquired immune deficiency syndromes*, 31 Suppl 2, pp.S62–S69.

Nath, A., 2015b. Neurologic Complications of Human Immunodeficiency Virus Infection. *Continuum (Minneap Minn)*, 21(6), pp.1557–1576.

Nath, A. et al., 2000. Neurotoxicity and dysfunction of dopaminergic systems associated with AIDS dementia. *Journal of psychopharmacology (Oxford, England)*, 14(3), pp.222–227.

Naumenko, V.S. et al., 2012a. Effect of brain-derived neurotrophic factor on behavior and key members of the brain serotonin system in genetically predisposed to behavioral disorders mouse strains. *Neuroscience*, 214, pp.59–67. Available at: http://dx.doi.org/10.1016/j.neuroscience.2012.04.031.

Naumenko, V.S. et al., 2012b. Effect of brain-derived neurotrophic factor on behavior and key members of the brain serotonin system in genetically predisposed to behavioral disorders mouse strains. *Neuroscience*, 214, pp.59–67.

Naumenko, V.S. et al., 2013a. Effects of brain-derived and glial cell line-derived neurotrophic factors on startle response and disrupted prepulse inhibition in mice of DBA/2J inbred strain. *Neuroscience Letters*, 550, pp.115–118. Available at: http://dx.doi.org/10.1016/j.neulet.2013.06.056.

Naumenko, V.S. et al., 2013b. Effects of brain-derived and glial cell line-derived neurotrophic factors on startle response and disrupted prepulse inhibition in mice of DBA/2J inbred strain. *Neuroscience Letters*, 550, pp.115–118.

New York State Department of Health AIDS Institute., 2014. Comprehensive Harm Reduction Reverses the Trend in New HIV Infections. , p.30.

Nguyen, T.P., Soukup, V.M. & Gelman, B.B., 2010. Persistent hijacking of brain proteasomes in HIV-associated dementia. *American Journal of Pathology*, 176(2), pp.893–902.

Ngwainmbi, J. et al., 2014. Effects of HIV-1 Tat on enteric neuropathogenesis. *The Journal of neuroscience : the official journal of the Society for Neuroscience*, 34(43), pp.14243–51.

Norman, J.P. et al., 2007. HIV-1 Trans Activator of Transcription Protein Elicits Mitochondrial Hyperpolarization and Respiratory Deficit, with Dysregulation of Complex IV and Nicotinamide Adenine Dinucleotide Homeostasis in Cortical Neurons. *The Journal of Immunology*, 178(2), pp.869–876. Available at: http://www.jimmunol.org/cgi/doi/10.4049/jimmunol.178.2.869.

Nowlin, B.T. et al., 2018. Encephalitis Lesions Are Composed of CD163 D Macrophages Present in the Central Nervous System during Early SIV Infection and SIV-Positive Macrophages Recruited Terminally with AIDS. *The American Journal of Pathology*, 185(6), pp.1649–1665. Available at: http://dx.doi.org/10.1016/j.ajpath.2015.01.033.

Olsen, G.D., 1974. Morphine binding to human plasma proteins. *Clin. Pharmacol. Ther.*, 17(Ref {#}1841 of 2800 in sirius july 20 2007.ref), pp.31–35.

Paris, J.J. et al., 2016. 5α-reduced progestogens ameliorate mood-related behavioral pathology, neurotoxicity, and microgliosis associated with exposure to HIV-1 Tat. *Brain Behav Immun*, 55, pp.202–14.

Pau, A.K. & George, J.M., 2014. Antiretroviral therapy: Current drugs. *Infectious Disease Clinics of North America*, 28(3), pp.371–402. Available at: http://www.ncbi.nlm.nih.gov/pmc/articles/PMC4143801/pdf/nihms-603290.pdf.

Persidsky, Y., Ghorpade, A., et al., 1999. Microglial and Astrocyte Chemokines Regulate Monocyte Migration through the Blood-Brain Barrier in Human Immunodeficiency Virus-1 Encephalitis. *American Journal of Pathology*, 155(5), pp.1599–1611.

Persidsky, Y., Ghorpade, A., et al., 1999. Microglial and astrocyte chemokines regulate monocyte migration through the blood-brain barrier in human immunodeficiency virus-1 encephalitis. *The American journal of pathology*, 155(5), pp.1599–1611.

Persidsky, Y. et al., 2000. Mononuclear phagocytes mediate blood-brain barrier compromise and neuronal injury during HIV-1-associated dementia. *Journal of leukocyte biology*, 68, pp.413–422.

Persidsky, Y. et al., 2006. Rho-mediated regulation of tight junctions during monocyte migration across the blood-brain barrier in HIV-1 encephalitis (HIVE). *Blood*, 107(12), pp.4770–4780.

Peters, P.J. et al., 2016a. HIV Infection Linked to Injection Use of Oxymorphone in Indiana, 2014–2015. *New England Journal of Medicine*, 375(3), pp.229–239. Available at: http://www.nejm.org/doi/10.1056/NEJMoa1515195.

Peters, P.J. et al., 2016b. HIV Infection Linked to Injection Use of Oxymorphone in Indiana, 2014–2015. *New England Journal of Medicine*, 375(3), pp.229–239.

Peterson, P.K. et al., 1993. Enhancement of HIV-1 replication by opiates and cocaine: the cytokine connection. *Advances in experimental medicine and biology*, 335, pp.181–188.

Peterson, P.K. et al., 1994. Morphine amplifies HIV-1 expression in chronically infected promonocytes cocultured with human brain cells. *Journal of neuroimmunology*, 50(2), pp.167–175.

Peterson, P.K. et al., 1990. Morphine promotes the growth of HIV-1 in human peripheral blood mononuclear cell cocultures. *AIDS (London, England)*, 4(9), pp.869–873.

Peterson, P.K. et al., 1990. Morphine promotes the growth of HIV-1 in human peripheral blood mononuclear cell coculturres. *AIDS*, 4, pp.869–873.

Petito, C.K. & Cash, K.S., 1992. Blood-brain barrier abnormalities in the acquired immunodeficiency syndrome: immunohistochemical localization of serum proteins in postmortem brain. *Annals of neurology*, 32(5), pp.658–66. Available at: http://onlinelibrary.wiley.com/doi/10.1002/ana.410320509/abstract.

Petito, C.K. & Roberts, B., 1995. Evidence of Apoptotic Cell Death in HIV Encephalitis. *American Journal of Pathology*,, 146(5), pp.1121–1130.

Polli, J.W. et al., 1999. Role of P-glycoprotein on the CNS disposition of amprenavir (141W94), an HIV protease inhibitor. *Pharmaceutical research*, 16(8), pp.1206–12.

Power, C. et al., 1993. Cerebral white matter changes in acquired immunodeficiency syndrome dementia: alterations of the blood-brain barrier. *Annals of neurology*, 34(3), pp.339–350.

Power, C. et al., 2009. NeuroAIDS: An Evolving Epidemic. *Can. J. Neurol.*, 36, pp.285–295.

Price, T.O. et al., 2005. HIV-1 viral proteins gp120 and Tat induce oxidative stress in brain endothelial cells. *Brain Research*, 1045(1–2), pp.57–63.

Pu, H. et al., 2005. HIV-1 Tat protein-induced alterations of ZO-1 expression are mediated by redox-regulated ERK 1/2 activation. *Journal of Cerebral Blood Flow & Metabolism*, 25(10), pp.1325–1335.

Pu, H. et al., 2003. HIV-1 tat protein upregulates inflammatory mediators and induces monocyte invasion into the brain. *Molecular and Cellular Neuroscience*, 24(1), pp.224–237.

Pu, H. et al., 2007. Limited role of COX-2 in HIV Tat-induced alterations of tight junction protein expression and disruption of the blood-brain barrier. *Brain Research*, 1184(1), pp.333–344.

Pulliam, L. et al., 1997. Unique monocyte subset in patients with AIDS dementia. *The Lancet*, 349, pp.692–695.

Ramirez, S.H. et al., 2012. Activation of Cannabinoid Receptor 2 Attenuates Leukocyte – Endothelial Cell Interactions and Blood – Brain Barrier Dysfunction under Inflammatory Conditions. *J Neurosci*, 32(12), pp.4004–4016.

Ransohoff, R.M., Kivisäkk, P. & Kidd, G., 2003. Three or more routes for leukocyte migration into the central nervous system. *Nature Reviews Immunology*, 3(7), pp.569–581.

Reddy, P.V.B. et al., 2012. Interactive effects of morphine on HIV infection: role in HIV-associated neurocognitive disorder. *AIDS Research and Treatment*.

Reese, M.J. et al., 2013. In vitro investigations into the roles of drug transporters and metabolizing enzymes in the disposition and drug interactions of dolutegravir, a hiv integrase inhibitor. *Drug Metabolism and Disposition*, 41(2), pp.353–361.

Reis, J.M. et al., 2013. Lamivudine permeability study: A comparison between PAMPA, ex vivo and in situ Single-Pass Intestinal Perfusion (SPIP) in rat jejunum. *European Journal of Pharmaceutical Sciences*, 48(4–5), pp.781–789.

Robinson-Papp, J. et al., 2012. Substance abuse increases the risk of neuropathy in an HIV-infected cohort. *Muscle Nerve*, 45, pp.471–476.

Roy, S. et al., 2011. Opioid Drug Abuse and Modulation of Immune Function: Consequences in the Susceptibility to Opportunistic Infections. *J Neuroimmune Pharmacol*, 6, pp.442–465.

Rudd, R.A., 2016. Increases in drug and opioid-involved overdose deaths—United States, 2010–2015. *MMWR.Morbidity and mortality weekly report*, 65, pp.2010–2015.

Sacktor, N. et al., 2002. HIV-associated cognitive impairment before and after the advent of combination therapy. *Journal of NeuroVirology*, 8, pp.136–142.

Sansing, H.A., Renner, N.A. & Maclean, A.G., 2012. An inverted blood-brain barrier model that

permits interactions between glia and inflammatory stimuli. *J Neurosci Methods*, 207(1), pp.91–6.

Saukkonen, J.J. et al., 1997. In vitro transendothelial migration of blood T lymphocytes from HIV-infected individuals. *AIDS (London, England)*, 11(13), pp.1595–1601.

Saylor, D. et al., 2016. HIV-associated neurocognitive disorder - pathogenesis and prospects for treatment. *Nature reviews. Neurology*, 12(4), pp.234–248.

Schier, C.J. et al., 2017. Selective Vulnerability of Striatal D2 versus D1 Dopamine Receptor-Expressing Medium Spiny Neurons in HIV-1 Tat Transgenic Male Mice. *The Journal of Neuroscience*, 37(23), pp.5758–5769.

Schwarz, J.M., Sholar, P.W. & Bilbo, S.D., 2012. Sex differences in microglial colonization of the developing rat brain. *Journal of Neurochemistry*, 120(6), pp.948–963.

Shaik, N. et al., 2007. P-glycoprotein-mediated active efflux of the anti-HIV1 nucleoside abacavir limits cellular accumulation and brain distribution. *Drug Metabolism and Disposition*, 35(11), pp.2076–2085.

Sharma, H.S. & Ali, S.F., 2006. Alterations in Blood-Brain Barrier Function by Morphine and Methamphetamine. *Annals of the New York Academy of Sciences*, 1074(1), pp.198–224.

Shiu, C. et al., 2007. HIV-1 gp120 as well as alcohol affect blood-brain barrier permeability and stress fiber formation: Involvement of reactive oxygen species. *Alcoholism: Clinical and Experimental Research*, 31(1), pp.130–137.

Silva, J.N. et al., 2014. Chronic Central Nervous System Expression of HIV-1 Tat Leads to Accelerated Rarefaction of Neocortical Capillaries and Loss of Red Blood Cell Velocity Heterogeneity. *Microcirculation*, 21(7), pp.664–676.

Singh, I.N. et al., 2004. Apoptotic death of striatal neurons induced by human immunodeficiency virus-1 Tat and gp120: Differential involvement of caspase-3 and endonuclease G. *Journal of neurovirology*, 10(3), pp.141–51. Available at: http://www.ncbi.nlm.nih.gov/pubmed/15204919 [Accessed January 12, 2014].

Smurzynski, M. et al., 2011. Effects of central nervous system antiretroviral penetration on cognitive functioning in the ALLRT cohort. *AIDS (London, England)*, 25(3), pp.357–65. Available at:

http://www.pubmedcentral.nih.gov/articlerender.fcgi?artid=3022370&tool=pmcentrez&rendertype=abstract [Accessed December 17, 2013].

Spudich, S.S. & Ances, B.M., 2012. Neurologic complications of HIV infection. *Top Antivir Med*, 20(2), pp.41–47.

Stiene-Martin, A., Zhou, R. & Hauser, K.F., 1998. Regional, Developmental, and Cell Cycle-Dependent Differences in μ, and δ, and κ-Opioid Receptor Expression among Cultured Mouse Astrocytes. *Glia*, 22(3), pp.249–259.

Strazza, M. et al., 2016. Prolonged Morphine Exposure Induces Increased Firm Adhesion in an in Vitro Model of the Blood–Brain Barrier. *International Journal of Molecular Sciences*, 17(6).

Sun, H. & He, P., 2009. Characterization of interaction between doxycycline and human serum albumin by capillary electrophoresis-frontal analysis. *Electrophoresis*, 30(11), pp.1991–1997.

Thieblemont, N. et al., 1995. CD1410wCD16high : a cytokine-producing monocyte subset which expands during human immunodeficiency virus infection. *Eur. J. Immunol.*, (33), pp.3418–3424.

Toborek, M. et al., 2005. Mechanisms of the blood-brain barrier disruption in HIV-1 infection. *Cellular and Molecular Neurobiology*, 25(1), pp.181–199.

Towgood, K.J. et al., 2013. Regional cerebral blood flow and FDG uptake in asymptomatic HIV-1 men. *Human Brain Mapping*, 34(10), pp.2484–2493.

Tozzi, V. et al., 2005. Neurocognitive Impairment and Survival in a Cohort of HIV-Infected Patients Treated with HAART. *AIDS RESEARCH AND HUMAN RETROVIRUSES*, 21(8), pp.706–713.

Tozzi, V. et al., 2007. Persistence of neuropsychologic deficits despite long-term highly active antiretroviral therapy in patients with HIV-related neurocognitive impairment: prevalence and risk factors. *Journal of acquired immune deficiency syndromes (1999)*, 45(2), pp.174–182.

Trickey, A. et al., 2017. Survival of HIV-positive patients starting antiretroviral therapy between 1996 and 2013 : a collaborative analysis of cohort studies. *The Lancet HIV*, 4, pp.349–356.

Troutman, M.D. & Thakker, D.R., 2003. Rhodamine 123 requires carrier-mediated influx for its activity as a P-glycoprotein substrate in Caco-2 cells. *Pharmaceutical research*, 20(8), pp.1192–1199.

Turchan-Cholewo, J. et al., 2009. Morphine and HIV-Tat increase microglial free radical production and oxidative stress: possible role in cytokine regulation. *Journal of Neurochemistry*, 108(1), pp.202–215.

UNAIDS, 2016. Global AIDS Update 2016.

Valcour, V., 2011. Evaluating cognitive impairment in the clinical setting: practical screening and assessment tools. *Top Antivir Med*, 19(5), pp.175–80.

Valcour, V.G. et al., 2013. HIV DNA reservoir increases risk for cognitive disorders in cART-naïve patients. *PloS one*.

Venturoli, D. & Rippe, B., 2005. Ficoll and dextran vs. globular proteins as probes for testing glomerular permselectivity: effects of molecular size, shape, charge, and deformability. *American journal of physiology. Renal physiology*, 288(4), pp.F605-13.

Verani, A., Gras, G. & Pancino, G., 2005. Macrophages and HIV-1: Dangerous liaisons. *Molecular Immunology*, 42(2), pp.195–212.

Vivithanaporn, P., Gill, M.J. & Power, C., 2011. Impact of current antiretroviral therapies on neuroAIDS. *Expert Review of Anti-infective Therapy*, 9(4), pp.371–374.

Wachtel, M. et al., 2001. Down-regulation of occludin expression in astrocytes by tumour necrosis factor (TNF) is mediated via TNF type-1 receptor and nuclear factor- k B activation. *Journal of Neurochemistry*, pp.155–162.

Wang, X. & Ho, W.Z., 2011. Drugs of abuse and HIV infection/replication: Implications for mother-fetus transmission. *Life Sciences*, 88((21-22)), pp.972–9.

Weber, R. et al., 2009. Uptake of and virological response to antiretroviral therapy among HIV-infected former and current injecting drug users and persons in an opiate substitution treatment programme: The Swiss HIV Cohort Study. *HIV Medicine*, 10(7), pp.407–416.

Weiss, J. et al., 1999. HIV-1 Tat Induces Monocyte Chemoattractant Protein-1-Mediated

Monocyte Transmigration Across a Model of the Human Blood-Brain Barrier and Up-Regulates CCR5 Expression on Human Monocytes. *J Immunol*, 163, pp.2953–2959.

Weiss, J.M. et al., 1999. HIV-1 Tat induces monocyte chemoattractant protein-1-mediated monocyte transmigration across a model of the human blood-brain barrier and up-regulates CCR5 expression on human monocytes. *Journal of immunology (Baltimore, Md. : 1950)*, 163(5), pp.2953–2959.

Wen, H. et al., 2011. Morphine induces expression of platelet-derived growth factor in human brain microvascular endothelial cells: implication for vascular permeability. *PloS one*, 6(6), p.e21707.

Wiley, C.A. et al., 1986. Cellular localization of human immunodeficiency virus infection within the brains of acquired immune deficiency syndrome patients. *Neurobiology*, 83, pp.7089–7093.

Williams, D.W. et al., 2015. JAM-A and ALCAM are therapeutic targets to inhibit diapedesis across the BBB of CD14+CD16+ monocytes in HIV-infected individuals. *Journal of Leukocyte Biology*, 97(2), pp.401–412.

Williams, D.W. et al., 2013. Mechanisms of HIV entry into the CNS: increased sensitivity of HIV infected CD14+CD16+ monocytes to CCL2 and key roles of CCR2, JAM-A, and ALCAM in diapedesis. *PloS one*, 8(7), p.e69270.

Williams, D.W. et al., 2012. Monocyte maturation, HIV susceptibility, and transmigration across the blood brain barrier are critical in HIV neuropathogenesis. *Journal of leukocyte biology*, 91(3), pp.401–415.

Williams, K.C. et al., 2001. Perivascular macrophages are the primary cell type productively infected by simian immunodeficiency virus in the brains of macaques: implications for the neuropathogenesis of AIDS. *The Journal of experimental medicine*, 193(8), pp.905–915. Available at: http://www.pubmedcentral.nih.gov/articlerender.fcgi?artid=2193403&tool=pmcentrez&rendertype=abstract.

Williams, K.C. & Hickey, W.F., 2002. Central nervous system damage, monocytes and macrophages, and neurological disorders in AIDS. *Annu. Rev. Neurosci.*, 25, pp.537–62.

Wing, E.J., 2016. International Journal of Infectious Diseases HIV and aging. , 53, pp.61–68.

Wright, C.I., 1940. The Enzymatic Deacetylation of Heroin and Closely Related Morphine Derivatives by Blood Serum. *Science*, 92(2385), pp.244–245.

Wu, D.T. et al., 2000. Mechanisms of leukocyte trafficking into the CNS. *Journal of neurovirology*, 6 Suppl 1, pp.S82–S85.

Wybran, J. et al., 1979. Suggestive evidence for receptors for morphine and methionine-enkephalin on normal human blood T lymphocytes. *J Immunol*, 123(3), pp.1068–70.

Xie, R., Bouw, M.R. & Hammarlund-Udenaes, M., 2000. Modelling of the blood-brain barrier transport of morphine-3-glucuronide studied using microdialysis in the rat: involvement of probenecid-sensitive transport. *British journal of pharmacology*, 131(8), pp.1784–92.

Xu, R. et al., 2012. HIV-1 Tat protein increases the permeability of brain endothelial cells by both inhibiting occludin expression and cleaving occludin via matrix metalloproteinase-9. *Brain Research*, 1436, pp.13–19. Available at: http://dx.doi.org/10.1016/j.brainres.2011.11.052.

Yamada, H. et al., 2003. Formation of highly analgesic morphine-6-glucuronide following physiologic concentration of morphine in human brain. *The Journal of Toxicological Sciences*, 2828(55), pp.395–401.

Yeh, S.Y., Gorodetzky, C.W. & Krebs, H.A., 1977. Isolation and identification of morphine 3- and 6-glucuronides, morphine 3,6-diglucuronide, morphine 3-ethereal sulfate, normorphine, and normorphine 6-glucuronide as morphine metabolites in humans. *Journal of Pharmaceutical Sciences*, 66(9), pp.1288–1293.

Yilmaz, A. et al., 2010. Treatment Intensification Has no Effect on the HIV-1 Central Nervous System Infection in Patients on Suppressive Antiretroviral Therapy. *JAIDS Journal of Acquired Immune Deficiency Syndromes*.

Yousif, S. et al., 2008. Effect of chronic exposure to morphine on the rat blood-brain barrier: Focus on the P-glycoprotein. *Journal of Neurochemistry*, 107(3), pp.647–657.

Yuen, G.J., Weller, S. & Pakes, G.E., 2008. A review of the pharmacokinetics of abacavir. *Clinical pharmacokinetics*, 47(6), pp.351–71.

Van Zee, A., 2009. The promotion and marketing of oxycontin: Commercial triumph, public health tragedy. *American Journal of Public Health*, 99(2), pp.221–227.

Zembala, M., Bach, S. & Colizzi, V., 1997. Phenotypic Changes of Monocytes Induced by HIV-1 GP 120 Molecule and its Fragments. *Immunobiol.*, 197, pp.110–121.

Zhong, Y. et al., 2008. Caveolin-1 regulates human immunodeficiency virus-1 Tat-induced alterations of tight junction protein expression via modulation of the Ras signaling. *The Journal of neuroscience : the official journal of the Society for Neuroscience*, 28(31), pp.7788–7796.

Zou, S., Fitting, S., Hahn, Y.-K., et al., 2011. Morphine potentiates neurodegenerative effects of HIV-1 Tat through actions at m-opioid receptor-expressing glia. *Brain*, 134, pp.3613–3628. Available at: http://brain.oxfordjournals.org/.

Zou, S., Fitting, S., Hahn, Y.-K.K., et al., 2011. Morphine potentiates neurodegenerative effects of HIV-1 Tat through actions at mu-opioid receptor-expressing glia. *Brain*, 134(12), pp.3613–3628

VITA

Name: Crystal Reiko Leibrand
Birth Date: September 12, 1990
Birth Place: Chesapeake, Virginia
Citizenship: United States of America

Crystal Reiko Leibrand was raised in Chesapeake, VA where she graduated from Western Branch High School in 2008. She then received her undergraduate education from Randolph-Macon College where she received a Bachelor of Science in chemistry in 2012. She then pursued a Doctor of Pharmacy (Pharm.D.) degree at Virginia Commonwealth University School of Pharmacy in 2012 before joining the Pharm.D./Ph.D. program in the Department of Pharmacotherapy & Outcomes Science in 2014.